Azerbaijan Journal of Chemical News

Əlaqə

Ünvan: 20 Azadlıq pr., Bakı, AZ1010, Azərbaycan, Tel: +994124986533,
E-mail: minira_baku@yahoo.com, mayaabdullayeva@hotmail.com.

ISNN: print 2663-7006; online 2709-2666

Azerbaijan Journal of Chemical News

Contacts

Address: 20 Azadliq av., Baku, AZ1010, Azerbaijan, Phone: +994124986533, E-mail: minira_baku@yahoo.com, mayaabdullayeva@hotmail.com.

CONTENT

ISNN: print 2663-7006; online 2709-2666

AJCN, Vol 3, No. 3, 2021, pp. 4-12

UDC: 666.03

RESEARCH OF THE PROCESS OF CONCRETE PRODUCTION USING CULLET

H.B.Bafadarova
Azerbaijan State Oil and Industry University
hokuma.bafadarova@mail.ru

In this research work, was studied the possibility of using glass waste to produce concrete, while maintaining its quality.The problem of the shortage of natural raw materials for the production of materials for construction purposes has not lost its relevance over the past years. This is due to the rapidly developing pace of construction. In this regard, the task of the construction industry is to reorient enterprises towards the consumption of technogenic raw materials. In terms of structure and physicochemical properties, cullet is a mineral resource of anthropogenic origin.Cullet of crushed glass with a grain size of 0-20 mm was introduced into the plastic concrete mixture in the amount of 0, 30, 50, 70 and 100% of the mass of finely dispersed, replacing the sand with this amount of cullet. Concrete samples made from concrete mixtures of various compositions were kept for 7 and 28 days under normal hardening conditions, then a test was carried out to determine the strength and other characteristics of concrete. In order to increase the strength of concrete samples, crushed granite sand and cullet were used as aggregates for subsequent series of samples.*The conducted research allows us to confirm that replacing part of the sand with finely dispersed glass is an acceptable way to reduce the use of natural raw materials while maintaining the strength properties of the concrete mixture.*

Keywords: *concrete, cullet, grinding, fine dispersion, sand, strength, cement, composite materials, technogenic raw materials.*

INTRODUCTION

In the XXI century concrete will be developed as one of the main materials for construction. Already today, more than a thousand types of various concretes are used - from extra lightweight concretes with a density of 100 kg / m^3 - to extra strong ones with a strength of more than 100 MPa - and a wide variety of special concretes with different sets of properties.Modern construction is inconceivable without concrete. 2 billion m^3 per year - this is the volume of its use in the world today.This is one of the most popular building materials in many respects determining the level of development of civilization. At the same time, concrete is the most complex artificial composite material that can have completely unique properties.

It is used in a wide variety of operating conditions, harmoniously combines with the environment , has a limited raw material base and a relatively low cost. To this should be added high architectural and construction emphasis, comparative simplicity and availability of technology, the possibility of widespread use of local raw materials and disposal of man-made waste during its manufacture, low energy consumption, environmental safety and operational reliability. That is why concrete will undoubtedly remain the main structural material for the foreseeable future.The last decades of the twentieth century were marked by significant advances in concrete technology. During these years, new effective binders, modifiers for binders and concretes, additional mineral additives and fillers, reinforcement fibers, new technological methods and methods for producing construction composites appeared and became widespread.

All this made it possible not only to create and master the production of new types of concrete, but also to significantly expand the range of materials used in construction: from super-light heat-insulation materials (with a density of less than 100 kg/m^3) to high-strength construction materials (with a compression strength of about 200 MPa). Today, more than a thousand different types of concrete are used in construction, and the process of creating new concretes continues intensively. Concrete is widely used in residential, industrial, transport, hydrotechnical, energy and other types of construction.

Concretes are artificial stone materials obtained as a result of solidification of a thoroughly mixed and compacted mixture of a mineral or organic binder with water, fine or coarse aggregates, taken in certain proportions. Before hardening, this mixture is called concrete mixture [2,3].

In construction, concretes prepared on the basis of cements or other inorganic binders are widely used. A certain amount of water is added to the dry concrete mixture. Cement and water are the active constituents of concrete; as a result of the reaction between them, a cement stone is formed, which consolidate the aggregate grains into a single monolith.

There is usually no chemical interaction between cement and aggregate (with the exception of silicate concretes obtained by autoclave curing), therefore aggregates are often called inert materials. However, they significantly affect the structure and properties of concrete, changing its porosity, hardening time, behavior when exposed to load and the external environment. Aggregates significantly reduce concrete deformations during hardening and thereby ensure the production of large-sized products and structures. Local rocks and industrial wastes (slags, etc.) are mainly used as aggregates. The use of these cheap aggregates reduces the cost of concrete, since aggregates and water make up 85-90%, and cement 10-15% of the mass of concrete. To reduce the density of concrete and improve its thermotechnical properties, artificial and natural porous aggregates are used.

To regulate the properties of concrete and concrete mixture, various chemical additives and active mineral components are introduced into their composition, which accelerate or slow down the setting of the concrete mixture, make it more workable, accelerate the hardening of concrete, increase its strength and frost resistance, regulate the own deformations of concrete that occur during its hardening, as well as, if necessary, change other properties of concrete.

With increasing age of concrete, its strength, density, and resistance to environmental influences increase. The properties of concrete are determined not only by its composition and the quality of the raw materials, but also by the technology of preparation and placement of the concrete mixture into the structure, by the conditions of concrete hardening. All these factors are taken into account when designing the composition of concrete and producing structures based on it.

On organic binders (bitumen, synthetic resins, etc.), the concrete mixture is obtained without the introduction of water, which ensures high density and impermeability of concrete. The variety of binders, aggregates, additions of active mineral components and technological methods makes it possible to obtain concretes with a wide variety of properties.

Depending on the type, the purpose and features of the concrete usage, as well as concrete products, various binders are used.

Aggregates [7] occupy up to 80% of the volume in concrete and affect the properties of concrete, its durability and cost. The introduction of aggregates into

ISNN: print 2663-7006; online 2709-2666

concrete can dramatically reduce the consumption of cement, which is the most expensive component. In addition, aggregates improve the technical properties of concrete. Aggregates create a rigid skeleton in concrete and reduce concrete shrinkage by about 10 times, compared to cement paste. A rigid skeleton made of high-strength aggregate somewhat increases the strength and deformation modulus of concrete, reduces deformations of structures under load, as well as creep of concrete - irreversible deformations that occur during prolonged loading. Aggregates create a rigid skeleton in concrete and reduce concrete shrinkage by about 10 times compared to cement paste, contributing to obtaining a more durable material.

Porous natural and artificial aggregates, having a low density, reduce the density of lightweight concrete, improve its thermotechnical properties. In special concretes (heat-resistant, for protection from radiation, etc.), the role of the filler is significant, since its properties largely determine the special properties of these concretes.

Coarse [4] and fine aggregates [5, 6] are used in concrete. Coarse aggregate (more than 5 mm) is subdivided into gravel and crushed stone. The fine aggregate in concrete is natural or artificial sand.

Aggregates for concrete are of various types, natural or artificial: sand, crushed stone, gravel. Their properties are regulated by the relevant GOSTs, technical specifications, and other regulatory documents.

The water used for preparation of the concrete mixture must meet the requirements. For this purpose, it is recommended to use potable water. Also, technical circulating water and natural low-mineralized water with acceptable level of impurities can be used.

The use of cement of lower grades increases its consumption, and the use of cement of higher grades does not always lead to its savings. The type of cement for various working conditions of construction products must be selected taking into account the requirements of GOST.

An increase in the production of concrete and reinforced concrete is impossible without an increase in the amount of aggregates. With an average annual volume of concrete and reinforced concrete production of more than 60 million m^3, the need for non-ore filler is more than 50 million m^3, for fine aggregate 50-55 million m^3. However, the expansion of mining of the main types of aggregates for concrete cannot always be realized. The issue of developing compositions and technologies for obtaining building materials based on industrial waste is highly relevant. In recent years, the utilization of unsorted cullet has been of particular interest. Many leading research centers in the CIS countries and abroad have been actively working in the field of cullet utilization in recent years [1, 11, 12].

Materials based on cullet meet the relevant requirements of the applicable GOST. Moreover, they are highly competitive in their general construction and functional properties to modern similar materials based on traditional binders. And for a number of indicators, such as biostability, thermal conductivity, acid resistance, even surpass them [8]. Today cullet is an important part of our life and at the same time - a universal material. It is used in domestic consumption, in scientific research, in modern architecture, as well as in the branches of science and industry.

From an environmental point of view, glass is considered the most difficult waste to recycle. It is not subject to destruction under the influence of water, atmosphere, solar radiation, frost. In addition, glass is a corrosion-resistant material that does not destruct under the influence of the overwhelming amount of strong and weak organic, mineral

and bioacids, salts, as well as fungi and bacteria. Therefore, if organic waste completely decomposes after 1-3 years, polymeric materials - after 5-20 years, then glass, like steel, can remain without much damage for tens and even hundreds of years.

Glass has high strength and inertness, which allows it to be used as a material that replaces more expensive analogs as an aggregate in concrete, drainage and other systems.

The use of glass as an aggregate in concrete makes it possible to completely or partially replace gravel or crushed stone, and sometimes Portland cement and pozzolanic additives [10, 11].

Glass cullet is a valuable secondary raw material, the production of which has already consumed not only natural raw materials, but also large energy resources.

Utilization of glass cullet is a relevant scientific and technical task, the successful solution of which can bring significant economic and environmental benefits.

EXPERIMENTAL PART

From the point of view of chemical and physical structure, cullet can be considered as a mineral resource - amorphous silicate material of anthropogenic origin. Obtaining composite building materials - foam glass, light concrete from unsorted cullet will allow solving the following tasks: saving natural resources, reducing harmful emissions in glass production, reducing the volume of cullet accumulation.

The task is to correctly select the composition of the concrete where part of the fine aggregate of natural origin would be replaced by cullet.

To obtain concrete, it is necessary to observe the proportionality of the composition to other materials used, such as sand, cement, crushed stone and water [9,10].

Cullet used in the research was from container crushed glass with a grain size of 0-20 mm. Finely ground/powdered glass was used as an aggregate instead of natural sand, the chemical composition of the glass is given in table 1.

Table 1

Chemical composition of the container glass

Chemical element	SiO_2	Al_2O_3	Fe_2O_3	CaO	MgO	Na_2O+K_2O	SO_3
Content percentage %	71,5..73,7	0,2..3,3	1,7..3,2	5,2..9,1	0,1..0,6	15,2..16	up to..0,2

In order to study the possibility of using cullet as aggregates for the manufacture of concrete samples, granite crushed stone of 5-10 mm fraction and as a fine aggregate - natural sand and cullet with a grain size of 0-10 mm were used. The cullet was introduced into the composition of the workable concrete mixture in the amount of 0, 30, 50, 70 and 100% of the mass of fine aggregate, replacing the sand with the given amount of cullet. Sample sizes, technology of concrete pouring, as well as processing of samples and the amount of concrete are carried out in accordance with the requirements of the standard. The composition of the samples is shown in table 2.

ISNN: print 2663-7006; online 2709-2666

Table 2

The composition of the concrete mixture

№ of the experiment	1	2	3	4	5
The content of cullet from the mass of fine aggregate, %	0	30	50	70	100
Cement, g	150	150	150	150	150
Natural sand, g	205	143	102	61,5	0
Cullet, g	0	61	102	143	205
Crushed stone 5 – 10 mm, g	56	56	56	56	56
Water, g	70	70	69,5	69,5	69,5

Concrete specimens made from concrete mixtures of various compositions were kept for 7 and 28 days under normal hardening conditions.The research results are shown in fig.2. and in table 3.

When compressing concrete, the ultimate tensile strength was determined on cube samples with dimensions of 40x40x40 mm on a YAW-300D apparatus for building materials. Strength characteristics of concrete samples were determined in accordance with the requirements of GOST 10180-2012 “Concrete. Methods for Determining Strength Using Control Samples”.

Fig. 1. Apparatus YAW -300D

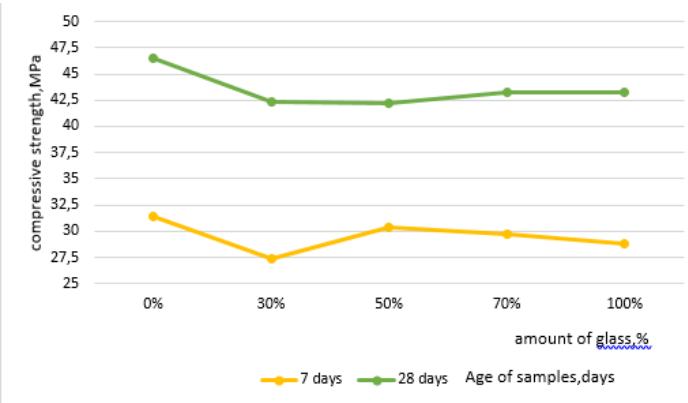

Fig. 2. Dependence of concrete strength on the amount of cullet

Table 3

Compressive strength (MPa) with the amount of cullet in % of the mass of fine aggregate

Age of samples	The amount of cullet from the mass of fine aggregate				
	0%	30%	50%	70%	100%
7 days	31,4	27,4	30,35	29,7	28,8
28 days	46,5	42,4	42,2	43,2	43, 2

The research carried out have shown that replacing fine sand with cullet in the amount of 30% decreases the strength of concrete at the age of 28 days by ≈ 9.2%, and with a further increase in the proportion of cullet in fine aggregate, a slight increase in concrete strength occurs. When replacing fine sand with cullet in the amount of 70%, the strength of concrete decreases at the age of 28 days by 7.2%. It can be assumed that the decrease in the strength of concrete when cullet is added to the fine aggregate is due to the fact that the glass grains have a smooth surface, and there is no adhesion to the cement stone.

In order to increase the strength of concrete samples, crushed stone of a fraction 5-10 mm was used as aggregates for samples of series II, and crushed sand from granite and cullet with a grain size of 0-10 mm was used as a fine aggregate. The cullet was introduced into the composition of the workable concrete mixture in the amount of 0, 30, 50, 70 and 100% of the mass of fine aggregate, replacing the sand with the given amount of cullet. The composition of the concrete mix is shown in table 4.

Table 4

The composition of concrete mixture

№ of the experiment	1	2	3	4	5	6
The content of cullet from the mass of a fine aggregate, %	0	15	30	50	70	100
Cement, g	150	150	150	150	150	150
Crushed sand from granite, g	214	182	150	107	64	0
Cullet, g	0	33	64	107	150	161
Crushed stone 5 – 10 mm, g	161	161	161	627	161	161
Water, g	75	75	75	75	75	75

The appearance of concrete specimens before testing and after testing for ultimate compressive strength is shown in fig.3

Fig.3. Appearance of concrete specimens before and after testing for compressive strength

ISNN: print 2663-7006; online 2709-2666

RESULTS AND DISCUSSION

The results of concrete samples testing at the age of 7, 14 and 28 days after curing under normal hardening conditions are shown in fig.3 and table 5.

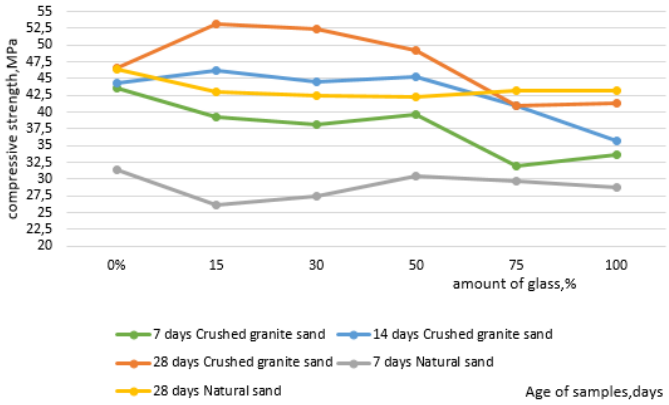

Fig.4. Dependence of concrete strength on the amount of cullet

Table 5

Results of concrete strength test

% glass by weight of fine aggregate	Compressive strength (MPa) at age, days				
	Crushed granite sand			Natural sand	
	7	14	28	7	28
0	43,6	44,4	46,6	31,4	46,4
15	39,2	46,2	53,1	26,2	43
30	38,1	44,6	52,4	27,4	42,4
50	39,7	45,3	49, 2	30,5	42,2
75	31,9	41	41	29,7	43,2
100	33,6	35,8	41,4	28,8	43,2

According to the test results, the strength of concrete samples on crushed granite sand is higher than the strength of samples with the same percentage of cullet on natural sand.

Data given in fig.4 and table 5 show a small (within 10%) strength gain of concrete with 15% cullet content in crushed granite sand. Then an increase in the amount of cullet in the crushed sand gradually leads to a decrease in the strength of the concrete. So, replacing crushed granite sand completely with cullet reduces the strength of concrete by about 11.3% compared to the strength of concretes made only on crushed sand.

Crushed glass reacts with cement hydrates and as a result, the chemical composition of the cement is improved. The cement becomes stronger and more durable and does not absorb water as quickly as conventional cement. The activity of a cullet binder is influenced by its chemical composition, fineness of grinding, water-binder ratio and parameters of autoclave treatment. With an increase in the fineness of grinding

of the binder, its specific surface area increases, as a result of which its solubility and the number of contact points between the cullet and aggregate particles increase. This is associated with an increase in the strength of glass concrete.

CONCLUSION

Thus, taking into account the results obtained, it can be concluded that at a late stage of hardening of composite materials, with partial replacement of the fine aggregate with cullet, a very dense and homogeneous structure of contact zone is formed. Strength properties on the basis of cullet are determined by the content of individual components in the composition.

In the context of the high cost of natural raw materials, scientific research work is of particular value, revealing new opportunities for the use of waste in the creation of building materials based on them.

The secondary use of this type of raw material will provide a significant economic and environmental effect. The research showed that the technology of the production of building materials based on cullet is quite simple, does not require special equipment and large material investments.

REFERENCES

1. Akimova T.V. Ecology. Man-Economy-Biota-Environment: Textbook for university students / T. A. Akimova, V. V. Haskin; 2nd ed., reprint. and supplement-Moscow: UNITY. 2006, 556 p
2. Bazhenov O.M. Technology of concrete. Textbook for universities of the construction ,specialty. - M.: ASV. 2003, 500 p
3. Bazhenov Yu.M. Betonovedenie- Textbook. M.: ASV. 2015,144 p
4. GOST 8267-93 " Crushed stone and gravel from dense rocks for construction work. Technical conditions"
5. GOST 8735-88. Sand for construction work. Test methods
6. GOST 8736-93. Sand for construction work. Technical conditions
7. Itskovich S. M., Chumakov L. D., Bazhenov Yu. M. Technology of concrete aggregates: Textbook for builders. vuzov - M.: Higher School.1991,272 p
8. Kozubskaya T.G. The use of technogenic waste in the production of building materials. Construction materials. 2022 №.2, 10 p
9. Ogloblina E.A. Calculation of the composition of concrete of various types. E.A.Ogloblina, Magnitogorsk: MSTU. 2016, 28 p
10. Chulkova I.L., Yurina T.A. Design of concrete mix compositions with the help of modern information technologies.Monograph. Moscow,Vologda, Info-Engineering. 2019, 36 p
11. Jani Y. & Hogland W.Waste glass in the production of cement and concrete – A review. Journal of Environmental Chemical Engineering. 2(3), 2014, pp.1767–1775
12. Rashad A.M., Recycled waste glass as fine aggregate replacement in cementitious materials based on Portland cement. Construction and Building Materials. 72, 2014, pp.340-357

ISNN: print 2663-7006; online 2709-2666

ИССЛЕДОВАНИЕ ПРОЦЕССА ПОЛУЧЕНИЯ БЕТОНА С ИСПОЛЬЗОВАНИЕМ СТЕКЛОБОЯ

H.B.Bafadarova
Azerbaijan State Oil and Industry University
hokuma.bafadarova@mail.ru

В данной исследовательской работе изучались возможность использования отходов стекла для получения бетона,при сохранении его качества.Проблема дефицита природного сырья для производства материалов строительного назначения на протяжении последних лет не теряет своей актуальности. Это обусловлено быстро развивающимися темпами строительства. В связи с этим, задачей строительной индустрии является переориентация предприятий на потребление техногенного сырья. По строению и физико-химическим свойствам стеклобой представляет собой минеральный ресурс антропогенного происхождения.. Стеклобой из измельченного стекла с крупностью фракции 0-20 мм, вводился в состав пластичной бетонной смеси в количестве 0, 30, 50, 70 и 100 % от массы мелкого заполнителя, заменяя песок данным количеством стеклобоя. Изготовленные бетонные образцы из бетонной смеси различных составов выдерживались в течение 7 и 28 суток в нормальных условиях твердения ,затем проводился тест на определение прочности и др характеристик бетона. С целью повышения прочности бетонных образцов в качестве заполнителей для последующих серии образцов были использованы в качестве мелкого заполнителя – дроблёный песок из гранита и стеклобой. Проведенныее исследования позволяют утверждать, что замена части мелкого заполнителя мелкодисперсным стеклом является приемлемым способом для уменьшения использования природного сырья с сохранением прочностных свойств бетонной смеси.
Keywords: *бетон, стеклобой, измельчение, мелкодисперсность, песок, прочность, цемент, композиционные материалы, техногенное сырье.*

BETONUN ALINMASINDA ŞÜŞƏ QIRINTILARININ İSTİFADƏSİ PROSESİNİN TƏDQİQİ

H.B.Bafadarova
Azərbaycan Dövlət Neft və Sənaye Universiteti
hokuma.bafadarova@mail.ru

Bu tədqiqat işində keyfiyyətini qoruyaraq beton əldə etmək üçün şüşə tullantılarından istifadə etmək imkanı araşdırılmışdır.Son illər ərzində tikinti materialların istehsalı üçün təbii xammal çatışmazlıq problemi aktuallığını itirmir. Buna səbəb,tikintidə sürətli inkişaf templəridir. Bu baxımdan tikinti sənayesinin vəzifəsi müəssisələri texnogen xammal istehlakına yönəltməkdir. Struktur və fiziki və kimyəvi xüsusiyyətlərinə görə şüşə qırıqları antropogen mənşəli mineral ehtiyat təmsil edir.Plastik beton qarışığının tərkibinə xırda doldurucu kimi, fraksiyasının ölçüsü 0-20 mm olan şüşə qırıntısı qum kütləsinin 0, 30, 50, 70 və 100% miqdarını şüşəqırıntısı ilə əvəz edilir.Müxtəlif tərkibli beton qarışığından hazırlanmış beton nümunələr 7 və 28 gün ərzində normal bərkimə şəraitində saxlanılmış, sonra betonun möhkəmliyinin və digər xüsusiyyətlərinin müəyyən edilməsi üçün test aparılmışdır.Beton nümunələrinin möhkəmliyini artırmaq üçün sonrakı seriya nümunələri üçün xırda doldurucu kimi xırdalanmış qranit qumu və şüşə qırıntısı istifadə edilmişdir.Aparılan araşdırma, qumun bir hissəsini xirda dispers şüşə ilə əvəzetməyin beton qarışığın möhkəmlik xüsusiyyətlərini qoruyaraq təbii təbii xammal istifadəsini azaltmaq üçün məqbul bir yol olduğunu iddia etməyə imkan verir.
Açar sözlər: *beton, şüşə qırıqları, daşlama, xırda dispersiya, qum, möhkəmlik, sement, kompozit materiallar, texnogen xammal*

AJCN, Vol 3, No. 3, 2021, pp. 13-19

UDC 547.569.665.66

STUDY OF INHIBITOR-BACTERICIDAL EFFECT OF ORGANIC AND INORGANIC COMPLEXES OF THE IMIDAZOLINES SYNTHESIZED ON THE BASIS OF SYNTHETIC PETROLEUM ACIDS ON MICROBIOLOGICAL CORROSION

N.N.Babanly
Y.H.Mammadaliyev Institute of Petrochemical Processes of Azerbaijan National Academy of Sciences
babanlinermin@gmail.com

Imidazoline was synthesized on the basis of synthetic-, oxysynthetic- petroleum acids and polyethylenepolyamine in the ratio (1:1), at 230°C for 4 h and their organic and inorganic complexes with hydrochloric and acetic acids were obtained. Solutions of the obtained complexes in isopropanol were prepared in three concentrations (25; 150; 250 mg/l), their effect on sulfate-reducing bacteria vital activity was tested in 7-14 days at 30-32°C. It was determined that imidazoline had 64.5%, imidazoline complex with hydrochloric acid - 87.5%, imidazoline complex with acetic acid - 91% of bacteria-destroying inhibitor-bactericidal effect at a concentration of 250 mg/l.

Keywords: *microbiological corrosion, imidazoline, synthetic petroleum acid, polyethylenepolyamine, sulfate-reducing bacteria.*

INTRODUCTİON

Biocorrosion is a special type of metal equipment destruction caused by microorganisms. Mechanism of materials biodegradation process is different and depends on the peculiarities of a destructive object, as well as biofactors [1-4]. Microorganisms affect metal corrosion but not directly on it. It's explained by the fact that they change corrosive medium composition and destroy an oxide layer on metal surface. Metabolic products are formed and gas regime, electrolyte composition, its pH, etc. varies in the process of their vital activity. This corrosion can also be studied as an independent destructive system, but more often biocorrosion occurs in non-electrolytes, aqueous solutions along with other corrosion processes, such as atmospheric, soil, marine corrosion. Biocorrosion is one of the causes for equipment and pipeline failures in aquatic environment.

Hydrogen sulfide is considered the metabolic product of SRB that reduces petroleum quality, complicates refining, and accelerates the corrosion of petroleum industry equipment. It is known that 80% of equipment corrosion in oil refining industry is caused by SRB that creates an active environment for corrosion as a result of vital activities. In a short period of time, they increase their numbers using sulfur compounds of oil in their food chain.

Microbiological corrosion occurs faster in long-term deposits, especially in the absence of bactericidal action against SRB, amount of dissolved hydrogen sulfide increases in the products extracted, and corrosion processes are intensified in the presence of H_2S. Therefore, effect of the proposed inhibitor-bactericides on hydrogen sulfide corrosion should also be studied. The most effective way to prevent biocorrosion of equipment during oil extraction is the use of bactericidal reagents that stop vital activity of SRB [5-7].

One of the most effective ways applied to stop SRB vital activity is the use of

ISNN: print 2663-7006; online 2709-2666

nitrogen-containing reagents [8-11].

The object of our research was to synthesize imidazoline on the basis of synthetic petroleum acids (SPA), oxysynthetic petroleum acids (OSPA) and polyethylenepolyamine (PEPA), obtain their complexes with organic and inorganic acids (with hydrochloric and acetic acids) and study bactericidal activity against SRB.

EXPERIMENTAL PART

The IR spectroscopy of the synthesized imidazoline was recorded on "ALFA" IR-Fourier spectrometer by the German company "Bruker" in the range of 400-4000 cm^{-1} wavelength, initial crystallization temperature was determined on ASTM 2386 Stanhope-Seta device according to GOST 5066-91, refractive index on "Abbemat" 350/500 refractometer and density on "DMA" 4500 M device.

Initially, 1:1 molar ratio of SPA+OSPA [14] obtained by the catalytic oxidation of naphthene-paraffinic hydrocarbons separated from the diesel fraction of Azerbaijani petroleum mixture and polyethylenepolyamine (PEPA) was taken and imidazoline was synthesized in 97% yield at 240°C by separation of 2 mole of water.

Imidazoline was synthesized on the basis of SPA+OSPA and PEPA in 1:1 molar ratio according to the following scheme:

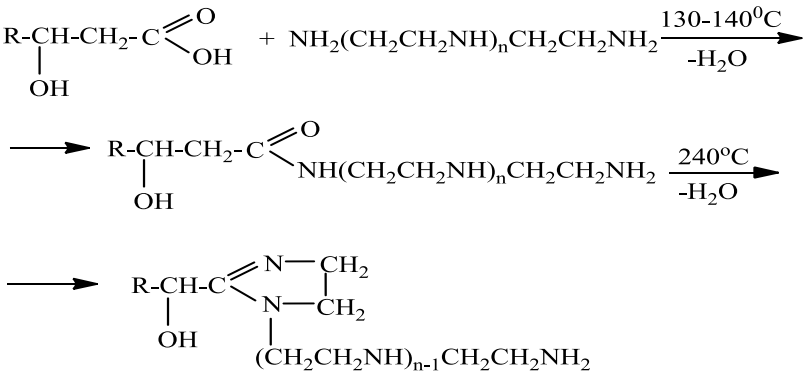

Table 1

Physicochemical properties of SPA+OSPA and PEPA-based imidazoline

№	Properties	Imidazoline
1	Aggregate form	Viscous liquid
2	Odour	Pungent
3	Colour	Dark brown
4	Average molecular weight	524
5	Freezing point, °C	5
6	Specific weight kg/m^3; 20°C	1131.2

Physicochemical properties of the synthesized imidazoline were studied and set into table 1.

The structure of the synthesized imidazoline was confirmed by IR spectroscopic method (fig. 1).

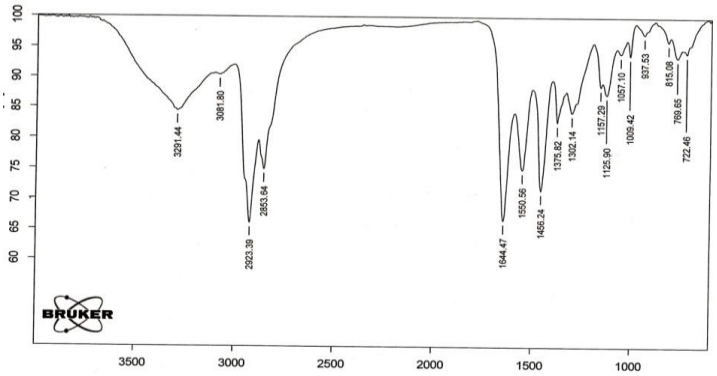

Fig.1. IR spectrum of the imidazoline synthesized on the basis of SPA+OSPA and PEPA

The following absorption bands were registered in the spectrum:

- mathematical vibration of CH_2 group C-H bond at 722 cm^{-1} ;
- CH_2 and CH_3 groups C-H bond deformation and stretching vibrations at 1375, 1456, 2853, 2923 cm^{-1};
- alcohol C-O bond at 1126, 1157 cm^{-1};
- stretching vibration of imidazoline N-H bond at 1550 cm^{-1};
- imidazoline C=N bond at 1644 cm^{-1};
- imidazoline N-H bond at 3081 cm^{-1};
- oxyacid OH group and imidazoline NH group N-H bond vibrations overlap at 3291 cm^{-1};
- OH group O-H bond deformation vibration at 1009, 1057 cm^{-1}.

Organic and inorganic complexes of the synthesized imidazoline with HCl and CH_3COOH acids were obtained in 1:1 ratio at room temperature, 20% isopropyl alcohol was selected as the dissolution medium for the complexes and completely transparent solutions of the complexes were obtained in the medium. The reaction for obtaining SPA+OSPA and PEPA-based imidazoline derivative complexes with organic and inorganic acids occurs on the following equation:

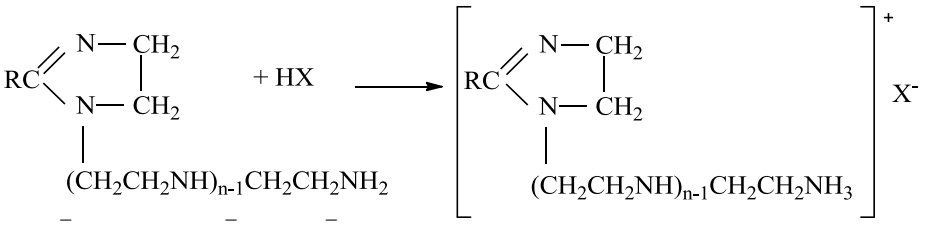

Here X^- = CH_3COO^- and Cl^-

Physical properties of 20% solutions of the complexes were studied and set into table 2.

Table 2

Physical properties of 20% solitions of inorganic complexes of obtained imidazoline

№	Samples	Refractive index, n_d^{20}	Density,g/cm^3	Freezing point,˚C
1	T-2	1.3968	0.8742	- 42
2	T-3	1.3992	0.8533	not frozen at – 60

Note: T-1- imidazoline synthesized on the basis of SPA+OSPA and PEPA, T-2 – imidazoline complex with HCl, T-3 imidazoline complex with CH_3COOH in 1:1 ratio.

ISNN: print 2663-7006; online 2709-2666

RESULTS AND DİSCUSSİON

Effect of T-1, T-2 and T-3 complexes on SRB vital activity was studied as follows.

Desulfovibrio desulfurican genus and 1143 strain of SRB were used for the tests. SRBs are obligate anaerobic bacteria reducing sulfates to hydrogen sulfide. The most suitable nutrient medium for the growth of SRBs is the Postgate B medium. The medium pH should be between 7.0-7.5 [12].

The experiment was performed in a pre-sterilized 10 ml test tube by a known method. For the purpose of determining the number of bacteria in an inhibitor-free medium, the bacteria were first diluted, cultured and kept in a thermostat at 30-32°C for 7-14 days and incubated for 7-14 days. The number of bacteria in the inhibitor-free medium was n = 108 at the end of the experiment. Further, the complexes were added to the medium at the concentrations of 25, 150 and 250 mg/l and kept in a thermostat at 30-32° C for 7-14 days again. The complexes were observed to have a significant effect on the growth of bacteria in the first 72 h of the experiment. Graphical representation of the complexes effects on SRB growth at the concentrations of 25, 150 and 250 mg/l is presented in fig. 2.

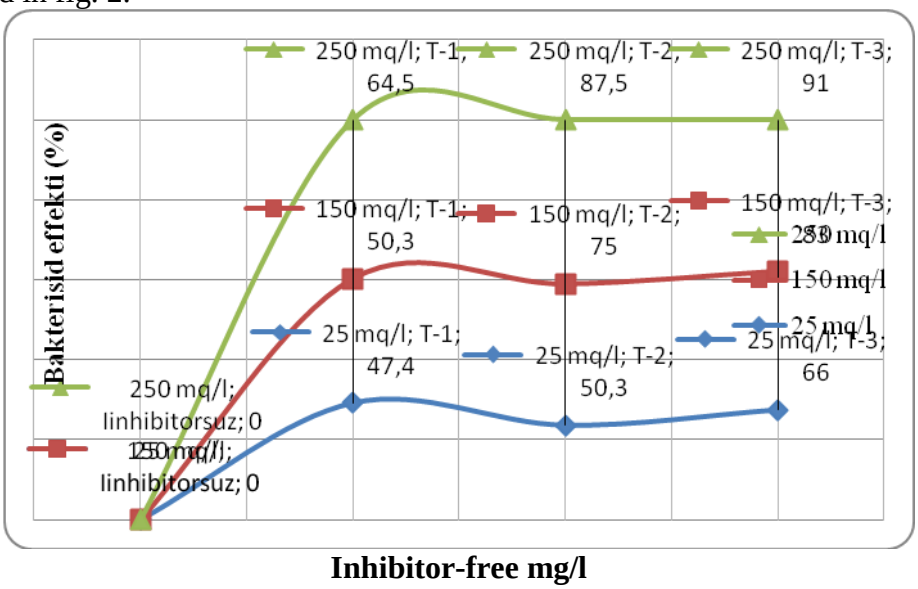

Fig. 2. Graphical representation of T-1, T-2 and T-3 bactericidal effects on SRB vital activity.

The inhibitor protective effect is calculated on the following formula according to the found H_2S amount.

$$Z = \frac{(C_0 - C_{inh})}{C_0} \cdot 100\%$$

C_0- hydrogen sulfide amount in the controlled medium, mg/l;

C_{inh}- hydrogen sulfide amount in the medium with reagent, mg/l.

Bactericidal effect of the samples (T-1, T-2, T-3) was calculated and the results are presented in the table 3.

Table 3

The results of concentration dependent bactericidal effects of T-1, T-2, T-3 complexes

Conventional symbols and compositions of the complexes	Substance concentration, C-mg/l	Bacteria number (cell number/ml)	H_2S amount, mg/l	Bactericidal effect, Z-%
T-1	25	10^5	143	47.4
	150	10^5	135	50.3
	250	10^4	96.5	64.5
T-2	25	10^5	135	50.3
	150	10^3	67	75
	250	10^1	34	87.5
T -3	25	10^3	93.5	66
	150	10^2	47	83
	250	10^1	25	91
Control-I H_2S amount in SRB-free medium		25 mg/l		
Control-II H_2S amount in SRB medium		272 mg/l		
Control-III- bacteria number in nutrient medium		10^8 cell number/ml		

*Test I and Test II show H2S amount in controlled bacteria-free and bacterial media. (Test I - H_2S amount in SRB-free medium -25 mg/l, test II -H_2S amount in SRB medium -272 mg/l), test III shows the number of bacteria in the nutrient medium (108 cell number/ml).

As is evident from the table, T-1, T-2, T-3 complexes prevented SRB growth by bactericidal effect of 47.4-66% at a concentration of 25 mg/l, 50.3-83% at 150 mg/l, and 64.5-91% at 250 mg/l.

The studies proved that in comparison with the synthesized imidazolines, the complexes on the basis of them have a higher bactericidal effect and completely prevent the growth of sulfate-reducing bacteria.

CONCLUSION

1. Imidazoline in 97% yield was synthesized on the basis of SPA+OSPA and PEPA, the complexes were obtained with hydrochloric and acetic acids and the solutions were prepared at the concentrations of 25, 150, 250 mg/l, physicochemical properties were determined and sulfate-reducing bacteria vital activity was tested.
2. Effect of the inhibitors synthesized in microbiological corrosive medium on genus Desulfovibrio desulfuricans of SRB was tested and a high biocidal activity was determined.
3. Bactericidal effects of the studied samples were calculated on the formed H_2S amount. It was determined that at a concentration of 250 mg/l imidazoline complex T-1 had 64.5%, imidohydrochloride complex T-2 – 87.5% and imidoacetic complex T-3 – 91% bactericidal effect.
4. As a result of the studies, the complexes obtained on the basis of the synthesized imidazolines are recommended for industrial use due to the high bactericidal effect

ISNN: print 2663-7006; online 2709-2666

preventing the growth of sulfate-reducing bacteria.

REFERENCES

1. Andreyevich P.M. Influence of Concentration of Oxygen Dissolved in Water on the Rate of Internal Corrosion of Pipelines . Vestnik Udmurtskogo Universiteta. 2012, № 3, pp. 78-83
2. Bashayev M.A., Glazov N.N., Glazov N.P. Influence of the State of Pipelines Insulation on Corrosion Destruction Rate.Truboprovodnyy transport. Teoriya i praktika, 2009, №1, pp. 47-49
3. Belous V.N., Shut′ko K.I. Intergranular cracking of austenitic steels in boiling reactors . FRG. M., ATZR. 2000, №7, 9 p
4. Vigdorovich V.I., Sinyutina S.E., Bokareva L.V. Inhibition of hydrogen sulfide corrosion and hydrogenation of steel in slightly acidic mineralized media. Korroziya, materialy, zashchita. 2003,№2, pp. 35-39
5. Antony P.J., Singh Raman R.K., Raman R., Kumar P., Role of Microstructure on Corrosion of Duplex Stainless Steel in Presence of Bacterial Activity, Corrosion Science. 2010, Vol. 52, p. 1404-1412
6. Li S.Y., Kim Y.G., Jeon K.S., Kho Y.T., Microbiologically Influenced Corrosion of Carbon Steel Exposed to Anaerobic Soil. Met. Mater. 2000, Vol.6, pp.281
7. Abbasov V.M., Mamedbeyli E.G., Agamaliyeva D.B. et al. Synthesis of the Derivatives of Imidazolines Based on Synthetic Oil Acids and their Influence on the Microbiological Corrosion. Practice of Corrosion Protection. 2018, № 1 (87), pp. 17-23
8. Ibragimova M.D., Mamedkhanova S.A., Abdullazada A.B., Agamaliyeva D.B. et al. Influence of Oligomethylenarylsulphonates Based on the Light Gasoil of Catalytic Cracking on the Process of Biocorrosion. Practice of Corrosion Protection.2020, №25 (4), pp. 18-25
9. Mamedbeyli E.G., Babaeva V.G., Agamalieva D.B., Azizbeyli A.R. Synthesis of Imidazoline Based on Diethylentriamine and Norborn-5-en-2-carbonic Acid and its Inorganic Anion Complexes and Studying its Effect on Biocorrosion // Neftepererabotka i neftekhimiya. 2020,№ 3, pp. 22-26
10. Mamedbeyli E.G., Gadzhieva G.E., Ibragimli S.I., Agamalieva D.B. Mannikh Norbornene-containing Bases as Biocorrosion Inhibitors. Neftepererabotka i neftekhimiya. 2020, №2, pp. 20-23
11. Abbasov V.M., Zeynalov E.B., Aliyeva L.I., Efendiyeva L.M., Nuriyev L.H. Liquid_Phase Oxidation of Naphthenic Hydrocarbons Separated from Oil Fractions in the Presence of Pentanuclear Complexes of Co and Ni.Chemical Industry Today. 2013,№ 3, pp.21-29
12. Postgate J.R., Campbell L.L. Classification of Desulfovibrio cpecies the non sporulating sulfate-redusing bacteria. Bacteriol. Revs. 1966,Vol.30, №4, pp. 732-738

AJCN, Vol 3, No. 3, 2021, pp. 13-19

ИЗУЧЕНИЕ ИНГИБИТОР-БАКТЕРИЦИДНОГО ВЛИЯНИЯ ОРГАНИЧЕСКИХ И НЕОРГАНИЧЕСКИХ КОМПЛЕКСОВ СИНТЕЗИРОВАННЫХ ИМИДАЗОЛИНОВ НА ОСНОВЕ СИНТЕТИЧЕСКИХ НЕФТЯНЫХ КИСЛОТ НА МИКРОБИОЛОГИЧЕСКУЮ КОРРОЗИЮ

Н.Н. Бабанлы
Институт Нефтехимических процессов им. Ю. Г. Мамедалиева Национальной академии наук Азербайджана
babanlinermin@gmail.com

Синтезирован имидазолин на основе синтетических-, окси- нефтяных кислот и полиэтиленполиамина в соотношении (1: 1), при температуре 230°С, в течение 4 часов и получены их органические и неорганические комплексы с соляной и уксусной кислотами. Приготовлены растворы полученных комплексов в изопропаноле в трех концентрациях (25; 150; 250 мг/л), проверено влияние сульфатредуцирующих бактерий на жизненную деятельность в течение 7–14 дней при температуре 30–32°С. Установлено, что имидазолин показывает ингибитор-бактерицидное свойство, уничтожая бактерии при концентрации имидазолина 250 мг /л - 64,5%, хлорсодержащий комплекс имидазолина - 87,5%, уксуссодержащий комплекс имидазолина - 91%.
Ключевые слова: *микробиологическая коррозия, имидазолин, синтетическая нефтяная кислота, полиэтиленполиамин, сульфатредуцирующая бактерия.*

SİNTETİK NEFT TURŞULARI ƏSASINDA SİNTEZ OLUNMUŞ İMİDAZOLİNLƏRİN ÜZVİ VƏ QEYRİ-ÜZVİ KOMPLEKSLƏRİNİN MİKROBİOLOJİ KORROZİYAYA İNHİBİTOR-BAKTERİSİD TƏSİRİNİN ÖYRƏNİLMƏSİ

N.N.Babanlı
AMEA akademik Y.H. Məmmədəliyev adına Neft-Kimya Prosesləri İnstitutu
babanlinermin@gmail.com

Sintetik neft turşuları, oksi- turşular və polietilenpoliamin əsasında (1:1) nisbətdə, 230°C temperaturda, 4 saat müddətində imidazolin sintez olunmuş, və onların xlorid və sirkə turşuları ilə üzvi və qeyri-üzvi kompleksləri alınmışdır. Alınmış komplekslərin izopropanolda üç qatılıqda olmaqla (25; 150; 250 mq/l) məhlulları hazırlanmış, 7-14 gün ərzində 30–32˚C temperaturda sulfat reduksiyaedici bakteriyaların həyat fəaliyyətinə təsiri yoxlanılmışdır. Müəyyən edilmişdir ki, 250 mq/l qatılıqda imidazolin 64.5%, xlorid tərkibli imidazolin kompleksi 87.5%, sirkə tərkibli imidazolin kompleksi isə 91% bakteriyaları məhv edərək inhibitor-bakterisid xassəsi göstərmişdir.
Açar sözlər: *mikrobioloji korroziya, imidazolin, sintetik neft turşusu, polietilenpoliamin, sulfatreduksiyaedici bakteriya*

ISNN: print 2663-7006; online 2709-2666

AJCN, Vol 3, No. 3, 2021, pp. 20-25

UDC 547.624

INVESTİGATİON OF THE REACTİON OF OBTAİNİNG HYDROGEN FROM ETHANOL OVER BİNARY NİCKEL-SERIUM OXİDE CATALYSTS

D.V. Akhmedova, V.L. Baghiyev
Azerbaijan State Oil and Industry University
daxmedzade@bk.ru

In the presented work, we had investigated the reaction of steam conversion of ethanol to hydrogen over binary nickel-cerium oxide catalysts of various alignments. It is also resoluted that hydrogen yield at a maximum temperature of 600 ° C reaches 76.5%, and the reaction products above 500 ° C contained only hydrogen, methane and carbon monoxide. It was found that the atomic ratio of nickel to them affects the activity of oxide catalysts Ni-Ce-O in the reaction of steam reforming of ethanol. Thus, as the amount of nickel oxide in the catalyst increases, the hydrogen yield in the Ni-Ce = 5-5 catalyst gradually exceeds the maximum by 82.3%. Based over the X-ray phase analysis, it was initiated that two phases are formed in the Ni-Ce-O catalytic system: NiO and CeO_2, and the ratios change according to the directions.
The yields of the reaction products and the degree of crystallinity of the catalysts are compared. It was initiated that with an increase in the degree of crystallinity of the trial, the yield of hydrogen passes through a maximum, while the yield of methane passes through a minimum, and the yield of carbon monoxide declines.
Keywords: *binary catalysts, hydrogen, bioethanol, methane, crystallinity, steam reforming, activity, carbon monoxide.*

INTRODUCTION

From the periodic literature it is known that different catalytic systems are used to carry out the reaction of steam conversion of ethanol to hydrogen. High activity in this reaction is manifested by simple and multicomponent catalysts based on cerium oxide. According to earlier studies, binary cerium oxide catalysts have high activity in the reaction of steam conversion of ethanol. In connection with this, we studied the activity of binary nickel-cerium oxide catalysts in the reaction of steam conversion of ethanol to hydrogen [1].

The reaction of steam conversion of ethanol to hydrogen is of both theoretical and practical interest. On the one hand, hydrogen in the future will be one of the main sources of energy. On the other hand, ethanol, obtained from bioresources, is a renewable raw material [2].

The main scientific idea of the presented article is to obtain valuable compounds for the chemical industry from renewable raw materials such as ethanol, hydrogen, acetic acid, and acetone, to research the reactions, and to offer a scientific basis for the production of hydrogen, acetic acid, and acetone [3].

The anticipated venture is both economically and ecologically applicable. The economic significance is the renewable bioethanol is used as the primary raw material to attain hydrogen, acetic acid and acetone which are valuable chemical monomers The ecological significance is that the industry uses renewable raw materials and as the result – carbon dioxide emissions don't increase [4,5].

Hydrogen invention from ethanol is observed as a auspicious way for energy sustainable development, which is undergoing an quick-tempered development over the last decade. Besides operating conditions, hydrogen yield momentously dependent on

the countryside of metal and the support nominated [6,7].

Hydrogen is a promising fuel for various types of power plants, including low-power devices (1-50W). However, the accumulation and storage of molecular hydrogen is currently a problem. One of the possible ways to overcome the emerging problems may be the generation of hydrogen from hydrocarbons, for example, alcohols (ethanol) in the process of steam catalytic conversion. Ethanol in this case has a number of undoubted advantages in comparison with methanol: low cost, low toxicity, ease of transportation and operation, as well as the possibility of obtaining it from renewable sources (bioethanol)[8,9].

EXPERIMENTAL PART

Nickel-serum oxide catalysts are prepared by the method of co-precipitation of aqueous solutions of nickel nitrate and serium nitrate. The resulting mixture is evaporated at 95-100ºC, then the precipitate is dried at 100-120ºC and then decomposed at 250ºC until complete separation of nitrogen oxides. The obtained solid mass was incubated at 700ºC for 10 h. In general, we have prepared 9 samples of catalysts that meet the following conditions:

mNi/nCe, where m, n = 1÷9, m+n = 10

The activity of the synthesized catalysts was studied in a flow unit with a quartz reactor at a temperature range of 300-700°C. The reactor was loaded with 5 ml of the studied catalyst with a grain size of 1.0–2.0 mm and studied its activity in the reaction of steam conversion of ethanol.

Radiographic investigations of the phase composition of tresearched catalysts were carried out on an automatic powder diffractometer (CuKα-radiation, Ni-filter) of the company "Bruker" (Germany) "D2 Phaser"..

Radiographic investigation of Ni-Ce-O catalysts were performed in the range of $50 \leq 2\theta \leq 750$ reflection angles. The figure below fig.1 shows a diffraction pattern of all nine mNi / nCe ratios combined. NiO and CeO_2 oxides are also shown at the beginning and end of these diffraction patterns.

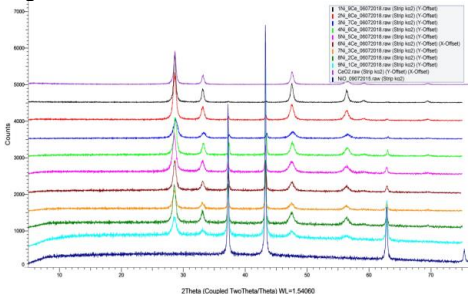

Fig.1. Radiographic investigation of Ni-Ce-O catalysts

Based on X-ray phase analysis, it was found that two phases are formed in the Ni-Ce-O catalyst system: NiO and CeO_2, and the ratios change according to the rules. We also calculated the degree of crystallinity of all trials table 1 on the D2 Phaser using the DIFFRAC.EVA program, the results of which are shown in the table below.

Table 1

The degree of crystallinity in trials

Atomic ratio of Ni:Ce	1-9	2-8	3-7	4-6	5-5	6-4	7-3	8-2	9-1
The degree of crystallinity , %	78.7	76.2	70.5	65.9	59.1	50.6	42	38.8	27.3

ISNN: print 2663-7006; online 2709-2666

As can be seen from the table, the crystallinity decreases in the samples as the amount of nickel increases. Researches of the vapor conversion reaction of ethanol to hydrogen on synthesized nickel oxide catalysts show that the main products of the reaction are hydrogen and carbon dioxide. Acetaldehyde, ethyl acetate, carbon monoxide and methane are also formed as by-products. Vinegar aldehyde and ethyl acetate are formed only at low temperatures.

RESULTS AND DISCUSSION

The activity of binary Ni-Ce oxide catalyst with different composition in the vapor conversion reaction of ethanol is shown below. The results of the conversion reaction of ethanol in the presence of water vapor on the catalyst Ni-Ce = 1-9 are shown below. Vapor conversion of ethanol begins at 200^0C. A small amount (6.0%) of acetaldehyde is obtained at this temperature. As can be seen from the (fig.2), subsequent increase in temperature leads to the formation of other reaction products. The figure also shows that the conversion of ethanol increases sharply with increasing temperature and reaches almost 90% at 500 ºC, and the subsequent increase in temperature does not affect the conversion of ethanol.

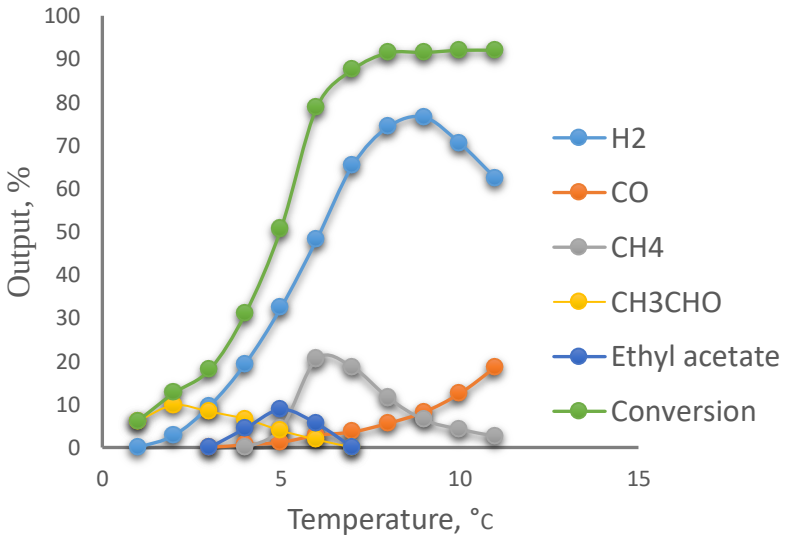

Fig.2. Influence of temperatures on the products of the reaction of steam conversion of ethanol in hydrogen on the catalyst Ni-Ce = 1-9.

As can be seen from the(fig.3),a yield of hydrogen at a maximum temperature of 600 %C reaches 76.5%, and the reaction products above 500°C contain only hydrogen, methane and carbon monoxide.

According to the results, binary nickel-serum oxide catalysts have a high activity in the vapor phase conversion of ethanol to hydrogen.

The activity of Ni-Ce-O oxide catalysts in the vapor conversion reaction of ethanol must, of course, be affected by the atomic ratio of nickel and cerium. As can be seen from the figure below, as the amount of nickel oxide in the catalyst increases, the hydrogen yield gradually exceeds the maximum of 82.3% in the Ni-Ce = 5-5 catalyst.

The figure 3 also shows that as the amount of nickel oxide in the catalyst increases, the methane output exceeds the minimum in the Ni-Ce = 5-5 catalyst, while the carbon monoxide yield increases and reaches 31% in the Ni-Ce = 9-1 sample. In nickel-rich catalysts, the conversion of ethanol reaches 100%. Acetaldehyde and ethyl acetate are practically not obtained.

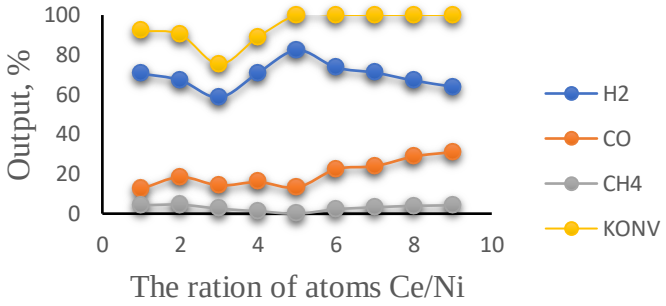

Fig. 3. Addiction of the product yields from reaction of steam conversion of ethanol to hydrogen on the atomic ratio of nickel to cerium.

The crystallinity of the sample can somehow affect its activity in the reaction of steam conversion of ethanol to hydrogen. Figure 4 shows the dependences of the yields of products of steam conversion of ethanol on the degree of crystallinity of nickel-cerium oxide catalysts. As can be seen from (fig.4), with an increase in the degree of crystallinity of the sample, the hydrogen yield passes through a maximum, while the methane yield passes through a minimum, and the carbon monoxide yield decreases. Based on the data obtained, we can say that a catalyst with a certain degree of crystallinity is required for a high hydrogen yield.

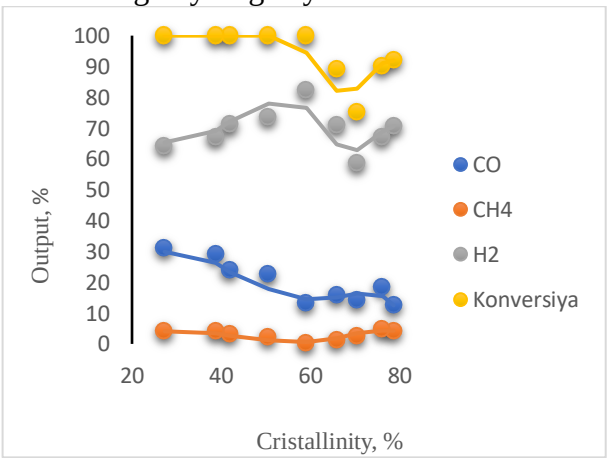

Fig. 4. Addiction of the product yields of the reaction of steam conversion from ethanol to hydrogen on the degree of crystallinity of the Ni-Ce-O catalyst

CONCLUSION

1.Binary Ni-Ce-O oxide catalysts have been synthesized and it has been determined that ethanol exhibits high activity in the vapor conversion reaction to hydrogen. It is shown that the yield of hydrogen reaches 85%.

ISNN: print 2663-7006; online 2709-2666

2.X-ray phase analysis of the binary Ni-Ce-O system revealed that all samples contained only the phases of the first two oxides, ie NiO and CeO_2.
3.The yield of hydrogen in the reaction of steam conversion of ethanol with an increase in the degree of crystallinity of the trial permits through a maximum.

REFERENCES

1. Michela Martinelli, Jonathan D.Castro, Nour Alhraki, Maria E.Matamoros, A. Jeremy Kropf, Donald C.Cronauer, Gary Jacobs. Effect of sodium loading on Pt/ZrO_2 during ethanol steam reforming, Applied Catalysis A: eneral. 2021, Vol 610, pp. 117-127
2. Ahmed Tijani, Afolabi F., Panagiotis N.Kechagiopoulos, Yurong Liu, Chun-Zhu Li. Kinetic features of ethanol steam reforming and decomposition using a biochar-supported Ni catalyst. Fuel Processing Technology. 2019, Vol. 212, pp. 106-112
3. Yanfei Li., Shigeru Kimura. Economic competitiveness and environmental implications of hydrogen energy and fuel cell electric vehicles in ASEAN countries: The current and future scenarios. Energy Policy. 2021, Vol.148, Part B, pp. 119-125
4. Markus Reuß, Lara Welder, Johannes Thürauf, Jochen Linßen, Thomas Grube, Lars Schewe, Martin Schmidt, Detlef Stolten, Martin Robinius. Modeling hydrogen networks for future energy systems: A comparison of linear and nonlinear approaches. International Journal of Hydrogen Energy. 2019, Vol. 44, I. 60, pp. 32136-32150
5. Ilenia Rossetti, AntonioTripodi, Gianguido Ramis. Hydrogen, ethylene and power production from bioethanol: Ready for the renewable market, International Journal of Hydrogen Energy. 2020, Vol.45, I.17, pp. 10292-10303
6. Camila Fernandes Ribeiro Machado, Ofélia de Queiroz Fernandes Araújo, José Luizde Medeiros, Rita Maria de Brito Alves. Carbon dioxide and ethanol from sugarcane biorefinery as renewable feedstocks to environment-oriented integrated chemical plants. Journal of Cleaner Production. 2018, Vol.172, pp. 1232-1242
7. FagenWang, Linjia Zhang, Jiayin Zhu, Bolin Han, Long Zhao, Hao Yu, Zhiyong Deng, Weidong Shi. Study on different CeO_2 structure stability during ethanol steam reforming reaction over Ir/CeO_2 nanocatalysts. Applied Catalysis A: General. 2018, Vol. 564, pp. 226-233
8. Lin Li, Dawei Tang, Yongchen Song, Bo Jiang, Qian Zhang. Hydrogen production from ethanol steam reforming on Ni-Ce/MMT catalysts. Energy. 2018, Vol.149, pp. 937-943

ИССЛЕДОВАНИЕ РЕАКЦИИ ПОЛУЧЕНИЯ ВОДОРОДА ИЗ ЭТАНОЛА НА ОСНОВЕ БИНАРНЫХ НИКЕЛЬ-ЦЕРИЕВЫХ ОКСИДНЫХ КАТАЛИЗАТОРАХ

Д. В. Ахмедова , В. Л. Багиев
Азербайджанский Государственный Университет Нефти и Промышленности
daxmedzade@bk.ru

В представленной работе исследована реакция паровой конверсии этанола в водород на бинарных никель-цериевых катализаторах различного строения. Найдено, что выход

водорода при максимальной температуре 600 ° C достигает 76,5%, а продукты реакции выше 500 ° C содержат только водород, метан и монооксид углерода. Было установлено, что атомное отношение никеля к церию влияет на активность оксидных катализаторов Ni-Ce-O в реакции парового риформинга этанола. Таким образом, по мере увеличения количества оксида никеля в катализаторе выход водорода в катализаторе Ni-Ce = 5-5 постепенно увеличивается и достигает своего максимума равного 82,3%. На основании рентгенофазового анализа было установлено, что в каталитической системе Ni-Ce-O образуются две фазы: NiO и CeO_2, и их соотношения меняются согласно закономерности.

Сравниваются выходы продуктов реакции и степень кристалличности катализаторов. Было определено, что с увеличением степени кристаллизации выход водорода проходит через максимум, а выход метана проходит через минимум, а также выход монооксида углерода уменьшается.

Ключевые слова: *бинарные катализаторы, водород, биоэтанол, метан, кристалличность, паровая конверсия, активность, оксид углерода.*

BİNAR NİKEL-SERİUM OKSİD KATALİZATORLARININ İŞTİRAKI İLƏ ETANOLDAN HİDROGENİN ƏLDƏ OLUNMA REAKSİYASININ TƏCRÜBİ ARAŞDIRILMASI

D. V. Əhmədova, V. L. Bağıyev
Azərbaycan Dövlət Neft və Sənaye Universiteti
daxmedzade@bk.ru

Təqdim olunan işdə, etanolun hidrogenə buxar çevrilməsinin müxtəlif quruluşlu binar nikel-serium katalizatorları üzərində reaksiyası araşdırılmışdır. Maksimum 600 ° C temperaturda hidrogen çıxımının % 76,5-ə çatması və 500 ° C-dən yuxarı reaksiya məhsullarında yalnız hidrogen, metan və karbon monoksid olduğu qərara alındı. Müəyyən edilmişdir ki nikelin seriuma atom nisbəti Ni-Ce-O katalitik sisteminin etanolun hidrogenə buxar konversiyası reaksiyasında aktivliyinə təsir edir. Beləliklə, Ni-Ce = 5-5 katalizatorundaı hidrogenin çıxımı tədricən maksimuma 82,3% çatır. Rentgen faza analizinə əsasən Ni-Ce-O katalitik sistemində iki fazanın yəni NiO və CeO2-nin əmələ gəlməsi aşkar edilmişdir:. Reaksiya məhsullarının çıxımı və katalizatorların kristallıq dərəcəsi müqayisə olunmuşdur. Kristallaşma dərəcəsinin artması ilə hidrogen çıxımının maksimumdan, metanın çıxımının minimumdan keçir və karbon monoksidin çıxımı isə azalır.

Açar sözlər: *binar katalizatorlar, hidrogen, bioetanol, metan, kristallaşma dərəcəsi, buxar çevrilməsi, aktivlik, karbon monoksidi.*

ISNN: print 2663-7006; online 2709-2666

AJCN, Vol 3, No. 3, 2021, pp. 26-31

UOT 66:65.015.11

RESEARCH OF REGULARITIES OF THE PROCESS OF CATALYTIC GAS-PHASE OXIDATION OF METHANOL TO FORMIC ACID

G.S.Aliyev[1], U.A.Abasova[2], Kh.M.Rustamli[1]
[1]Institute of Catalysis and Inorganic Chemistry named after acad. M.Naghiyev of ANAS
[2]Azerbaijan State Oil and Industry University
chemproblem@mail.ru

The article presents the results of a study of some regularities of the process of catalytic oxidation in the gas phase of methanol to formic acid. To do this, first, experiments were carried out on a unique laboratory setup at the nodal values of the initial parameters, and then a multiple regression equation for the process was created, the coefficients of the equation were calculated and their significance was determined. The adequacy of the equation was checked and a more sensitive parameter was identified. Using Fisher's criterion, the statistical significance of the equation was proved. Statistical analysis of the obtained regression equation was carried out: checking the significance of the equation and its coefficients, studying the absolute and relative errors of approximation. Paired correlation indicators of the equation coefficients are also calculated. Based on the maximum correlation coefficient, it was concluded that changes in the temperature of the reaction medium have the greatest effect on the yield of formic acid. It was also found that the parameters of the model are statistically significant.
Keywords: *methanol, formic acid, catalytic oxidation, regression equation, pair correlation.*

INTRODUCTION

An analysis of the patent and technical literature containing information about the named process indicates the absence of an efficient and cost-effective industrial process technology. Currently, there are two main methods of industrial production of formic acid: hydrolysis of methyl formate and hydrolysis of formamide. The disadvantage of these liquid-phase processes is the multistage nature, capital and energy costs, the formation of a number of by-products, pollution of the atmosphere and wastewater. However, all these methods are associated with very significant costs and consumption of valuable raw materials. The world demand for the production of formic acid is increasing every year. In this regard, the efforts of researchers working in this area are aimed at the development of effective highly active catalysts, the conjugation of technological stages, the creation of a cost-effective technology for the production of formic acid [1-6]. For a number of years, the Institute of Catalysis and Inorganic Chemistry has been carrying out original work on the study of gas-phase processes of oxidation of aliphatic alcohols on modified natural zeolites. The distinctive features of the processes under study are high yields of target products with high selectivity, as well as the simplicity of their technological design, which create good prospects for the widespread introduction of these processes into industry. Automation and optimal organization of experimental research with the use of PC contribute to the acceleration of the time and reduction in the development of new chemical-technological processes.

EXPERIMENTAL PART

As a result of systematic laboratory studies, an effective Pd^{+2} was developed

containing a modified zeolite catalyst, with the use of which experiments on the production of formic acid by gas-phase oxidation of methanol were carried out. This process is characterized by high yields of the target product with high selectivity, as well as simplicity of technological design, which creates a good prospect for its introduction into industry.

The experiments were carried out on a unique setup consisting of two parts: catalytic and analytical. The catalytic unit consisted of a U-shaped reactor with a fixed catalyst bed, with a volume of 6 cm^3. The reactor was placed in an air electric furnace, the heating of which was measured with a thermocouple and recorded using an electronic controller KVP-1-503. Vapors of raw materials entered one of the legs of the reactor to the catalyst bed. In the middle of the catalyst bed, it was measured with a thermocouple and recorded with a potentiometer. The thermostated cabinet was equipped with an electric spiral and a fan. A stable temperature in it was maintained using a contact thermometer connected to the MKU-48 relay, the feed was supplied using a saturator. The analytical part consisted of an X LKhM-80 MD with a thermal conductivity detector directly connected to the catalytic unit. The analysis of the reaction mixture is carried out every 30 minutes. Direct coupling of the catalytic unit to the analytical part increased the accuracy and facilitated the analysis by eliminating possible losses during the collection of reaction products.

Below are the experimental data carried out on a laboratory-scale plant. The following technological parameters were taken as controllable parameters, the values of which vary in the specified intervals 85≤T125°C, 850≤V≤3250h^{-1}, 0,13≤P_{O_2}≤0,6 atm, 0,09≤P_{CH_3OH}≤0,43atm, where T – temperature, V - volume speed, P_{CH_3OH} - partial pressure of methanol, P_{O_2} partial pressure of oxygen.

The experimental results are shown in table 1.

Table 1

Experimental results carried out on a laboratory-scale plant

№	T, ^{0}C	P_{CH_3OH}, *atm*	P_{O_2}, *atm*	V, h^{-1}	Y, Formic acid yield, mg/g
1	2	3	4	5	6
1	70	0.07	0.1	850	23,5
2	70	0.07	0.1	3250	20
3	70	0.07	0.7	850	23,8
4	70	0.07	0.7	3250	19,3
5	70	0.47	0.1	850	24,5
6	70	0.47	0.1	3250	20
7	70	0.47	0.7	850	28
8	70	0.47	0.7	3250	23
9	130	0.07	0.1	850	29,5
10	130	0.07	0.1	3250	23
11	130	0.07	0.7	850	31,5
12	130	0.07	0.7	3250	26,8
13	130	0.47	0.1	850	32,6
14	130	0.47	0.1	3250	26,3
15	130	0.47	0.7	850	36
16	130	0.47	0.7	3250	30,5

ISNN: print 2663-7006; online 2709-2666

RESULTS AND DISCUSSION

Using the well-known technique [7], we made regression equations for this process. The multiple regression equation is presented as:

$Y = f(\beta, X) + \varepsilon$, where $X = X(X_1, X_2, ..., X_m)$ - vector of independent variables; β - vector of parameters (to be determined); ε - deviation; Y - dependent variable. The theoretical linear multiple regression equation is:

$Y = \beta_0 + \beta_1 X_1 + \beta_2 X_2 + ... + \beta_m X_m + \varepsilon$, β_0 - an intercept that determines the value of Y, in the case when all explanatory variables X_j are equal to 0.

The empirical equation of multiple regression of the process of catalytic gas-phase oxidation of methanol can be represented as:

$$Y = b_0 + b_1 X_1 + b_2 X_2 + ... + b_m X_m + e,$$

where b_0, b_1, ..., b_m - theoretical estimates β_0, β_1, β_2, ..., β_m regression coefficients (empirical coefficients of the regression equation); e - deviation estimate ε.

To estimate the parameters of the multiple regression equation, the method of least squares (OLS) was used. According to this method, the vector s is obtained from the expression:

$$s = (X^T X)^{-1} X^T Y$$

The resulting regression equation has the form:

$$Y = 15.5893 + 0.1127 X_1 + 7.3438 X_2 + 4.0625 X_3 - 0.00211 X_4$$

Next, we carried out a statistical analysis of the obtained regression equation: checking the significance of the equation and its coefficients, studying the absolute and relative errors of approximation.

For an unbiased estimate of variance, the following calculations were performed:

Table 2

Calculation results for the unbiased variance estimate

Y	$Y(x)$	$\varepsilon = Y - Y(x)$	ε^2	$(Y - Ycp)^2$	|ε : Y|
23.5	22.606	0.894	0.799	6.989	0.038
20	17.544	2.456	6.033	37.746	0.123
23.8	25.044	-1.244	1.547	5.493	0.0523
19.3	19.981	-0.681	0.464	46.837	0.0353
24.5	25.544	-1.044	1.089	2.702	0.0426
20	20.481	-0.481	0.232	37.746	0.0241
28	27.981	0.0187	0.000352	3.446	0.00067
23	22.919	0.0812	0.0066	9.883	0.00353
29.5	29.369	0.131	0.0172	11.264	0.00445
23	24.306	-1.306	1.706	9.883	0.0568
31.5	31.806	-0.306	0.0938	28.689	0.00972
26.8	26.744	0.0562	0.00316	0.431	0.0021
32.6	32.306	0.294	0.0863	41.683	0.00901
26.3	27.244	-0.944	0.891	0.0244	0.0359
36	34.744	1.256	1.578	97.146	0.0349
30.5	29.681	0.819	0.67	18.977	0.0268
			∑=15.217	∑=358.939	∑=0.499

Where ε = Y - Y(x) = Y - X*s unbiased error or absolute error of approximation. The mean approximation error is

$$A = \frac{\sum|\varepsilon Y|}{n} \times 100\% = \frac{0.499}{16} \times 100\% = 3.12\%.$$

The multiple correlation coefficient is:

$$R = \sqrt{1 - \frac{0.0424}{1}} = 0.9786.$$

This means that the relationship between trait Y (formic acid yield) and X_i factors is strong.

We also checked the significance of the parameters of the multiple regression equation. The statistical significance of the regression coefficients b_0 , b_1 , b_2 , b_3, b_4 is confirmed.

The statistical significance of the equation was tested using the coefficient of determination and Fisher's test. It was also found that the parameters of the model are statistically significant.

$$r_{xy} = \frac{\overline{xy} - \bar{x}\bar{y}}{s(x)s(y)}$$

$$r_{yx_1} = \frac{2715.813 - 100 \times 26.144}{30 \times 4.736} = 0.714,\ r_{yx_2} = 0.31,\ r_{yx_3} = 0.257,\ r_{yx_4} = -0.534.$$

$$r_{x_1x_2} = 0,\ r_{x_1x_3} = 0,\ r_{x_1x_4} = 0,\ r_{x_2x_3} = 0,\ r_{x_2x_4} = 0,\ r_{x_3x_4} = 0.$$

Fisher's F-test was used to assess the significance of the regression equation.

From the Fisher-Snedokkor distribution table, the critical value of the F-criterion (F_{cr}) was found at a significance level = 0.05 and two numbers of degrees of freedom k_1 = m and k_2 = n-m-1. Fisher's criterion was calculated by the formula

$$R^2 = 1 - \frac{s_e^2}{\sum(y_i - \bar{y})^2} = 1 - \frac{15.217}{358.94} = 0.9576.$$

$$F = \frac{R^2}{1 - R^2} \times \frac{n - m - 1}{m} = \frac{0.9576}{1 - 0.9576} \times \frac{16 - 4 - 1}{4} = 62.118$$

Table value for degrees of freedom k_1 = 4 and k_2 = n-m-1 = 16 - 4 - 1 = 11, F_{cr} (4; 11) = 3.36. Since the actual value is F > F_{cr}, the coefficient of determination is statistically significant and the regression equation is statistically reliable (i.e., the coefficients b_i are jointly significant).

CONCLUSION

As a result of calculations, a multiple regression equation was obtained for the process of catalytic gas-phase oxidation of methanol to formic acid. Statistical analysis of the obtained regression equation was carried out: checking the significance of the equation and its coefficients, studying the absolute and relative errors of approximation. According to the maximum coefficient r_{yx_1}=0.714, we conclude that changes in the temperature of the reaction medium have the greatest effect on the yield of formic acid. The statistical significance of the equation was tested using the coefficient of determination and Fisher's test. It was also found that the parameters of the model are statistically significant.

ISNN: print 2663-7006; online 2709-2666

REFERENCES

1. Aliev A.M., Medzhidova S.M., Shakhtakhtinsky T.N., Guseinov K.A. Vapor-phase oxidation of methyl alcohol to formic acid on a modified zeolite catalyst // Journal of Chemistry and Chemical Technology, Ivanova. 2010, Vol.53, Issue 6, pp. 95-101
2. Aliyev A.M., Mammadov E.M., Aliyev Q.S., Abasova U.A. Research process gas-phase oxidation of methanol on the modified zeolite on a pilot plant. XX International Conference on Chemical Reactors "CHEMREAKTOR-20". Luxemburq. 2012, pp.233-234
3. Aliyev A.M., Mammadov E.M., Aliyev Q.S., Abasova U.A. Optimization and development technological scheme of production formic acid of methanol oxidation on a modified zeolite catalyst. 1st International chemistry and chemistry and chemical engineering conference. Abstracts & Proceedings. Baku 2013, pp. 993-997
4. Andrushkevich T., Popova G., Danilevich E., Zolotarskii I., Nakrokhin V., Nikoro T.V., A new gas-phase method for formic acid production: Tests on a pilot plant. Journal Catalysis in Industry. 2014, Vol. 6, pp.17–24
5. Yeo B.R., Pudge G.J., Bugler K.G., Rushby A.V., Kondrat S., Bartley J., Golunski S., Taylor S.H., Gibson E., Wells P.P., Brookes, C. The Surface of Iron Molybdate Catalysts Used for the Selective Oxidation of Methanol.Surface Science, 648:2018, pp.163-169
6. Peyrovi1 M.H., Parsafard N., Hasanpour H. Catalytic Study of the Partial Oxidation Reaction of Methanol to Formaldehyde in the Vapor Phase.Bulletin of Chemical Reaction Engineering & Catalysis. 13 (3) 2018, pp.520-528
7. Norman Draper, Harry Smith. Applied Regression Analysis, 3-th edition. John Wiley & Sons. 1998, 736 p

ИССЛЕДОВАНИЯ ЗАКОНОМЕРНОСТЕЙ ПРОЦЕССА КАТАЛИТИЧЕСКОГО ГАЗОФАЗНОГО ОКИСЛЕНИЯ МЕТАНОЛА В МУРАВЬИНУЮ КИСЛОТУ

Г.С.Алиев[1], У.А.Абасова[2], Х.М.Рустамли[1]
[1]Институт Катализа и Неорганической химии им.акад. М.Нагиева НАНА
[2]Азербайджанская Государственная Нефтяная Академия
chemproblem@mail.ru

В статье приведены результаты исследования некоторых закономерностей процесса каталитического окисления в газовой фазе метанола в муравьиную кислоту. Для этого сначала были проведены эксперименты при узловых значениях исходных параметров, а затем было создано множественное регрессионное уравнение для процесса, рассчитаны коэффициенты уравнения и определена их значимость. Проверена адекватность уравнения и идентифицирован более чувствительный параметр. С использованием критерия Фишера была доказана статистическая значимость уравнения. Проведены статистический анализ полученного уравнения регрессии: проверке значимости уравнения и его коэффициентов, исследованию абсолютных и относительных ошибок аппроксимации. Также вычислены парные показатели корреляции коэффициентов уравнения. По максимальному коэффициенту корреляции сделан вывод, что наибольшее влияние на выход муравьиной кислоты оказывает изменение температуры реакционный среды. Установлено также, что параметры модели статистически значимы.

Ключевые слова: *метанол, муравьиная кислота, каталитическое окисление, уравнение регрессии, парная корреляция.*

METANOLUN QARIŞQA TURŞUSUNA QAZ FAZADA KATALITIK OKSIDLƏŞMƏSININ QANUNAUYĞUNLUQLARININ TƏDQİQİ

Q.S.[1]Əliyev , Ü.Ə.[2]Abasova , X.M.[1] Rüstəmli [1]
[1]AMEA Akademik Murtuza Nağıyev adına Kataliz və Qeyri-üzvi Kimya İnstitutu
[2] Azərbaycan Dövlət Neft və Sənaye Universiteti
chemproblem@mail.ru

Məqalədə metanolun qaz fazada qarışqa turşusuna katalitik oksidləşməsi prosesinin bəzi qanunauyğunluqlarının öyrənilməsindən bəhs edilir. Bu məqsədlə əvvəlcə ilkin parametrlərin düyün nöqtələrində təcrübələr aparılmış, sonra isə prosesin çoxparametrli reqressiya tənliyi qurulub, tənliyinin əmsalları hesablanıb və onların əhəmiyyətlilik dərəcəsi təyin edilib. Reqressiya tənliyinin adekvatlığı yoxlanılıb, daha həssas parametr müəyyənləşdirilib. Tənliyin parametrlərinin korrelyasiya məsələləri araşdırılıb, Fişer meyarından istifadə edilərək tənliyin statistik əhəmiyyətliliyi sübut olunub. Həmçinin tənliyin əmsallarının cüt-cüt korrelyasiya dərəcələri hesablanıb. Korrelyasiya əmsallarının maksimal qiymətinə görə belə bir nəticəyə gəlmək olar ki, qarışqa turşusunun çıxımına ən böyük təsiri reaksiya mühitinin temperaturu göstərir. Model parametrlərinin statistik cəhətdən əhəmiyyətli olduğu da müəyyən edilib.
Açar sözlər. *metanol, qarışqa turşusu, katalitik oksidləşmə, çoxparametrli reqressiya tənliyi, korrelyasiya.*

ISNN: print 2663-7006; online 2709-2666

AJCN, Vol 3, No. 3, 2021, pp. 32-37

UDC: 543.1:541.3:547.442

SPECTROPHOTOMETRIC METHOD FOR STUDYING THE COMPLEX FORMATION OF COPPER (II) WITH BIS [3- (CHLOROPHENYLAZO-PENTADIENE-2,4) ETHYLENEDIIMINE] IN THE PRESENCE OF ANTIPYRINE AND 4-AMINOANTYPYRINE

F.O.Mamedova
Ganja State University
ciraqov@mail.ru

The complex formation of copper (II) with bis [3- (chlorophenylazo-pentadiene-2,4) ethylenediimine] in the presence of antipyrine and 4-aminoantipyrine was studied by spectrophotometric method. It was found that in binary compounds (Cu (II) -R) the yield of the complex is maximum at pH = 4, the optimal wavelength is 437 nm. In the presence of antipyrine (Ant) and 4-aminoantipyrine (4-Ant), three-component compounds Cu-R-Ant and Cu-R-4-Ant are formed. In these complexes, the optimal conditions for complex formation are pH_{opt} = 3.2, λ_{opt} = 444 nm; pH_{opt} = 3.08; λ_{max} = 447 nm. The ratio of the reacting components in the binary complex is 1: 1, in the mixed-ligand 1: 1: 1. The influence of foreign ions and masking substances on the determination of Cu (II) has been studied.

Keywords: *Copper(II), spectrophotometric method, bis-[3- (chlorophenylazo-pentadiene-2,4) ethylenediimine, antipyrine, 4-aminoantipyrine.*

INTRODUCTION

It is known that copper and its alloys are widely used for the production of wire, copper pipes, jewelry, glass dyes, etc. [1, 2]. Large amounts of copper are very harmful to the body. Copper poisoning leads to severe consequences - anemia, liver disease. Lack of copper in the body is observed with hair loss, changes in skin color [3-5].

The prevalence of copper in various fields of science and technology, in nature, in living organisms, put forward the need for strict control of the copper content in objects.

It is known in the literature that azo-sulfur-containing reagents are usually used for the photometric determination of copper with organic reagents [6]. Among such reagents, carbazones, thiosemicarbazones, diaminopyridine derivatives, β-diketones. Azocompound ketones are often used, which form the most stable chelates [7-14]. It should also be noted that recently, to improve the parameters of analytical reactions in spectrophotometric analysis, mixed-ligand complexes have been used [15].

Therefore, the study of the complexation of Cu (II) with bis [3- (chlorophenylazo-pentadiene-2,4) ethylenediimine] in the presence of antipyrine and 4-aminoantipyrine is considered highly relevant.

EXPERIMENTAL PART

Reagents, solutions and equipment. The reagent bis [3- (chlorophenylazo-pentadiene-2,4) ethylenediimine] was synthesized earlier according to the method [16]. A stock solution of $1 \cdot 10^{-1}$ M copper was prepared by dissolving an accurate weighed sample of copper of analytical grade in concentrated hydrochloric acid when heated [17]. Working solutions with a lower copper content were prepared by diluting the initial solution with distilled water. We used $1 \cdot 10^{-3}$ M solutions of the reagent and $1 \cdot 10^{-3}$ M of antipyrine and 4-aminoantipyrine. All reagents are highly soluble in ethanol.

The absorbances of the solutions was measured on a Lambda-40

spectrophotometer (PerkinElmer) and a KFK-2 photocolorimeter in a cuvette with a layer thickness of 1 cm. The pH of the solution was monitored using a pHS-25 ionomer calibrated with standard buffer solutions.

RESULTS AND DISCUSSION

We have previously found that the reagent used forms a colored complex compound. The maximum yield of the complex is observed at pH=4, the optimal wavelength is 437 nm. Under these conditions, the reagent has a maximum light absorption at 341 nm. When antipyrine and 4-aminoantipyrine interact, three-component compounds Cu-R-Ant and Cu-R-4-Ant are formed. The maximum light absorption of mixed-ligand complexes of Cu (II) is shifted bathochromically relative to the absorption maximum of the binary complex λ_{max}=452 and 464 nm, respectively. The optimal pH of complexation shifts to the acidic region: 3.5 and 3.0, respectively (fig. 1).

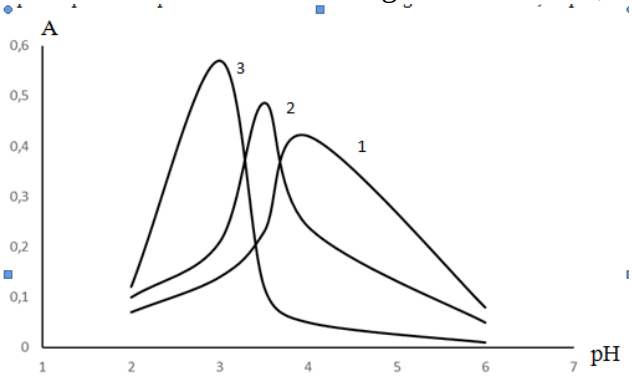

Fig. 1. Dependence of the optical density of solutions of copper (II) complexes on pH 1.Cu (II) -R, 2.Cu (II) -R-amine, 3.Cu (II) -R-4-aminoantipyrine

The effect of the concentration of antipyrine and 4-aminoantipyrine on complexation was studied. The maximum yield of Cu-R complexes at optimal pH is $8 \cdot 10^{-5}$ M R, Cu-R-Ant $8 \cdot 10^{-5}$ M R and $7.2 \cdot 10^{-5}$ M Ant; Cu-R-4-Ant $8 \cdot 10^{-5}$ M R and $6 \cdot 10^{-5}$ M 4-Ant, respectively.

Homogeneous and mixed ligand complexes are formed after mixing solutions. So if the binary complex is stable for 2 hours and when heated to 600 ^{0}C, then mixed-ligands - for more than a day and when heated to 80 ^{0}C. By the method of isomolar series, the relative yield of the Starick-Barbanel and the shift of equilibrium, the ratios of the reactants were established, which are 1: 2, 1: 2: 2 [18]. The Astakhov`s method was used to determine the number of protons displaced during complexation (equal to 2). Given these data, the following complexation scheme can be written:

$$Cu+2H_3R \rightarrow Cu(H_2R)_2+2H^+$$
$$Cu(H_2R)_2+2Ant \rightarrow Cu(H_2R)_2(Ant)_2$$

The molar coefficients of light absorption at λ_{opt} of the complexes Cu-R, Cu-R-Ant, Cu-R-4-Ant are 4380, 4860 and 5570, respectively. The copper complex obeys Beer's law in the range 2.0-2.8 mg/ml, 1.8 -2.56 mg/ml (Cu-R-AntCu-R-4-Ant).

The effect of foreign ions and masking substances on the complexation of Cu (II) has been studied. As can be seen from these data, the selectivity of the determination of

ISNN: print 2663-7006; online 2709-2666

Cu (II) in the presence of hydrophobic amines is significant. Therefore, the developed method for the photometric determination of copper (II) in the form of a mixed-ligand complex of Cu-R-4-Ant can be used to determine its in complex objects.

Construction of a calibration graph. 1.8-2.56 mg/ml Cu (II) was injected into a 25 ml volumetric flask, 2.0 ml of $1 \cdot 10^{-3}$ M solution was added to the reagents, 1.3 ml of $1 \cdot 10^{-3}$ M solution of 4-aminoantipyrine was brought to labels with buffer solution pH = 3. The absorbances of the solution was measured on a KFK-2 instrument at 440 nm in a cuvette with a layer thickness of 1 cm, relative to a blank solution (R-4-Ant) prepared under similar conditions. Based on the data obtained, a calibration graph was constructed and the standard deviation and the confidence interval of the determined concentrations were calculated for each point. The average standard deviation does not exceed 0.04.

A graph of the dependence of the light absorption of Cu (II) complexes on the background of the control experiment on pH was plotted (fig. 2).

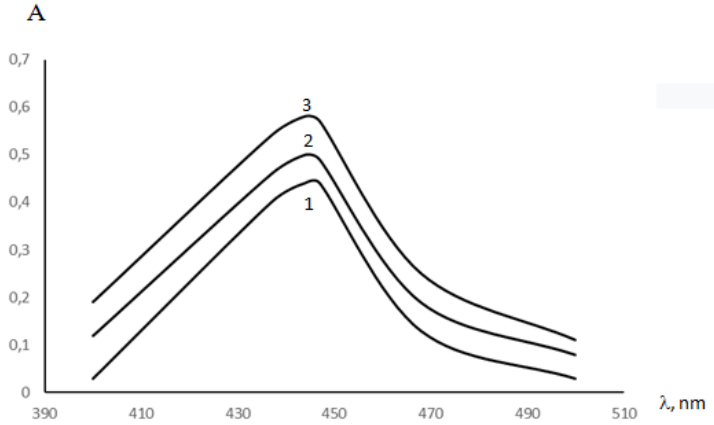

Fig. 2 Absorption spectra of a solution of the reagent and its complexes with copper (II) in the presence and absence of amine 4-aminoantipyrine at the optimum pH of the corresponding systems: 1.Cu (II) -R, 2.Cu (II) -R-amine, 3.Cu (II) -R-4-aminoantipyrine

Determination of copper (II) in the composition of the Akstafa river of Gazakh region. Photometric determination of the concentration of the investigated metal in the sample was used in the practice of chemical analysis of "Method of additions". This method allows you to create the same conditions for the photometry of the test and standard (with an addition) colored solutions, therefore it is advisable to use it for the determination of small amounts of various elements in the presence of large amounts of foreign substances in the analysis of saline solutions.Based on the studies carried out to optimize the conditions for the direct photometric determination of copper (II) in real objects and to obtain an optimal estimate of the selectivity of their determination in individual and complex mixtures, an express photometric method for analyzing natural waters to determine the content of the metals under study was developed. The water samples selected for the study were systems of complex composition, containing, in addition to mineral macrocomponents, also various cations of heavy and toxic metals. Sampling for the determination of copper (II) R-4-Ant by the method in glassware of various brands.

Method for the determination of copper in river water. A 1.0 L sample taken from the Akstafa River was placed in a heat-resistant glass with a capacity of 2 L, 10-12

ml of a 1.0 N nitric acid solution was added, heated in a sand bath, and evaporated until wet salts were formed. The precipitate was dissolved in 10.0 ml of distilled water, quantitatively filtered in a beaker with a capacity of 50.0 ml. The solution was transferred into a 25.0 ml flask, standard solutions of copper (II), 2 ml of $1 \cdot 10^{-3}$ M R and 1.3 ml of $1 \cdot 10^{-3}$ M 4-aminoantipyrine were added (0.5-2.5 mg) and up to the mark with a buffer solution of pH 3.0. In order to improve the selectivity of the method, the following masking agents were added: 8.0 ml of F^- and 2.0 ml of OH^- to bind ions of manganese, iron, zinc, aluminum, arsenic. The absorbance was measured on KFK-2, l = 1 sm, λ=440 nm relative to the R-4-Antpo solution. Based on the data obtained, the concentration of copper (II) was established - 0.003 mg/ml. The accuracy of the analysis results has been proven by the atomic absorption method.

CONCLUSION

Complex compound of Cu(II) with organic reagent synthesized on the basis of acetylacetone has been investigated by spectrophotometric method and method of determimation of Cu(II) ions developed. This method was used for determination of copper (II) ions in the river waters.

REFERENCES

1. Nekrasov B.V. Fundamentals of General Chemistry. 1973, Vol. 2, 688 p
2. Akhmedov N.S.General and inorganic chemistry, Ed. "Academy".2001, 743 p
3. Pichishcheva N.B., Shknaev K.Yu. The use of luminescence for the determination of low copper contents. Journal of Analytical Chemistry. 2008, Vol. 63, №3, pp. 454-466
4. Semenova E., Kunina M., Stuklov N. The role of copper and manganese in iron metabolism, Zh. Pharmacology 12, 2013, pp. 47-52
5. Rakhmedova A.A. Study of the biological activity of copper nanoparticles differing in dispersion and phase composition. Abstract of Candidate's Dissertation in Biological Sciences 02., 2011, 25 p
6. Podchaynova V.N., Simonova L.N. Analytical chemistry of copper. Charise S.E., El-Sharly R.M., Almy A.A., El-Shahahawi M.S. Spectrophotometric determination of copper(II) in natural waters, vitamins and certified steel scrap samples using acetophenone-p-chlorophenylthiosemicarbazone. Journal of the Iranian Chemical Society. Vol.3, №2, 2006, pp. 140-150
7. Admasu D., Reddy D.N. & Mekonnen K.N. Spectrophotometric determination of Cu(II) in soil and vegetable samples collected from Abraha Atsbeha, Tigray, Ethiopia using heterocyclic thiosemicarbazone. Springer Plus. 2016,1169 p
8. Sarma L.S., Kumar J.R., Reddy K.J., Reddy A.V. Development of an extractive spectrophotometric method for the determination of copper(II) in leafy vegetable and pharmaceutical samples using pyridoxal-4-phenyl-3-thiosemicarbazone. J Agric Food Chem. 2005,Vol.53, №14, pp.5492-5498
9. Babayeva K., Serkan Demir, Müberra Andac. A novel spectrophotometric method for the determination of copper ion by using a salophen ligand, N,N′-disalicylidene-2,3-diaminopyridine. Journal of Taibah University for Science. 2017, №5, pp. 808-814
10. Dayou F., Dong Y., Spectrophotometric determination of trace copper in water samples with thiomichlersketone. Spectrochim. Acta A. 2007, Vol.66,№ 2,

ISNN: print 2663-7006; online 2709-2666

pp. 434-437
11. Ramanjaneyulu G., Reddy P.R., Reddy V.K., Reddy T.S. Direct and derivative spectrophotometric determination of copper(II) with 5-bromosalicylaldehyde thiosemicarbazone. Open Anal. Chem. J. 2008, №2, pp. 78-82
12. Turabov N.T., Emmurzaev I.Sh., Godzhaev Zh.N. Some analytical characteristics of the reaction of complexation of copper ions with a new oxyazoreagent. Journal V. MUUZ. Tashkent. 2012, № 13, pp. 29-34
13. Makhmudov K.T. Analytical study of the use of copper complexes formed with azo derivatives of β-diketones. Dis. Cand. chem. sciences. Baku 2005, 214 p
14. Pilipenko A.T., Tananaiko M.M. Mixed-ligand complexes and their application in analytical chemistry. Chemistry. 1983, 221 p
15. Busev A.I. Synthesis of new organic reagents for inorganic analysis M: MGU. 1972, 245 p
16. Korostelev P.P. Preparation of solutions for chemical analytical work M: Nauka. 1964, 261 p
17. Bulatov M.I., Kalinkin N.P. Practical guide to photometric methods of analysis L: Chemistry. 1986, 432 p

СПЕКТРОФОТОМЕТРИЧЕСКИЙ МЕТОД ИЗУЧЕНИЯ КОМПЛЕКСООБРАЗОВАНИЯ МЕДИ(II)С БИС[3-(ХЛОРФЕНИЛАЗО-ПЕНТАДИЕН-2,4)ЭТИЛЕНДИИМИНОМ] В ПРИСУТСТВИИ АНТИПИРИНА И 4-АМИНОАНТИПИРИНА

Ф.О.Мамедова
Гянджинский Государственный Университет
ciraqov@mail.ru

Спектрофотометрическим методом изучено комплексообразование меди(II) с бис[3-(хлорфенилазо-пентадиен-2,4)этилендиимином] в присутствии антипирина и 4-аминоантипирина. Установлено, что в бинарных соединениях (Cu(II)-R) выход комплекса максимален при pH=4, оптимальная длина волны составляет 437 нм. В присутствии антипирина (Ant) и 4-аминоантипирина (4-Ant) образуются трехкомпонентные соединения Cu-R-Ant и Cu-R-4-Ant . В данных комплексах оптимальные условия комплесообразования $pH_{опт}$=3,2, $\lambda_{опт}$=444 нм; $pH_{опт}$=3,08; $\lambda_{мах}$=447 нм. Соотношение реагирующих компонентов в бинарном комплексе 1:1, в разнолигандном 1:1:1. Изучено влияние посторонних ионов и маскирующих веществ на определениеCu(II).
Ключевые слова: *медь(II), спектрофотометрический метод, бис[3-(хлорфенилазо-пентадиен-2,4)этилендиимин], антипирин, 4-аминоантипирин.*

MİS(II)-nin BİS [3- (XLORFENİLAZO PENTADİYEN-2,4) ETİLENDİİMİNLƏ]ANTİPİRİN VƏ 4-AMİNOANTİPİRİN İŞTİRAKINDA KOMPLEKSƏMƏLƏGƏLMƏSİNİN SPEKTROFOTOMETRİK METODLA ÖYRƏNİLMƏSİ

F.O.Məmmədova
Gəncə Dövlət Universiteti
ciraqov@mail.ru

Antipirin və 4-aminoantipirin iştirakında misin(II) bis [3-(xlorfenilazo-pentadiyen-2,4) etilendiimin] ilə əmələ gətirdiyi kompleks birləşməsi spektrofotometrik olaraq tədqiq edilmişdir.

Binar birləşmələrdə (Cu(II) -R) kompleksin çıxımının pH = 4-də maksimum olduğu, optimal dalğa uzunluğunun 437 nm olduğu aşkar edildi. Antipirin (Ant) və 4-aminoantipirin (4-Ant) iştirakı ilə üç komponentli Cu-R-Ant və Cu-R-4-Ant birləşmələri əmələ gəlir. Bu komplekslərdə kompleks əmələ gəlmənin optimal şəraitləri pH_{opt} = 3.2, λ_{opt} = 444 nm; pH_{opt} = 3.08, λ_{max} = 447 nm. Binar kompleksdəki reaksiyaya daxil olan komponentlərin nisbəti 1:1, qarışıq ligandda 1:1:1. Kənar ionların və pərdələyici maddələrin Cu(II) təyininə təsiri öyrənilmişdir.

Açar sözlər: *mis(II), spektrofotometrik metod, bis [3- (xlorfenilazo pentadiyen-2,4) etilendiimin], antipirin, 4-aminoantipirin.*

ISNN: print 2663-7006; online 2709-2666

AJCN, Vol 3, No. 3, 2021, pp. 38-45

UDC:66.074.5

INVESTIGATION OF THE GAS MIXTURE ADSORPTION PROCESS IN A FIXED LAYER OF THE NaX ADSORBENT

A.S. Bayramova
Azerbaijan State Oil and Industry University
aygun.b74@mail.ru

The paper describes a 4-adsorbent installation for cleaning gas mixtures from H_2S, CO_2 and NO_2 with zeolite. The lower and upper limits of the condensate level in the separator were controlled by electric contact pressure gauges, and the pressure was recorded on the operator panel. The number of adsorbers is 4, the height of the fixed zeolite layer is 3.6 m. Long-term operation of the adsorption unit under real operating conditions has shown that the temperature of zeolite regeneration largely depends on the quality of the gas entering the adsorption unit. As can be seen, the desorption of carbon dioxide is completed at the beginning, then hydrogen sulfide, and at the end - moisture vapor, and the time for complete desorption of all adsorbed components is limited by internal diffusion inhibition of the sorbed components. The greatest desorption time, as expected, is due to moisture vapors. It has been experimentally established that when heated with hot gas at the maximum permissible speed, the time for complete desorption of moisture is 150-160 minutes. For practical calculations, the time required for complete dehydration of the zeolite is taken at least 3 hours, which is confirmed experimentally.

Keywords: *adsorption, synthetic zeolite NaX, fixed adsorbent layer, gas mixture, desorbed substances.*

INTRODUCTION

In an experimental study, the curves of the adsorption isotherm of CO_2, H_2S and NO_2 from gas mixtures were studied. The adsorption isotherms are determined in NaX zeolite. The results of studies of the adsorption capacity of various adsorbents for CO_2, H_2S and NO_2 from gas mixtures under identical conditions are obtained. The predominant use of NaX zeolite for sorption separation of CO_2, H_2S and NO_2 was revealed. The calculation of industrial adsorbers and their number have important practical values. Therefore, the dynamic activity of synthetic zeolite NaX and the rate of gas desorption are calculated from experimental data. Also, the regeneration of zeolite should correspond to experimental data.

When studying the effect of the concentration of H_2S and CO_2 on their adsorption by zeolite, it was found that the component composition of substances adsorbed by zeolite strongly depends on the amount of H_2S/CO_2 in the gas. With a change in the concentration of hydrogen sulfide in the crude gas from 0.025 to 0.8% by volume, the percentage of hydrogen sulfide in the adsorbate increased from 26 to 60%, while the proportion of adsorbed CO_2 remained almost unchanged. It was also found that during the regeneration of zeolite, the concentration of hydrogen sulfide in the raw gas was equal to 0.05% of its (hydrogen sulfide) percentage in the regeneration gas was in the range of 0.2-2.5%, then with an increase in the amount of H_2S in gas mixtures to 3%, its concentration in the regeneration gas under identical conditions increases to 15% by volume.

EXPERIMENTAL PART

It was found experimentally that at least 3 hours of time is required for complete desorption of moisture. After establishing the optimal parameters of the processes of adsorption, desorption and regeneration, long-term experiments were carried out on the separation of gas mixtures from H_2S by an adsorbent in fishing conditions. The results of the experiments are presented in table 1.

During the experiments, the grinding of zeolite, the formation and entrainment of zeolite dust were observed. The gas consumption for regeneration was 4-6% of the total amount of purified gas. Natural gas with a hydrogen sulfide content of up to 1000 mg/m^3 was supplied to the input thread block, where a certain gas flow rate was set with the help of regulating fittings. The gas pressure before the fitting fluctuated in the intervals of 5.2-7.1 atm., and after 20-25^{0}C.

Table 1

Experimental results obtained in the pilot plant Q=10000nm^3/day [6];
P_{ads}=6,0 MPa, P_{des}=5,5 MPa, t_{ads}=15-20^{0}C, t_{ads}=325-360^{0}C

Zeolites	The amount of H_2S in gas mixtures, mg/m^3		Temperature (dew point), ^{0}C		Pre-slip adsorption	Degree of desorption, %
	Source code	Cleared	Source code	Cleared		
NaA	600	2,6	+16	-64	2,2	87,0
	800	3,2	+19	-62	2,5	91,0
	1400	3,8	+ 15	-62	2,9	89,0
CaA	600	4,2	+ 16	-57	3,5	93,0
	800	4,7	+ 20	-56	3,7	92,0
	1400	5,7	+15	-59	4,1	91,0
NaX	600	3,5	+16	-53	4,6	95,0
	800	4,0	+19	-51	5,2	94,0
	1400	5,4	+17	-50	6,9	95,0

After the block of input threads, the gas entered the horizontal separator C-1, where it was freed from mechanical impurities and droplet liquid and sent to the zeolite purification unit [1].

The lower and upper limits of the condensate level in the separator were controlled by electric contact pressure gauges, and the pressure was recorded on the operator panel.

The number of adsorbers is 4, the height of the fixed zeolite layer is 3.6 m.

When gas is passed through a fixed layer of the adsorber zeolite, it is simultaneously dried and purified from hydrogen sulfide. At this time, desorption occurs in the second adsorbent, and in the third, cooling of the adsorbent and in the fourth, regeneration of the adsorbent.

The end of the adsorption process was monitored continuously by an automatic gas analyzer " FGC -16". Thus, the gas separation process was continuous. The valves were switched manually (this stage will be fully automated in the future). The pressure in the adsorbers was monitored locally and recorded on the control panel in the operator room, the temperature at the inlet and outlet of the adsorbers was measured by resistance thermometers with a record on the control panel in the operator room.

For continuous monitoring of the number of gas mixtures on the commercial gas line, a device for determining the content of H_2S in the gas mixture (the FGC-16 gas

ISNN: print 2663-7006; online 2709-2666

analyzer with a scale of 0.3 mg/m^3) and a moisture meter of the KIVGDI brand were installed. A part of the commercial gas of 0.36-2.8 MPa is fed to the adsorber, which is in the cooling stage, where the gas, cooling the zeolite, is heated to a temperature of 100-150^{0}C and fed to the furnace P-1, from where it enters the adsorber apparatus, which is in the desorption mode, at a temperature of 370-400^{0}C. Regeneration gases with desorbate (hydrocarbons, hydrogen sulfide, moisture) are discharged to the torch and burned. The gas flow during cooling and desorption is directed from the bottom up, and during adsorption-from the top down.

To heat the regeneration gas, the dehumidified gas is supplied to the furnace (P-1), reduced by two control valves to a pressure of 0.30 MPa. In cases of an increase (above 0.6 MPa) or a decrease (below 0.03 MPa) of the pressure, an electromagnetic shut - off valve is triggered, which stops the gas supply to the injectors, while sound and light signals are given on the panel in the operator room.

It is possible to periodically measure the flow of gas and condensate for each well. To do this, the gas from the wells enters the measuring separator C-1, where it is released from the drip liquid and mechanical impurities and sent through the flow meter to the purification unit. The condensate is discharged into the E-1 tank by the level controller. The flow rate and pressure in the separator C-1 are regenerated locally [2].

The treated gas mixture is passed through vinicine filters F-1, F-2 and after measurement is sent to the main gas pipeline. A drainage tank (V-25 m^3) is provided for the release of the installation devices.

All gas discharges are distributed through pipes of various diameters: regeneration gases - through a pipe with a diameter of 114 mm, discharges with safety valves - with a diameter of 89 mm, discharges from the purge of plumes - with a diameter of 152 mm, as well as gases from "small" technological tanks and condensate weathering gases are fed to a torch with a diameter of 300 mm, a height of 35 m. Thus, in addition to emergency discharges, the torch receives an adjustable technological discharge of regeneration gases. The torch is placed at a distance of 120 m: from the installation, its performance is designed for maximum discharge from the safety valves.

The absorption capacity of the adsorbent of gas mixtures at the inlet to the adsorber was studied at the installation.

When the gas temperature was reduced to minus 10^{0}C (with the help of the NTS installation), the plant's productivity increased almost three times, reaching 800 thousand m^3 per day.

Regeneration gases are usually supplied from the bottom up, and the purified gas is supplied in the opposite direction. In this case, the most strongly adsorbed substances extracted from the gas stream by a stationary zeolite layer are desorbed and removed from the adsorber without polluting the entire sorption layer. During desorption, the heat of the regenerating gas introduced into the adsorber is first consumed for evaporation of the adsorbed components from the zeolite pores. It is experimentally proved that all adsorbed substances, including moisture, evaporate completely from the pores at a temperature of 260-275^{0}C within 2 hours. After that, the temperature of the layer begins to increase and the surface of the adsorbent is cleaned from the most strongly sorbed polar micro-impurities.

Complete purification of the zeolite surface from polar highly sorbed micro-impurities occurs at a temperature of 310-320^{0}C in the interval of 2.5-3.5 hours. Heating the layer to 320^{0}C and holding it at this temperature for 3 hours is necessary in order to remove from the surface of the adsorbent hard-to-desorb substances that do not

evaporate at a temperature of 275-300^{0}C.

Long-term operation of the adsorption unit under real operating conditions has shown that the temperature of zeolite regeneration largely depends on the quality of the gas entering the adsorption unit. As can be seen, the desorption of carbon dioxide is completed at the beginning, then hydrogen sulfide, and at the end - moisture vapor, and the time for complete desorption of all adsorbed components is limited by internal diffusion inhibition of the sorbed components. The greatest desorption time, as expected, is due to moisture vapors. It has been experimentally established that when heated with hot gas at the maximum permissible speed, the time for complete desorption of moisture is 150-160 minutes. For practical calculations, the time required for complete dehydration of the zeolite is taken at least 3 hours, which is confirmed experimentally.

As can be seen, the maximum concentration of H_2S in desorption gas mixtures is reached at a layer temperature of 155-185^{0}C. The degree of desorption of hydrocarbons adsorbed by zeolite takes an intermediate position between moisture and hydrogen sulfide, and their complete desorption occurs at a layer temperature of 260-270^{0}C.

The data on metal corrosion obtained in the actual operating conditions of the installation show the possibility of manufacturing the installation equipment, supply lines, etc.from 17 GS steel. At the same time, it is necessary to take into account the temperature factor and the frequency of heating and cooling of the adsorbers, as well as the pipelines adjacent to them.

It is known that the main obstacle to the wide implementation of the process of sorption separation of gas components is the difficulty of utilization of zeolite regeneration gases. As already noted, in the proposed process, regeneration gases after the desorption cycle are fed to the oxidation unit, where at a temperature of 270-290^{0}C, direct oxidation of H_2S occurs until pure S is obtained on the surface of the solid catalyst.

Gas regeneration and the process of catalytic oxidation of H_2S is exothermic, which practically does not require heating of the gas entering the catalytic unit.

For the adsorption separation of gas from H_2S by adsorbents, two-chamber, three-chamber, four-chamber, and other gas purification schemes are used in practice. The most widespread are three-dimensional schemes. Depending on the working conditions, different conditions of the saturated zeolite layer are used.

The paper describes a 4-adsorber installation for cleaning gas mixtures from H_2S with zeolite. The purified gas passes through each adsorber in turn until the zeolite is completely saturated. Regeneration of the adsorbent is carried out by feeding sulfur dioxide into the zeolite layer at a temperature of 315^{0}C.

The paper uses a two-bucket scheme. The adsorption time was 3 hours, of which 1 hour was hot; 2 hours was cold.

During the long-term operation of the zeolite, complete purification of the gas mixtures from H_2S was achieved. At the same time, there was no noticeable decrease in the adsorption activity of zeolite.

Zeolites NaX, CaX are used to separate those components that have critical molecular sizes greater than 5Å.

To ensure the continuity of the process of adsorption of gas mixtures along the flow of raw materials and the finished product, four adsorbers are provided in the installation scheme, in each of which one of the stages of the process is carried out for a certain period of time [3].

ISNN: print 2663-7006; online 2709-2666

The paper discusses the adsorption purification of gas mixtures from CO_2, NO_2 and H_2S with zeolites NaX, NaA and CaA.

During the experimental study, the curves of the adsorption isotherm of CO_2, H_2S and NO_2 from gas mixtures were studied. The adsorption isotherms are determined in NAX zeolite. The results of studies of the adsorption capacity of various adsorbents for CO_2, H_2S and NO_2 from gas mixtures under identical conditions are obtained. The predominant use of NaX zeolite for sorption separation of CO_2, H_2S and NO_2 was revealed. The calculation of industrial adsorbers and their number have important practical values. Therefore, the dynamic activity of synthetic zeolite NaX and the rate of gas desorption are calculated from experimental data. Also, the regeneration of zeolite should correspond to experimental data.

A gas mixture of H_2S, CO_2 and NO_2 was passed through a fixed layer of zeolite NaX 1-6 MPa, fed at $20 \div 40^0$C to the upper part of the adsorber. The adsorption of H_2S, CO_2 and NO_2 occurs on a fixed layer of NaX zeolite. The process is carried out in 4 adsorption devices. The first adsorber operates in the mode of adsorption, the second desorption, the third regeneration and the fourth cooling. The speed of natural gas is determined by the hydraulic resistance of the adsorbent layer. The NaX zeolite layer is gradually saturated with undesirable components H_2S, CO_2 and NO_2. After complete saturation of the zeolite, the adsorber is switched to the regeneration mode directly in the adsorber and further, respectively.

The calculation of the adsorption units of the process during the purification of gas mixtures is reduced to determining their amount necessary for the continuous absorption of undesirable components. In our case, these components are H_2S, CO_2 and NO_2. Usually, at the installation at a pressure of 5-6 MPa and a temperature of 20 – 40^0C, approximately 41414 thousand m^3 of natural gas per month is cleaned from various gas fields. And 1380 thousand m^3 of natural gas is purified by the adsorption method per day.

As a result, the amount of H_2S increases at the output of the stationary adsorbent layer. Also at this time, H_2S continues to be absorbed until the moment of the slip. By increasing the time of the stage of the adsorption process, it is possible to achieve the desired degree of carbon dioxide extraction, if H_2S at a high content in the composition of gas mixtures is necessary to carry out the adsorption process under isothermal conditions. It should be noted that from an economic point of view, it is preferable to carry out desulfurization of gas mixtures if the gas mixture contains CO_2: H_2S >2.8. The calculation of industrial adsorbers and their number have important practical values. Therefore, the dynamic activity of synthetic zeolite NaX and the rate of gas desorption are calculated from experimental data. Also, the regeneration of zeolite should correspond to experimental data [4].

RESULTS AND DISCUSSION

Let's determine the number of adsorbers for the adsorption purification of gas mixtures, determine the daily amount of gas mixture entering the adsorption apparatus [3, 4]. The monthly amount of gas mixture coming from the deposits is equal to: 41413 644 thousand m^3.

$$41413.644 \text{ thous.m}^3 \approx 41414 \text{ thous.m}^3$$

$$\frac{41414\ \text{thous.m}^3}{30} = 1380\ \text{thous.m}^3$$

Synthetic zeolite NaX is used as an absorber. Dynamic activity of zeolite NaX a_g =0.036 kg CO_2/kg zeolite. Let's calculate the total amount (H_2S, CO_2 and NO_2) to be adsorbed: these components contain 1.6% by weight.

$$V = 1380\ \text{thous.m}^3 \cdot 0{,}016 = 22080\ \text{m}^3$$

$$m = \rho \cdot V = 0{,}80\ \text{kg/m}^3 \cdot 22080\ \text{м}^3 = 17664\ \text{kg}$$

The amount of undesirable components absorbed within 1 hour (for one adsorption operation) will be:

$$m_o = m \cdot \tau_1/24 = 17664 \cdot 1/24 = 736\ \text{kg}$$

The amount of synthetic zeolite loaded into one industrial adsorbent of a fixed adsorbent layer:

$$F = \frac{m_0}{a_g} = \frac{717}{0{,}036} = 19917\ \text{kg}$$

The number of adsorption stages on the entire adsorption unit per day:

$$a = \frac{m}{m_0} = \frac{17664}{736} = 24$$

The main operating modes of industrial adsorbers consist of the following stages: adsorption – τ_a =1,0 hour, desorption – $\tau_д$ =1,8 hour, regeneration - τ_p =1.0 hour, $\Sigma\tau$ = 3,8 hour.

The number of stages of the adsorption process that can be carried out in one adsorber during the day:

$$b = \frac{24}{\tau} = \frac{24}{3{,}8} = 6{,}31$$

Required number of adsorbers:

$$N = \frac{a}{b} = \frac{24}{6{,}3} = 3{,}8 \approx 4$$

Based on the calculation, we obtain the number of adsorbers 4.

We also optimized the process of adsorption of gas mixtures based on the previously developed model [5]. The calculated and theoretical results for the required number of adsorbers are in good agreement.

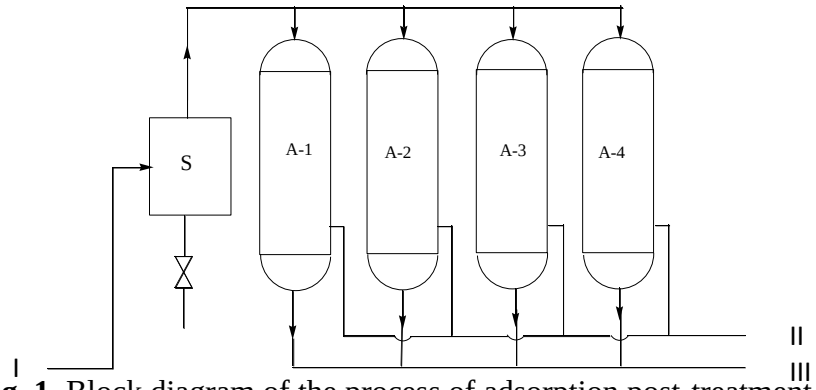

Fig. 1. Block diagram of the process of adsorption post-treatment of gas mixtures in a fixed adsorbent layer: A-1:A-4 - adsorbers, S-separator, I- raw materials; II- inert gas; III- commercial gas.

ISNN: print 2663-7006; online 2709-2666

CONCLUSION

The analysis of various adsorbents for the adsorption of CO_2, H_2S and NO_2 from a gas mixture showed that it is advisable to use NaX zeolite. In computer modeling, the adsorption isotherms are particularly important, as well as the exact numerical value of the dynamic activity. The dynamic activity of adsorbents is the main indicator that determines the size of the adsorbers and the sorption cycle time.

The coefficients of the equations are found based on the "Matlab" system in the "Optimization Toolbox"environment.

Thus, the proposed method of separation of gas mixtures allows for adsorption with respect to a three-component $H_2S/NO_2/CO_2$ gas mixture, the initial composition of which in %volume corresponds to - H_2S - 80%, CO_2 - 15%, NO_2 - 5%, using NaX as a zeolite while maintaining a pressure drop in the adsorption layer of 0.173÷0.203 kg/cm^2. The optimal conditions for the adsorption process of the gas components contained in the mixture is to conduct the process at a pressure drop in the adsorption layer a layer of 0.193 kg/cm^2, which provides after cleaning the content of H_2S - 0.040, CO_2 - 0.010, NO_2-0.061.

Based on the optimization of the adsorption process, it was found that (for NaX zeolite) the height of the adsorber is 6.37 m, the diameter of the adsorber is 1.69 m, the height of the working adsorbent layer is 92 cm, which guarantees the complete absorption of H_2S–0.040, CO_2-0.011 and NO_2-0.061% at a productivity of 41414 thousand m^3 per month.

REFERENCES

1. Youssef Belmabkhout., Rodrigo Serna-Guerrero., Abdel Hamid. Sayari Adsorption of CO_2 from dry gases MCM-41 silica at ambient temperature and high pressure 1: Pure CO_2 adsorption Chemical Engineering Science. 2009, Vol. 64, İssue 17, pp.3721-3934
2. Laurent F., Pope C.J., Mahzoul H., Delfosse L., Gilot P. Modelling of NO_x adsorption over NO_x adsorbers// Chemical Engineering Science. 2003,58 (9), pp.1793 – 1803
3. Bayramova A.S., Yusubov F.V., Babaev R.K. Investigation of the process of adsorption of H_2S, CO_2 and NO_2 from natural gas for the purpose of computer modeling. Austrian Journal of Technical and Natural Sciences. № 5-6, May June, Austria, Vienna 2015, pp.123-127
4. Vinay Mulgundmath., F. Handan Tezel. Optimization of carbon dioxide recovery from flue gas in a TPSA // Adsorption. 2010, 16, pp.587 – 598
5. Yusubov F.V., Bayramov A.S. Study and computer simulation of the process of separation of gas mixtures. Journal "Chemical Technology". Moscow 2020,Vol.21, №9, pp.428-432

ИССЛЕДОВАНИЕ ПРОЦЕССА АДСОРБЦИИ ГАЗОВОЙ СМЕСИ В НЕПОДВИЖНОМ СЛОЕ АДСОРБЕНТА NaX

А.С. Байрамова
Азербайджанский Государственный Университет Нефти и Промышленности
aygun.b74@mail.ru

В работе описана 4-х адсорберная установка очистки газовых смесей от H_2S, CO_2 и NO_2 цеолитом. Нижние и верхние пределы уровня конденсата в сепараторе контролировались электроконтактными манометрами, а давление регистрировалось на операторном щите.
Число адсорберов - 4, высота неподвижного слоя цеолита - 3,6 м. Длительная работа адсорбционной установки в реальных условиях работы показала, что температура регенерации цеолита во многом зависит от качества газа, поступающего на адсорбционный блок. Как видно, в начале завершается десорбция углекислого газа, затем сероводорода, а в конце - паров влаги, причем время для полной десорбции всех адсорбируемых компонентов лимитируется внутренне - диффузионным торможением сорбируемых компонентов. Наибольшее время десорбции, как и следовало ожидать, принадлежит парам влаги. Экспериментально установлено, что при нагреве горячим газом с максимально-допустимой скоростью время для полной десорбции влаги составляет 150-160 мин. Для практических расчетов время, необходимое для полной дегидратации цеолита, берется не менее 3 часов, что подтверждено экспериментально.
Ключевые слова: *адсорбция, синтетический цеолит NaX, неподвижный слой адсорбента, газовая смесь, десорбируемые вещества.*

NaX ADSORBENTİNİN HƏRƏKƏTSİZ QATINDA QAZ QARIŞIĞININ ADSORBSİYA PROSESİNİN TƏDQİQİ

A.S. Bayramova
Azərbaycan Dövlət Neft və Sənaye Universiteti
aygun.b74@mail.ru

İşdə 4 adsorber qurğusu H_2S, CO_2 və NO_2 qaz qarışıqlarından seolitlə təmizlənməsini təsvir edilir. Separatorda kondensat səviyyəsinin aşağı və yuxarı hüdudları elektrokontakt manometrlər tərəfindən nəzarətdə saxlanılırdı, təzyiq isə operator lövhəsində qeydə alınırdı.Adsorberlərin sayı 4, seolitin hərəkətsiz təbəqəsinin hündürlüyü 3,6 metrdir. Real şəraitdə adsorbsiya qurğusunun uzun müddətli işi göstərdi ki, seolitin regenerasiyasının temperaturu çox vaxt adsorbsiya blokuna daxil olan qazın keyfiyyətindən asılıdır. Göründüyü kimi, başlanğıcda karbon dioksid, daha sonra hidrogen sulfidi, sonda isə nəm buxarlarının desorbsiyası başa çatır, özü də bütün adsorb olunan komponentlərin tam desorbsiyası üçün vaxt sorblaşdırılan komponentlərin daxili - diffuziya tormoziyası ilə məhdudlaşdırılır. Gözlənildiyi kimi, ən böyük desorbsiya müddəti nəm cütlüklərə aiddir. Eksperimental olaraq müəyyən edilmişdir ki, isti qazla maksimal icazə verilən sürətlə qızdırıldığı zaman nəmin tam desorbsiyası üçün vaxt 150-160 dəqiqə təşkil edir. Praktiki hesablamalar üçün seolitin tam dehidratasiyası üçün lazım olan vaxt 3 saatdan az olmayaraq alınır ki, bu da eksperimental olaraq təsdiqlənir.
Açar sözlər: *adsorbsiya, sintetik seolit NaX, adsorbentin sabit təbəqəsi, qaz qarışığı, desorbasiya olunan maddələr.*

ISNN: print 2663-7006; online 2709-2666

AJCN, Vol 3, No. 3, 2021, pp. 46-52

UDC 544.478.13

OXIDATION OF ETHANOL OVER BINARY COPPER-TUNGSTEN OXIDE CATALYSTS

K.Kh. Aghayeva
Azerbaijan State Oil and Industry University
aghayeva1972@mail.ru

The oxidation reaction of ethanol on binary copper-tungsten oxide catalysts has been studied. It was shown that at temperatures up to 300°C, acetaldehyde is practically the only product of the ethanol oxidation reaction on copper-tungsten oxide catalysts. At higher temperatures, in addition to acetaldehyde, acetone, carbon dioxide and ethylene are also formed. It is found that the isomerization of butene-1 on the Cu-W-O catalysts begins from a temperature of 200°C and with an increase in temperature, the yield of butenes-2 increases and at 350°C reaches its maximum. It was shown that the dependence of the yields of butenes-2 on the atomic ratio of copper to tungsten has the form of a curve with a maximum on the sample Ti-W=3-7. On this sample, the maximum yield of butenes-2 reaches 57%. It is found that with an increase in the degree of isomerization, the yields of acetaldehyde and ethylene increase, and the yield of the product of deep oxidation decreases, which is due to formation of carbon dioxide at sites of basic nature.

***Keywords**: Ethanol oxidation, isomerization, binary catalysts, tungsten oxide, copper oxide, acetaldehyde.*

INTRODUCTION

The use of renewable resources for the production of fuels and valuable chemicals is the next important step in the development of the chemical industry. On the one hand, it is important that natural gas and oil resources will not be used, which will lead to a decrease in emissions of toxic and greenhouse gases into the atmosphere. On the other hand, the use of renewable sources of raw materials and fuels will lead to long-term and sustainable development of the chemical industry. Ethanol obtained by fermentation of lignocellulose, referred to as “second generation bioethanol”, may become the main intermediate in the new industrial organic chemistry based on renewable raw materials [1,2].

The products of the direct conversion of ethanol are ethylene, acetaldehyde, acetic acid, ethyl acetate, and diethyl ether [3-5].

It is known from the periodical literature that catalysts based on tungsten oxide are highly active in the reactions of partial oxidation of organic compounds [6-8]. Also, catalytic systems based on such elements as molybdenum, titanium and copper are often used as catalysts for ethanol conversion reactions [9-11]. In this regard, in this work, we studied the effect of additions of copper on the activity of binary tungsten oxide catalysts in the ethanol oxidation reaction.

EXPERIMENTAL PART

Mixed copper-tungsten containing oxide catalysts of various compositions were prepared by coprecipitation from aqueous solutions of copper nitrate and ammonium tungstate. The obtained mixture was successively evaporated and dried at 100-120°C, decomposed at 250°C until nitrogen oxides were completely liberated, and then calcined

at a temperature of 600°C for 10 hours. Thus, we have prepared a total of 9 catalysts that meet the following conditions:

mCu/nW, where m, n = 1 ÷ 9, m + n = 10.

The activity of the synthesized catalysts in the ethanol oxidation reaction was studied in a flow-through unit with a tubular reactor in the temperature range 100-500°C. The reactor was loaded with 5 ml of the investigated catalyst with a grain size of 1.0–2.0 mm, and a mixture of ethanol with water vapor and air with a ratio of ethanol:water:air=1:4:5 was passed. The volumetric feed rate of the initial mixture was 1200 h^{-1}. Carbon dioxide was determined on a chromatograph with a thermal conductivity detector and a 3 m column filled with Vaseline oil applied to an Celite sorbent. Ethanol and its conversion products were determined on a chromatograph with a flame ionization detector on a 3 m column filled with a specially treated polysorb-1 sorbent.

RESULTS AND DISCUSSION

The research of the activity of the studied samples showed that the products of the reaction of ethanol conversion on the Cu-W-O catalytic system are acetaldehyde, acetone, ethylene, and carbon dioxide. The temperature dependence of the activity of the Cu-W=2-8 catalyst in the ethanol conversion reaction is shown in figure 1. As can be seen from (fig.1), the ethanol conversion starts from a temperature of 200°C. At this temperature, only acetaldehyde is formed in an amount of 3.6%. With an increase in the reaction temperature, the yield of acetaldehyde increases to 50.8% at a selectivity of 56,8% at 400°C after which it begins to decrease and at 500°C it is already equal 35,6% with a selectivity of 38m6%. In addition to acetaldehyde, the formation of ethylene, acetone and carbon dioxide is also observed on the studied sample. The formation of ethylene and carbon dioxide begins at 300°C and with an increase in the reaction temperature, their yields increase over the entire temperature range studied. The maximum yields of ethylene and carbon dioxide are, respectively, 20.9 and 27.3%. As can be seen from (fig.1), the formation of acetone on this sample begins at 350°C and its maximal value (6%) observed at 400°C. The conversion of ethanol at a temperature of 500°C reaches 92%.

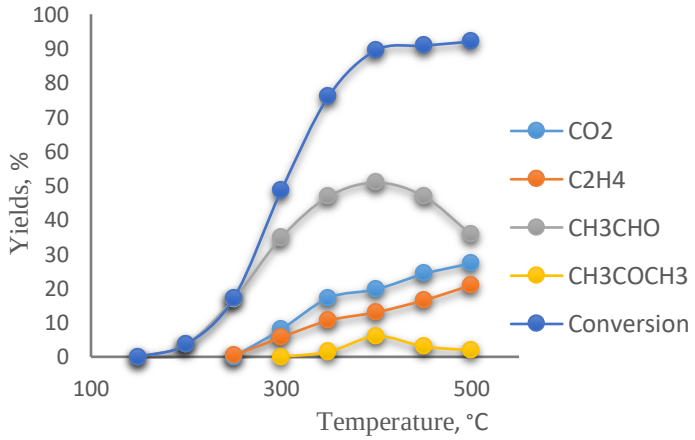

Fig. 1. Influence of temperature on the yields of products of the reaction of ethanol oxidation on the catalyst Cu-W=2-8.

It is found that activity of copper- tungsten oxide catalysts strongly depend on catalyst composition. Table 1 shows at a temperature of 250°C the dependences of the

ISNN: print 2663-7006; online 2709-2666

yields of the reaction products of the conversion of ethanol on the atomic ratio of copper to tungsten in the composition of Cu-W-O catalysts. It can be seen that with an increase in the copper content in the catalyst, the yield of acetaldehyde passes through a maximum on the Cu-W = 6: 4 sample, reaching 30%. From table 1 it can be seen that on the samples rich in tungsten in the reaction products, the formation of only acetaldehyde is observed. An increase in the copper content in the binary catalyst also leads to the formation of carbon dioxide.

Table 1

Influence of the atomic ratio of copper to tungsten on the yields of ethanol oxidation products. T = 250°C

Atomic ratio copper/tungsten / Reaction products	Ethanol oxidation reaction product yields, %								
	1:9	2:8	3-7	4:6	5:5	6:4	7:3	8:2	9:1
CO_2	0	0	0	0	0	2,6	5,6	6,3	7,2
C_2H_4	0	0,3	0	0	0	0	0	0	0
CH_3CHO	13,6	16,8	18	15,8	21,9	30	20	21,8	27,6
CH_3COCH_3	0	0	0	0	0	0	0	0	0
Conversion	13,6	17,1	18	15,8	21,9	32,6	25,6	28,1	34,8

In contrast to low reaction temperatures at higher temperatures, in the oxidation of ethanol on binary copper-tungsten oxide catalysts, in addition to acetaldehyde and carbon dioxide, acetone and ethylene are also formed. Table 2 shows the dependence of the yields of the reaction products of the conversion of ethanol on the atomic ratio of copper to tungsten in the composition of Cu-W-O catalysts. It can be seen that with an increase in the copper content in the catalyst, the yield of acetaldehyde passes through two maxima for the samples Cu-W=3:7 (56.4%) and Cu-W=6:4 (52.6%). Similar dependences of the yield on the catalyst composition are observed for the reaction of acetone formation. The ethylene yield decreases with an increase in the copper content in the catalyst and is practically zero in the samples rich in copper. The yield of the product of deep oxidation of ethanol of carbon dioxide with an increase in the copper content in the catalyst first slightly decreases, and then, starting with the Cu-W=3-7 sample, it increases to 24.6% for the Cu-W=9-1 sample. As can be seen from table 3, the dependence of the ethanol conversion on the catalyst composition also has the form of a curve with two maxima, and the highest ethanol conversion reaches 89.5%.

Table 2

Influence of the atomic ratio of copper to tungsten on the yields of ethanol oxidation products. T = 400°C

Atomic ratio copper/tungsten	Ethanol oxidation reaction product yields, %								
Reaction products	1:9	2:8	3-7	4:6	5:5	6:4	7:3	8:2	9:1
CO_2	21,6	19,7	16,8	17,8	20,4	19,8	23,2	20,3	24,6
C_2H_4	18	13	9,4	5,4	4,8	4,3	0	0	0
CH_3CHO	32,2	50,8	56,4	52,4	44,4	52,6	45,6	40,4	37,4
CH_3COCH_3	0	6	5,2	0	0	6,2	1,5	1,2	0
Conversion	71,8	89,5	87,8	75,9	69,9	83	70,3	66,3	63,5

Summarizing the above, we can say that the main product of ethanol oxidation on

copper-tungsten oxide catalysts is acetaldehyde. At temperatures up to 300°C, acetaldehyde is practically the only product of the ethanol oxidation reaction, while at higher temperatures, in addition to acetaldehyde, acetone, carbon dioxide and ethylene are also formed.

The acid-base properties of the surface of heterogeneous catalysts quite often correlate with their catalytic properties. In this regard, we studied the dependence of the activity of binary tungsten-containing catalysts in the ethanol oxidation reaction on their acidity, by the measure of which we chose the rate of the isomerization of butene-1 to butenes-2. Studies have shown that the isomerization of butene-1 on the Cu-W-O catalysts begins from a temperature of 200°C and with an increase in temperature, the yield of butenes-2 increases and at 350°C reaches its maximum. However, it should be noted that an increase in the amount of copper in the catalyst leads to a decrease in the yields of butenes-2 and a shift in their formation towards higher temperatures. Thus, on the Cu-W = 1-9 sample, the formation of butenes-2 is observed at a temperature of 400°C and their total yield does not exceed 2.4%. It can be seen from the results obtained that the ratio of the yields of the trans and cis isomers of butenes-2 on the studied catalysts, with rare exceptions, varies from 0.2 to 0.6. The study of the dependence of the yields of trans and cis butenes-2 on the atomic ratio of copper to tungsten at a temperature of 300°C showed that with an increase in the amount of copper in the composition of the binary catalyst, the yields of butenes-2 pass through a maximum of 22.1% on the catalyst Cu-W=3-7. A further increase in copper in the composition of the binary copper-tungsten oxide catalyst leads to a decrease in the yields of butenes-2 and on the samples beginning from Cu-W=7-3 at this temperature isomerization of butene-1 does not occur.

At temperatures above 400°C, the formation of butenes-2 is observed in all studied samples. Figure 2 shows the dependence of the yields of trans and cis butenes-2 on the atomic ratio of copper to tungsten at a temperature of 400°C. As can be seen from Figure 2, the dependence of the yields of butenes-2 on the atomic ratio of copper to tungsten has the form of a curve with a maximum on the sample Ti-W=3-7. On this sample, the maximum yield of butenes-2 reaches 57%.

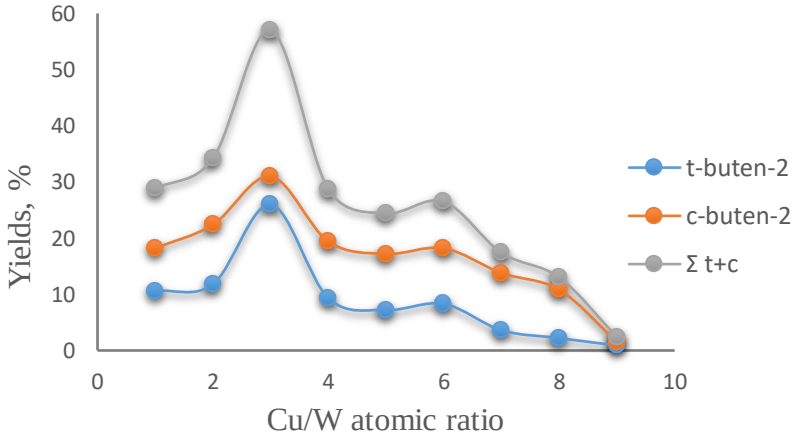

Fig.2. Dependence of the degree of isomerization of butene-1 on the atomic ratio of copper to tungsten.

The dependences of the yields of acetaldehyde, ethylene, acetone, and carbon dioxide in the reaction of ethanol conversion on copper-tungsten oxide catalysts on the degree of butene-1 isomerization are shown in fig.3. It can be seen that with an increase

ISNN: print 2663-7006; online 2709-2666

in the degree of isomerization, the yields of acetaldehyde and ethylene increase, and the yield of the product of deep oxidation decreases.

These data allow us to assume that, in the oxidation of ethanol on copper-tungsten oxide catalysts the formation of ethylene and acetaldehyde occurs at acid sites, while the formation of carbon dioxide occurs at sites of basic nature. Figure 3 also shows that the yields of acetaldehyde and ethylene change symbatically with a change in the degree of butene-1 isomerization, that is, it can be assumed that the formation of these products proceeds at the same centers.

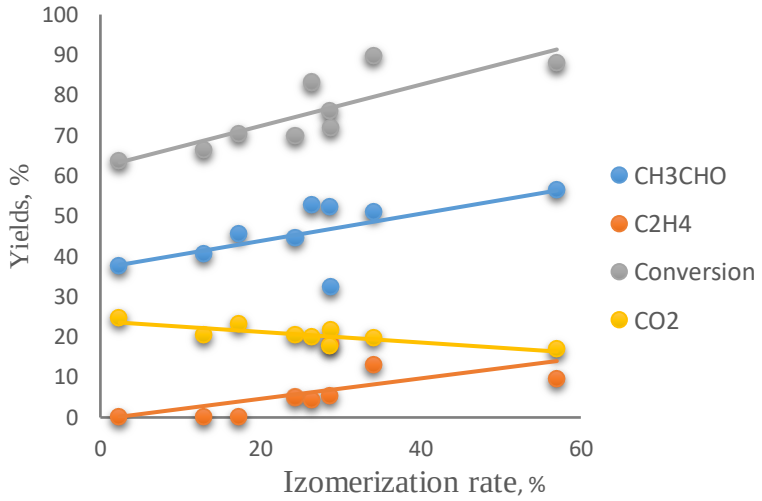

Fig.3. Dependence of the ethanol oxidation reaction products yields on degree of isomerization of butene-1

CONCLUSION

In the oxidation reaction of ethanol on copper-tungsten oxide catalysts the formation of ethylene and acetaldehyde occurs at acid sites, while the formation of carbon dioxide occurs at sites of basic nature. The formation of acetaldehyde and ethylene proceeds at the same centers.

REFERENCES

1. Alya Limayem, Steven C.Ricke. Lignocellulosic biomass for bioethanol production: Current perspectives, potential issues and future prospects. Progress in Energy and Combustion Science. 2012, Vol. 38, Issue 4, pp. 449-467
2. Mustafa Balat. Production of bioethanol from lignocellulosic materials via the biochemical pathway: A review. Energy Conversion and Management. 2011, Vol. 52, Issue, 2, pp. 858-875
3. Claudio Bianchini, Valentina Bambagioni, Jonathan Filippi, Andrea Marchionni, Francesco Vizza, Paolo Bert, Alessandro Tampucci. Selective oxidation of ethanol to acetic acid in highly efficient polymer electrolyte membrane-direct ethanol fuel cells // Electrochemistry Communications, 2009, Vol.11, Issue 5, pp. 1077-1080
4. Inusa Abdullahi., Taylor J.Davis, Dong M.Yun, Jose E.Herrera. Partial oxidation of ethanol to acetaldehyde over surface-modified single-walled carbon nanotubes. Applied Catalysis A: General. 2014, Vol. 469, pp. 8-17
5. Thanh Khoa Phung, Guido Busca. Ethanol dehydration on silica-aluminas: Active

sites and ethylene/diethyl ether selectivity. Catalysis Communications. 2015, Vol. 68, pp. 110-115
6. Chenghang Zheng, Hao Li, Yang Yang, Shuo Zhang, Xinning Yu, Qi Xin, Shaojun Liu, Xiang Gao. Promotional effects of ruthenium oxide on catalytic oxidation of dichloromethane over the tungsten-titanium binary oxides catalyst. Proceedings of the Combustion Institute, 2021, Vol. 38, Issue 4, pp. 6461-6471
7. Zinaida P.Pai, Yuriy A.Chesalov, Polina V.Berdnikova, Evgeny A.Uslamin, Dmitry Yu.Yushchenko, Yulia V.Uchenova, Tatiana B.Khlebnikova, Vladimir P.Baltakhinov, Dmitry I.Kochubey, Valerii I.Bukhtiyarov. Tungsten Peroxopolyoxo Complexes as Advanced Catalysts for the Oxidation of Organic Compounds with Hydrogen Peroxide. Applied Catalysis A: General. 2020, Vol. 604, 117786 p
8. Uriel Caudillo-Flores, Mario J.Muñoz-Batista, Ana B.Hungría, Miguel López Haro, Marcos Fernández-García, Anna Kubacka. Toluene and styrene photo-oxidation quantum efficiency: Comparison between doped and composite tungsten-containing anatase-based catalysts. Applied Catalysis B: Environmental. 2019, Vol. 245, pp. 49-61
9. Xiaoxiang Chen, Wuyi Li, Zhanchang Pan, Yanbin Xu, Gen Liu, Guanghui Hu, Shoukun Wu, Jinghong Li, Chun Chen, Yingsheng Lin. Non-carbon titanium cobalt nitride nanotubes supported platinum catalyst with high activity and durability for methanol oxidation reaction. Applied Surface Science. 2018, Vol. 440, pp. 193-201
10. Ryoji Kuma, Tomoyuki Kitano, Takuya Tsujiguchi, Tsunehiro Tanaka. Effect of molybdenum on the structure and performance of V2O5/TiO2–SiO2–MoO3 catalysts for the oxidative degradation of o-chlorotoluene. Applied Catalysis A: General. 2020, Vol. 595, 117496 p
11. Ling-Ling Guo, Jing Yu, Miao Shu, Lu Shen, Rui Si. Silicon nitride as a new support for copper catalyst to produce acrolein via selective oxidation of propene with very low CO_2 release. Journal of Catalysis. 2019, Vol. 380, pp. 352-365

ОКИСЛЕНИЕ ЭТАНОЛА НА БИНАРНЫХ МЕДЬ-ВОЛЬФРАМ ОКСИДНЫХ КАТАЛИЗАТОРАХ

К.Х. Агаева
Азербайджанский Государственный Университет Нефти и Промышленности
aghayeva1972@mail.ru

Изучена реакция окисления этанола на бинарных медь-вольфрам оксидных катализаторах. Показано, что при температурах до 300°C ацетальдегид является практически единственным продуктом реакции окисления этанола на медь-вольфрам оксидных катализаторах. При более высоких температурах, помимо ацетальдегида, также образуются ацетон, диоксид углерода и этилен. Установлено, что изомеризация бутена-1 на катализаторах Cu-W-O начинается с температуры 200°C и с повышением температуры выход бутенов-2 увеличивается и при 350°C достигает максимума. Было показано, что зависимость выходов бутенов-2 от атомного отношения меди к вольфраму имеет вид кривой с максимумом на образце Ti-W = 3-7. На этом образце максимальный выход бутенов-2 достигает 57%. Установлено, что с увеличением степени изомеризации выходы ацетальдегида и этилена увеличиваются, а выход продукта глубокого окисления уменьшается, что обусловлено их образованием на основных центрах.

Ключевые слова: *окисление этанола, изомеризация, бинарные катализаторы, оксид вольфрама, оксид меди, ацетальдегид.*

ISNN: print 2663-7006; online 2709-2666

BİNAR MİS-VOLFRAM OKSİD KATALİZATORLARI ÜZƏRİNDƏ ETANOLUN OKSİDLƏŞMƏSİ

K.X. Ağayeva
Azərbaycan Dövlət Neft və Sənaye Universiteti
aghayeva1972@mail.ru

Binar mis-volfram oksid katalizatorları üzərində etanolun oksidləşmə reaksiyası tədqiq olunmuşdur. Göstərilmişdir ki mis-volfram oksidi katalizatorları üzərində 300°C-yə qədər olan temperaturda asetaldehid praktiki olaraq etanolun oksidləşmə reaksiyasının yeganə məhsuludur. Yüksək temperaturlarda isə asetaldehiddən başqa aseton, karbon dioksid və etilen də əmələ gəlir. Müəyyən edilmişdir ki Cu-W-O katalizatorlarında buten-1-in izomerləşməsi 200°C temperaturdan başladığı və temperaturun artması ilə buten-2-in çıxımları artır və 350°C-də maksimuma çatır. Göstərilmişdir ki buten-2 çıxımının misin volframla atom nisbətindən asılılığı Ti-W = 3-7 nümunəsində maksimumdan keçir. Bu nümunədə buten-2-in maksimum çıxımı 57%-ə çatır. Aşkar edilmişdir ki izomerləşmə dərəcəsinin artması ilə asetaldehidin və etilenin çıxımları artır və dərin oksidləşmə reaksiyanın məhsulları azalır.

Açar sözlər: *Etanolun oksidləşməsi, izomerləşmə, binar katalizatorlar, volfram oksidi, mis oksidi, asetaldehid.*

AJCN, Vol 3, No. 3, 2021, pp. 53-58

UDK 541.49:546.719

REGULARITIES OF RHENIUM COORDINATION WITH PHENANTHROLINE DONOR LIQAND

G.I.Safarli, M.M.Aghahuseynova
Azerbaijan State Oil and Industry University
gunel.safarli.1995@gmail.com

Effective methods for the synthesis of a number of complex compounds of rhenium (V) with 1, 10 - phenanthroline have been developed. The composition and structure of the obtained compounds were proved by physico-chemical methods, and their properties were studied by methods of elemental analysis, IR and electron (ESP) spectroscopy and thermogravimetry. Compounds of the composition $PhenH_2[ReOCl_5]$(I) and $PhenH_2[ReOBr_5]$(II) were obtained. The $[ReOX_3Phen]$- (III and IV) (x=Cl, Br) compounds were synthesized by thermal decomposition I and II. It is shown that thermal decompositions I and II proceed with the release of the corresponding hydrogen halide and the rearrangement of the phenanthroline molecule. The transition of phenanthroline from the external sphere (I and II) to the sphere of the ligand environment of rhenium (V) (compounds III and IV) was confirmed by the results of spectrophotometric measurements (IRS, ESP).

Keywords: *complexes of rhenium, nitrogen containing organic liqands, o-phenantroline.*

INTRODUCTION

Recently, rhenium compounds in high oxidation states have been of particular interest, due to their having a number of important properties, the study of which makes a significant contribution to the development of the theory of the structure of complex compounds and opens the way for the purposeful synthesis of a substance with specified properties. In most papers regarding this problem [1-3], complex compounds of rhenium with S- and P-containing ligands are studied, and the complex formation of rhenium with N- containing ligands is not fully covered in the literature. Therefore, it was of interest to synthesize and study the properties of rhenium (V) complexes with 1, 10-phenanthroline (Phen), which has two donor nitrogen atoms in its composition and is coordinated with metals as a bidentate ligand [4-6].

The coordination chemistry of rhenium has received significant development in recent years, due to the interest in creating radiopharmaceutical drugs based on complex rhenium compounds for the diagnosis and treatment of cancer diseases. Most of the rhenium complexes used in radio medicine are oxocomplexes, and therefore compounds containing the polar group Re=0 are of great interest, the addition of which to the molecule has a strong influence on the properties and behavior of the latter [7-11]. This circumstance played a significant role in the formulation of this study.

This paper deals with the research of the processes of Re(V) compound complex formations with o-phenanthroline, the development methods for the synthesis of previously undescribed complexes, as well as the study of the synthesized sample composition, structure and properties.

EXPERIMENTAL PART

The process of complex formation of rhenium with o-phenanthroline is comprehensively considered, for which various starting substances were used.

ISNN: print 2663-7006; online 2709-2666

H2[ReOX5], where X=Cl, Br, obtained by us according to the methods given in [5,6], were used as starting substances. Rhenium was determined in the form of nitron perrenate [7], carbon, hydrogen and nitrogen-on an automatic analyzer manufactured by "Carlo Erba" company. The IR spectra of the obtained complexes were taken on SpecordM-80 and Specord 75-IR spectrometers, and the electronic absorption spectra on the SpecordM-40 device. The ЯМР′Н spectras were taken by Bruker-400 devices. The thermal analysis was performed on a Q-1500 D derivatograph of the Paulik-Paulik-Erdei system. The molar electrical conductivity of the complex solutions was determined through the conductometric method.

[$PhenH_2$][$ReOCl_5$](I) Synthesis. The 1,10-phenanthroline solution in hydrochloric acid was added to H2[ReOCl5] solution in HCl. The reaction occurs at room temperature and stirring for 1.0 h. The precipitated fine-crystalline precipitate of light brown color was filtered out after a day, treated with a weak HCl solution, washed with ether and dried at 105°C to a constant mass

It is found that, %: Re-25,01; C-19,10; H-1,72; N-4,03.

For [$PhenH_2$][$ReOCl_5$]

It is calculated that, %: Re-24,44; C-18,90; H-1,58; N-3,68.

[$PhenH_2$][$ReOBr_5$](II) Synthesis. An equivalent amount of 1,10-phenanthroline solution in HBr was added to the oxobromorenic acid solution in concentrated HBr. Upon stirring for 1.5 hours, the precipitation is completed in the form of small crystals of a reddish color. The precipitate was filtered out after a day, washed with 5 mol/ l HBr, benzene, ether and dried in a thermostat at 105°C to a constant mass.

It is found that, %: Re-23,68; C-17,64; H-1,81; N-3,22.

For [$PhenH_2$][$ReOBr_5$]

It is calculated that, %: Re-23,22; C-17,96; H-1,50; N-3,49.

[$ReOCl_3$Phen](III) Synthesis. 0.5 g of [PhenH2][ReOCl5] was placed in a test tube with two taps. The dry argon was passed through the test tube, and heated in an argon current at a temperature of 195°C during 1.5 hours. Then the test tube was cooled, without stopping the supply of argon, to room temperature. After thermal decomposition (I), the color of the substance changed to yellow-green.

It is found that, %: Re-38,24; Cl-21,40; N-5,74.

For [$ReOCl_3$Phen]

It is calculated that, %: Re-38,10; Cl-21,76;N-5,73.

[$ReOBr_3$Phen](IV) Synthesis. In argon current, the solution of PhenH2[ReOBr5] (0.5 g) in a two-pipe test tube was kept at 190°C for 3.0 hours, then cooled in an inert atmosphere. After dehydrohalogenation and rearrangement (II), substance IV was of a light green color.

It is found that, %: Re-29,36; C-22,85; H-1,07; N-5,10.

For [$ReOBr_3$Phen]

It is calculated that, %: Re-29,36; C-23,15;H-1,29;N-4,50.

RESULTS AND DISCUSSION

The interaction of a solution of oxochlororenic acid in hydrochloric acid with an equivalent amount of hydrochloric acid solution of o-phenanthroline resulted in elimination of [PhenH2][ReOCl5]-(I) compound. The [PhenH2][ReOBr5]-(II) complex was obtained by adding the o-phenanthroline solution in HBr to the oxobromorenic acid

solution in hydrobromic acid. Oxochloro - and oxobromorenates of o-phenanthroline were deposited in the form of small crystals of light brown (I) and reddish (II) color.

$$Phen+H_2[ReOX_5]\rightarrow[PhenH_2][ReOX_5]$$

These formulas were attributed based on the elemental analysis data and the IR spectroscopy. Thus, the IR spectra of compounds I and II have wide absorption bands in the 3300-3340 cm-^{1} scope. These bands are characteristic for protonated nitrogen atoms in the heterocycle and confirm the formation of an outer-sphere cation $[PhenH_2]^{2+}$.

On the heating curves of compounds I and II, decomposition is accompanied by two endothermic effects – at 84 and 186°C for $[PhenH_2][ReOCl_5]$ and 87, 188°C$[PhenH_2][ReOBr_5]$. The first endothermic effect corresponds to the removal of crystallization water, the second is associated with dehydrohalogenation. In order to obtain substances formed after the removal of HX (x=Cl, Br), compounds I and II were subjected to thermal exposure in an inert atmosphere. By heating at the temperature slightly higher (190-195°C) of the second endothermic effects, compounds of the $[ReOCl_3Phen]$-(III) and $[ReOBr_3Phen]$-(IV) composition were obtained. Upon heating, dehydrohalogenation occurs and the ligand passes from the outer sphere to the inner sphere of the complex, and the color of the substances changes to yellow-green (III) and light green (IV). The reaction proceeds according to the scheme:

$$[PhenH_2][ReOX_5]\rightarrow[ReOX_3Phen]+2HX. \qquad (x=Cl, Br)$$

This thermal decomposition scheme with the release of two hydrogen halide molecules and the entry of the o-phenanthroline molecule into the inner sphere of the complexing agent atom is confirmed by the elemental analysis data and a comparative study of the IR spectra of the initial and obtained compounds. In the IR spectra of compounds III and IV, the absorption bands in the 3300-3340 cm^{-1} scope disappear due to the presence of protonated nitrogen atoms of the heterocycle in the outer-sphere cation $[PhenH2]^{2+}$ of compounds I and II.

The intense band in the 848 cm^{-1} scope, caused by fluctuations of free o-phenanthroline, in the IR spectra of compounds III, IV is split into two bands: - less intense at 848 cm^{-1} and low-intensity at 843 cm^{-1} (III) and 840 cm^{-1} (IV), which confirms the entry of the phenanthroline molecule into the internal coordination sphere of the rhenium atom (V). Changes in the intensities and the shift of the absorption bands on the electronic spectra of compounds III-IV relative to I-II in the visible and close UV sites characterizing the phenanthroline chromophore system indicate the transition of the phenanthroline molecule from the outer sphere (I and II) to the inner sphere of the complexing agent atom (III and IV). The band at 19050 cm^{-1} splits into two bands with a significant hyperchromic shift at 23500 and 22500 cm^{-1}, and for the long-wave absorption band in the 12020 cm^{-1} area, a hypsochromic shift is observed (Δ550 cm^{-1}).

The transition of phenanthroline from the external sphere to the rhenium ligand environment sphere is confirmed by a change in the ESP nature (fig. 1,2) and is characterized by a change in the spectral characteristics in the UV area due to the phenanthroline chromophore system, which is accompanied by a redistribution of the absorption band intensities and a hypsochromic shift. This indicates that structural transitions affect the parameters of electronic transitions both in the metal-ligand system and in the ligand system itself, which confirms the relationship of these chromophore systems.

ISNN: print 2663-7006; online 2709-2666

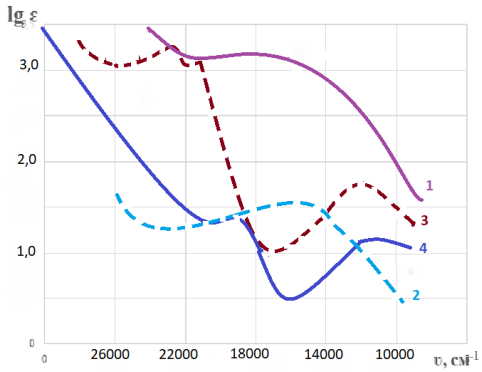

Fig.1. Electronic absorption spectra of complex compounds of rhenium (V) 1-4 substances, respectively I,II,III,IV.

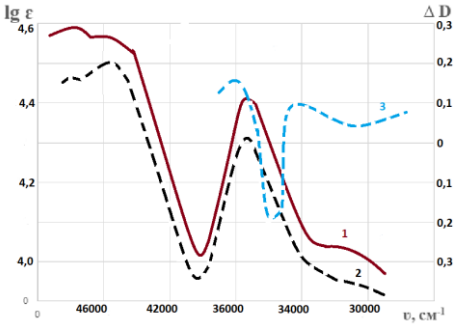

Fig.2. Electronic absorption spectra of acetonitrile solutions of rhenium (V) complex compounds in the UV area.

Based on the above and taking into account the fact that the complex anions $[MeOX_5]^{2-}$ (x=Cl, Br) have the configuration of a flattened octahedron, compounds III and IV may be designated by one of two possible structural formulas (A and B) as shown below:

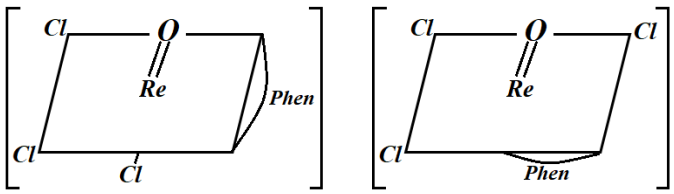

CONCLUSION

1. Compounds of the composition $PhenH_2[ReOCl_5]$(I) and $PhenH_2[ReOBr_5]$(II) were obtained. The $[ReOX_3Phen]$- (IIIиIV) (x=Cl, Br) compounds were synthesized by thermal decomposition I and II.
2. It is shown that thermal decompositions I and II proceed with the release of the corresponding hydrogen halide and the rearrangement of the phenanthroline molecule.
3. The transition of phenanthroline from the external sphere (I and II) to the sphere of

the ligand environment of rhenium (V) (compounds III and IV) was confirmed by the results of spectrophotometric measurements (IRS, ESP).

REFERENCES

1. Hanack M., Kamenzin S., Kamentin C., Subramanian L.R. Synthetic Metals. 2000, Vol. 110, № 2, 93 p
2. Ospanova L.L., Ospanov Kh.K., Shabikova G.Kh., Khachaturova T.G. Journal inorgan. Chemistry.1990, Vol. 35, №10, pp. 2564-2568
3. Amindzhanov A.A., Kurbanov N.M., Kotegov K.V. Journal inorgan. Chemistry.1992, Vol.37, №1, pp. 126-131
4. Dzhabbarova N.E., Agaguseynova M.M. Coordination compounds of transition metals in catalysis (monograph). 2006, 86 p
5. Dudnik A.S., Ivanov A.V., Tomilova L.G., Zefirov N.S. Coord. Chemistry. 2004, Vol.30, №2, 120 p
6. Rither B.D., Kenney M.S., Ford W.L., Rodqers A.I. I.Am. Chem. Soc. 2002, Vol.112, №22, 8064 p
7. Jennifer Schroer, Ulrich Abram. Rhenium (V) complexes with tridentate *P*,*N*,*S* ligands. 2012, Vol.33, Issue 1, pp.218-222
8. Miguel A. Huertos, Julio Pérez, Lucía Riera, Amador Menéndez-Velázquez *J.*From *N*-Alkylimidazole Ligands at a Rhenium Center: Ring Opening or Formation of NHC Complexes. *Chem. Soc.* 2008, 130, 41, pp.13530–13531
9. Purcell W., Visser H. G. Rhenium(V)-nitrido complexes with different nitrogen donor bidentate ligands.W. Transition Metal Chemistry. 2015,Vol.40, pp.899–906
10. Mironov Yu.V., Naumov N.G., Brylev K.A., Efremova O.A, Fedorov V.E., Hegechweiler K. "Chiral coordination polymers based on rhenium cluster complexes" . Coordination Chemistry. 2005, 31, №4 pp.289-301
11. Tarasenko M.S., Naumov N.G., Virovets A.V., Naumov D.Yu., Kurat'eva N.V., Mironov Yu.V., Ikorsky V.N., Fedorov V.E. “New coordination polymers based on paramagnetic cluster anions and rare-earth cations: synthesis and structure of [{Ln (H_2O) 3} {$Re_6Se_8(CN)_6$}] 3.5H_2O”. Journal Structural Chemistry. 2005, Vol.46, pp.134-141

ЗАКОНОМЕРНОСТИ КООРДИНАЦИИ РЕНИЯ С ДОНОРНЫМ ЛИГАНДОМ-ФЕНАНТРОЛИНОМ

Г.И.Сафарли, Г.Г.Агагусейнова
Азербайджанский государственный университет нефти и промышленности
gunel.safarli.1995@gmail.com

Разработаны эффективные методы синтеза ряда комплексных соединений рения (V) с 1,10-фенантролином. Состав и структура полученных соединений доказаны физико-химическими методами, а их свойства изучены методами элементного анализа, ИК, электронной (ЭСП) спектроскопии и термогравиметрии. Получены соединения состава $PhenH_2$ [$ReOCl_5$] (I) и $PhenH_2$ [$ReOBr_5$] (II). Соединения [$ReOX_3Phen$] - (III и IV) (x = Cl, Br) синтезированы термическим разложением I и II. Показано, что термические разложения I и II протекают с выделением соответствующего галогенида водорода и перегруппировкой молекулы фенантролина. Переход фенантролина из внешней сферы

ISNN: print 2663-7006; online 2709-2666

(I и II) в сферу лигандного окружения рения (V) (соединения III и IV) подтвержден результатами спектрофотометрических измерений.
***Ключевые слова**: комплексы рения, азотсодержащие органические лиганды, о-фенантролин.*

RENİUMUN DONOR LİQAND-FENANTROLİNLƏ KOORDİNASİYA QANUNAUYĞUNLUQLARI

G.I.Səfərli, M.M.Ağahüseynova
Azərbaycan Dövlət Neft və Sənaye Universiteti
gunel.safarli.1995@gmail.com

Reniumun (V) 1,10-fenantrolinlə bir sıra kompleks birləşmələrinin sintezi üçün effektiv üsullar işlənib hazırlanmışdır. Alınan birləşmələrin tərkibi və quruluşu fiziki-kimyəvi üsullarla sübut edilmiş, xassələri elementar analiz, İQ, elektron (EUS) spektroskopiya və termoqravimetriya üsulları ilə öyrənilmişdir. $PhenH_2$ $[ReOCl_5]$ (I) və $PhenH_2$ $[ReOBr_5]$ (II) tərkibli birləşmələr əldə edilmişdir. $[ReOX_3Phen]$ - (III və IV) (x = Cl, Br) birləşmələri I və II -nin termal parçalanması ilə sintez edilmişdir. I və II -nin termal parçalanmasının müvafiq hidrogen halojenidin ayrılması və fenantrolin molekulunun yenidən qurulması ilə davam etdiyi göstərilmişdir. Fenantrolinin xarici sferadan (I və II) reniumun (V) ligand əhatəsinə, yəni kompleksin daxili sferasına (III və IV birləşmələr) keçidi spektrofotometrik nəticələri ilə təsdiq edilmişdir.
***Açar sözlər:** renium kompleksləri, azot tərkibli üzvi ligandlar, o-fenantrolin.*

AJCN, Vol 3, No. 3, 2021, pp. 59-63

UDC: 504.45.064.36

INVESTIGATION OF UNDERGROUND WATER SOURCES WITH HYDROGEN SULFIDE CONTENT ON THE TERRITORY OF SHIMALI

N.A.Guliyeva , Z.V.Abdulazimova
Azerbaijan State Oil and Industry University
zarifaabdulazimova@gmail.com

This paper examines the chemical composition of the hydrogen sulfide waters of the Khachmaz region from three hydrogen sulfide sources on the territory of Shimali, namely from the Khazar camp site from the Shafa camp site, as well as from one of the central villages, the population for which is famous for good health from the Shimali village-1. A comparative analysis of the relationship between the salinity of groundwater, chloride ions, HCO_3^- and the concentration of H_2S is carried out. We have carried out monitoring from several hydrogen sulfide sources for the presence and quantitative determination of Cl^- in them, as well as established environmental factors affecting the preservation of these sources.
Keywords: *chloride ion, hydrogen sulfide (H_2S), ecology, titration.*

INTRODUCTION

In the system of artesian waters, hydrogen sulfide waters belong to a reducing geochemical environment, which depends largely on the ecological state, in the zone of development of anaerobic processes. The main factors and environmental conditions for the formation of hydrogen sulfide waters are the lithological-facies composition of the water-bearing rocks, first of all, having sulfate-containing deposits and oil and gas complexes, which is very important when studying the composition of water and using it both for technical and other purposes. Geostructural conditions and hydrogeochemical setting are one of the key factors [1- 3]. The formation of hydrogen sulphide waters is a complex geochemical process that depends on a complex of geological factors and the natural and ecological situation in a given area [4,5]. The study of the ionic composition of hydrogen sulfide waters shows that the most common among them are chloride and sodium waters. Rare: sulfate, calcium, chloride-sulfate and sodium types. Very rarely meet: hydrogen sulphide waters of chloride-hydrocarbonate sodium composition, hydrocarbonate-sulphate calcium.

At present, the population of the Republic of Azerbaijan continues to be treated with mineral waters from local springs. Most of those who come to the springs in summer use the water on their own, without first seeking medical advice and without being subject to medical supervision. Such uncontrolled use of medicinal mineral waters can seriously harm health. The rational use of mineral hydrogen sulfide waters for medicinal purposes is impossible without a thorough study of their composition, properties and effects on the body. Hydrogen sulfide medicinal waters are represented mainly by thermal and cold springs. The therapeutic effect of hydrogen sulfide waters is associated with the free H_2S present in the water, which has active chemical properties.

EXPERIMENTAL PART

For our work we used: pipette 1 cm, graduated every 0.01 cm; measuring cylinder 100 cm; burette 25 cm with glass cock. Colorimetric tubes with a mark of 5 cm. Ashless

ISNN: print 2663-7006; online 2709-2666

filters "white tape", $AgNO_3$, NaCl, $KAl(SO_4)_2 \cdot 12H_2O$, K_2CrO_4, NH_3, 25% solution.

Samples were taken from three sources in the Shimali area in August 2019. When taking a water sample for analysis for H_2S. They allowed the water to drain a little, and immediately filled it. The water was delivered to the laboratory for analysis within 24 hours.

Sample 1. Fig . 1. Camp site " Shafa "

Sample 2. Fig . 2. " Shimali 1" village

Sample 3. Fig . 3. The source of the camp site " Khazar "

Sample 4. Fig . 4. Camp "Shafa", the pipe which was closed here due to the fact that this reservoir was installed .

Analysis of the relationships between groundwater salinity, SO_4^{2-}, HCO_3^- and H_2S concentration. The volume of water samples for determining the chloride content was taken with a volume of 250 cm^3 and not preserved in a conical flask. The chlorine ion content was determined by titration with $AgNO_3$.

5 cm^3 of water was poured into a colorimetric test tube, and three drops of a 10% $AgNO_3$ solution were dropped. The fact that there is chlorine ion in the test water was determined by the white precipitate, after the qualitative detection of the chlorine ion in the water, a quantitative determination was carried out.

Fig.1. Camp site "Shafa"

Fig.2. " Shimali 1" village

Fig.3. The source of the camp site "Khazar"

Fig.4. Camp "Shafa", the pipe which was closed here due to the fact that this reservoir was installed

RESULTS AND DISCUSSION

Studies of the chemical composition of hydrogen sulphide waters on the territory of Shimali. We have determined the ionic composition of water from several springs located on the territory of Shimali -1 village, on the territory of the "Shafa" camp site, which is a resting place for azi workers and a source on the territory of the "Khazar"

Camp site.

We have carried out monitoring from several hydrogen sulfide sources for the presence and quantitative determination of Cl in them. Of all the known anions, chlorides have the highest ability to migrate, which is explained by their high solubility, weakly expressed ability to sorption and consumption by living organisms.

The increased content of chlorides in drinking water gives it a salty taste and has a negative impact on human health; it is also not suitable for household and technical needs. Chlorides in water are harmful to health. Drinking water with chlorides, a person experiences a violation of the water-salt balance and the digestive tract, edema occurs. Therefore, it is necessary to monitor the correlation of the amount of chlorine ions in hydrogen sulfide sources in the territory where the resort zones and villages in which the population lives, using this water in everyday life. Both sulfates and carbonates in water were determined in parallel (fig. 5). We also studied the ratio of Ca^{2+} , Mg^{2+} and Na^{+} cations with K^{+} in water and thus compared them quantitatively relative to the sources (fig. 6).

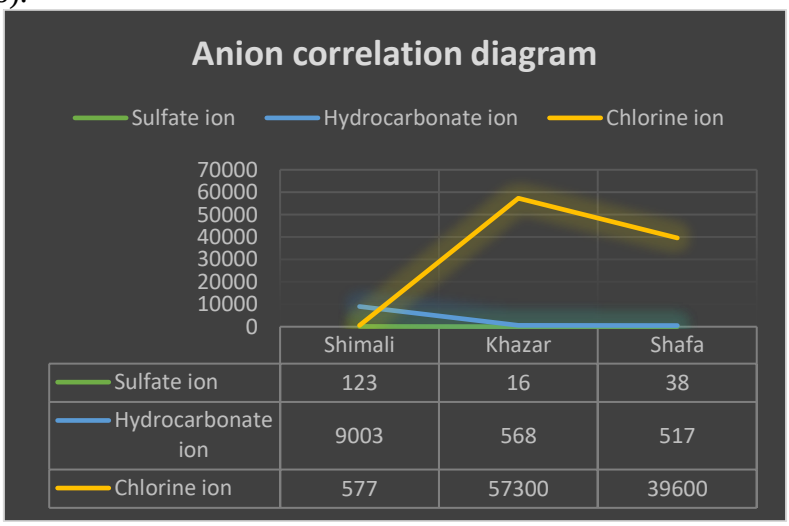

Fig.5. Correlation diagram of sulfate ion, hydrogen carbonate ion and chlorine ion

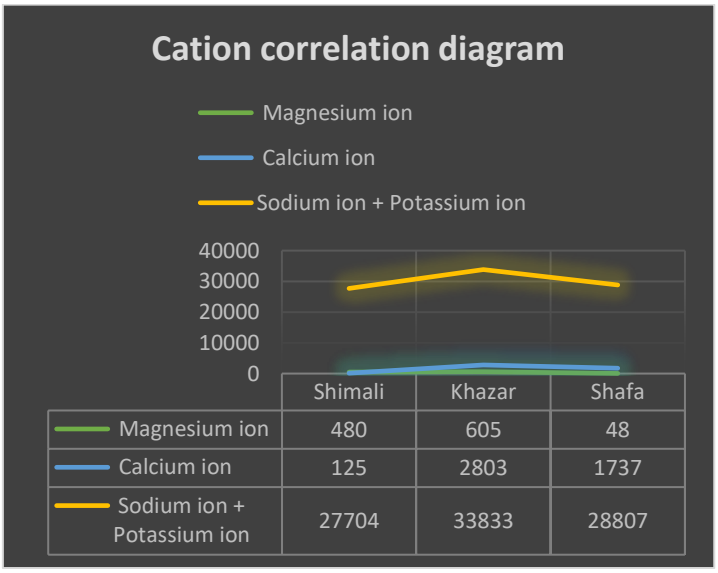

Fig.6. Correlation diagram of chlorine, calcium and sodium ions with potassium in general

ISNN: print 2663-7006; online 2709-2666

CONCLUSION

In conclusion, we can explain that the chemical composition we determined from three hydrogen sulfide sources : “Shimali-1” village , the camp site “Khazar” and camp site “Shafa” . They allows us to conclude that the good health of the population of the village of Shimali -1 is due to the fact that they use water from hydrogen sulfide sources as drinking water for daily consumption, which provides them with good complexion excellent skin and silky hair.

REFERENCES

1. Barbu M., Santin I., Vilanova R. Applying Control Actions for Water Line and Sludge Line To Increase Wastewater Treatment Plant Performance. Ind. Eng. Chem. Res. 2018, 57, pp. 5630–5638
2. Quadros S., Joao Rosa M., Alegre H., Silva C. A performance indicators system for urban wastewater treatment plants. Water Sci. Technol. 2010, 62, pp. 2398–2407
3. Mudriy I.V. Protection of water supply sources from static surfactants (review) Hygiene and sanitation. 1996, №4, pp. 6-8
4. Aliev A.M. Hydrogeodynamic conditions of seismicity of the territory of Azerbaijan. Azərb. EA News, Earth Sciences.1999, № 1, pp. 76-84
5. Memmedov A.V., Akhmadbeyli F.S., Shirinov A.N. Neotectonics of Azerbaijan (a short description of the neotectonic map). Proceedings of the Institute of Geology of AMEA.1998, №26, pp. 43-49

ИССЛЕДОВАНИЕ ХИМИЧЕСКОГО СОСТАВА ВОДЫ СЕРОВОДОРОДНЫХ ИСТОЧНИКОВ НА ТЕРРИТОРИИ ШИМАЛИ

Н.А.Гулиева , З.В.Абдулазимова
Азербайджанский Государственный Университет Нефти и Промышленности
zarifaabdulazimova@mail.com

В данной статье исследуется химический состав сероводородных вод Хачмазского района из трех источников сероводорода на территории Шимали, а именно из турбазы Хазар, из турбазы Шафа, а также из одного из центральных сел, население которого славится крепким здоровьем деревня Шимали-1. Проведен сравнительный анализ взаимосвязи между соленостью подземных вод, хлорид-ионами, HCO_3^- и концентрацией H_2S. Проведен мониторинг нескольких источников сероводорода на предмет наличия и количественного определения иона Cl^- в них, а также установленния факторов окружающей среды, влияющих на сохранность этих источников.

Ключевые слова: *хлорид-ион, сероводород (H_2S), экология, титрование.*

ŞİMALİ ƏRAZİSİNDƏ HİDROGEN SULFİD TƏRKİBLİ YERALTI SU MƏNBƏLƏRİNİN KİMYƏVİ ANALİZİ

N.A.Quliyeva , Z.V.Abduazimova
Azərbaycan Dövlət Neft və Sənaye Universiteti
zarifaabdulazimova@gmail.com

Məqalədə Shimali ərazisindəki üç hidrogen sulfid mənbəyindən, yəni Şəfa düşərgəsindən Xəzər

düşərgə sahəsindən, həm də əhalisi Şimali kəndinin sağlamlığı ilə məşhur olan mərkəzi kəndlərdən birindən Xaçmaz bölgəsinin hidrogen sulfid sularının kimyəvi tərkibi araşdırılmışdır. Yeraltı suların duzluluğu, xlorid ionları, HCO_3^- və H_2S konsentrasiyası arasındakı əlaqənin müqayisəli təhlili aparılmışdır. Hidrogen sulfid mənbələrinin içərisində Cl^- ionun olması və miqdarı, habelə bu mənbələrin təhlükəsizliyinə təsir edən müəyyən edilmiş ətraf mühit faktorları üçün analizi aparılmışdır.
Açar sözlər: *xlorid ionu, hidrogen sulfid (H_2S), ekologiya, titrləmə.*

ISNN: print 2663-7006; online 2709-2666

AJCN, Vol 3, No. 3, 2021, pp. 64-72

UDC:666.965.2

RESEARCH OF HEAT-INSULATING PROPERTIES OF FOAMED CONCRETES ON BASIS OF BRICK WASTES

Y.N.Gahramanli, R.V.Gurbanova, B.A.Samedzadeh
Azerbaijan State Oil and Industrial University
y.gahramanli@asoiu.edu.az

Researches on studying of heat-insulating properties of the obtained geopolymeric foamed concretes on basis of brick wastes were conducted. Content of alkali solution in the initial composite was varied at the level of 20%mass. The composite with ratio of brick wastes to binder equal 80:20 was taken for research. Volume weight of the researched specimens was varied from 558 kg/m^3 up to 1656 kg/m^3. Temperature of heat flow meter was kept up at the level of 40, 50 and 60^{0}C. It was established that specimens with volume weight 558 kg/m^3 at temperature 60^{0}C have the least value of coefficient of thermal conductivity which makes up 0.03 W/(mK). It was also established that the obtained specimens of geopolymeric foamed concrete can be recommended for the using as heat-insulating materials.
Keywords: *geopolymer, foamed concrete, coefficient of thermal conductivity, brick wastes.*

INTRODUCTION

On modern stage of mankind development, the questions connected with environmental protection from anthropogenic influence are very topical and important. It is known that as a result of life activity of human the huge amounts of industrial and domestic wastes are throwed out into the atmosphere, lithosphere, hydrosphere and biosphere of the Planet. Therefore, it is important to correctly utilize and to rationally use these wastes. Wastes, particularly solid wastes of construction and industry, can be reused for an obtaining of new materials with required properties. Importance of wastes is that they are generated in big industrial centers and towns and therefore there is not a necessity to transport them at long range. On the other hand, they have got low cost and this fact has a great importance. Therefore, the obtaining of new materials with predetermined properties on basis of wastes is important problem which is being studied by all world scientific community. Taking into account a specificity of local brick manufacturing and presence of huge amounts of brick wastes, such types of wastes of constructional and industrial origin were used.

The other and important problem is the decreasing of carbon dioxide emissions into the atmosphere. This problem has a great topicality nowadays, because the average temperature on the Planet rises due to greenhouse effect. Carbon dioxide emissions is mainly related to power industry. The greater consumption of heat and electric energy, the greater emissions of carbon dioxide into the atmosphere. Therefore, the decreasing of heat and electric energy consumption is one of ways of a decreasing of carbon dioxide emissions. It is achieved by using of heat-insulating materials in construction. These materials can be used in the masonry of walls and various ceilings. The using of heat-insulating materials makes it possible to keep a heat in winter and coolness in summer in the rooms. This circumstance promotes considerable saving of power resources. It means that emissions of carbon dioxide into atmosphere can be considerably decreased. Many researches in the field of creation of sound-proof and heat-insulating materials are being conducted. [1-7]

Thus, an obtaining and research of heat-insulating properties of the materials are

rather topical problem, therefore the attempt of a studying of heat-insulating properties of the obtained geopolymeric foamed concretes on basis of brick wastes was undertaken by us in this work.

EXPERIMENTAL PART

The composites of geopolymeric foamed concretes containing such main constituents as filler (brick wastes) and binder with ratio 80:20 were taken for research of their heat-insulating properties. The procedure of the obtaining of the given composites was explained in work [8].

Thermal conductivity of foamed concretes was researched according to GOST 7076-66. Tests were conducted on laboratory unit (fig.1).

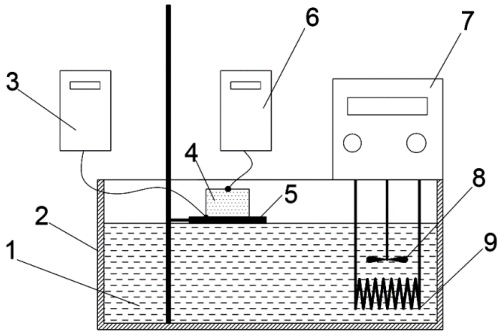

Fig.1. Laboratory unit for determination of coefficient of thermal conductivity: 1- heat-transfer agent; 2- thermostatic system; 3- temperature-sensing device for measuring of temperature of heat flow meter; 4- tested specimen; 5- heat flow meter; 6- temperature-sensing device for measuring of temperature of specimen; 7- control module; 8- stirrer; 9- heating element.

The laboratory unit involves a thermostatic system 2 containing heat-transfer agent 1 (water). The specimen is set on the table 5 made from the quick-response heat flow meter. Heat-transfer agent is heated at the expense of heating element 9. Its temperature is controlled by control module 7. The stirrer 8 continually agitates a heat-transfer agent for uniform distribution of temperature in all volume of thermostat. Temperatures of heat flow meter and top of the specimen are measured by means of two thermocouples 3 and 6.

The tested specimen must have a plane-parallel facets and cube form. The thickness of the specimen must make up 40 mm. Thickness of the specimen is measured by Vernier caliper with accuracy 0.1 mm and is a result of four measurements. Before testing, the specimens must be dried at 105-110^{0}C up to constant weight.

At conducting of testing, the specimen is set on the table of heat flow meter and clutched by special device on top. Thermocouples are set on top facet of specimen and on the heat flow meter. Then temperature of heating is set by means of control module. After installation of a steady-state regime the temperature is measured by two thermocouples 3 and 6. Herewith, temperature of heat flow meter must not be changed

ISNN: print 2663-7006; online 2709-2666

within 30 minutes.

Calculation of results of measurement is carried out as follows. Coefficient of thermal conductivity is determined in accordance with the formula:

$$\lambda = \frac{Q \cdot \delta}{t_1 - t_2},$$

where δ – is a thickness of specimen, m; t_1- is a temperature of hot surface of specimen, ^{0}C; t_2- is a temperature of cool surface of specimen, ^{0}C; Q- is a heat quantity passing through the specimen in direction which is perpendicular to its surface, kcal/m^{2}hour.

At measuring of heat quantity by quick-response heat flow meter the calculation is carried out in accordance with the following formula:

$$Q = \frac{0{,}86 \cdot R \cdot I^2}{F},$$

where R- is a constant resistance of heater of heat flow meter, Om; I- is a current strength, A; F- is a cross sectional area, m^2.

Temperature of specimen surfaces is measured at steady-state regime with accuracy of 0.1^{0}C. Coefficient of thermal conductivity is calculated with accuracy of 0.001 W/m·K.

RESULTS AND DISCUSSION

As it was said above, it was necessary to obtain the heat-insulating materials (foamed concretes) on basis of unconventional concretes. To this end, the researches of changing of materials thermal conductivity depending on various rate of foaming or volume weight were conducted according to GOST 7076-66. Main measure of thermal conductivity of material and their heat insulating properties is coefficient of thermal conductivity (λ, W/mK). As it is known, thermal conductivity is capability of a material to conduct a heat energy. Herewith, a heat transfer takes place from body with high temperature to body with low temperature at the expense of Brownian motion (thermal motion) of molecules, atoms etc. Thus, if there is non-uniform distribution of temperatures in the bodies, then heat transfer takes place. In this case, mechanism of heat transfer will depend on aggregate state of a matter. There are two main mechanisms of thermal conductivity in solids. This is mechanism of thermal conductivity by free electrons (electronic thermal conductivity) and mechanism of atomic oscillations (background or lattice conductivity). Besides, the first one is characteristic for metals and the second one (background conductivity) is characteristic for dielectrics. In case of lattice conductivity, atoms located in knots of crystal lattice are combined with each other by elastic forces. Due to this, oscillations appearing in some point of crystal lattice will be spread in all directions in the form of elastic waves. Thermal oscillations are spread by the similar way.

Thus, thermal conductivity is a wavelike transfer of thermal energy. This transfer is directed to such points of crystal lattice where the knots of the lattice is excited least. In other words, capability of a material to conduct heat is characterized by coefficient of thermal conductivity which represents a heat quantity transferring through the homogeneous specimen of a material of unit length and area for a unit time at unit temperature difference.

Researches of specimens of foamed concrete at certain ratio of constituents (brick wastes:binder = 80:20) were conducted. Herewith, a content of alkali solution in the initial mixture made up 20%mass, because only in this case the least values of volume weight and maximal values of rate of foaming were observed. [8] Research was

conducted at three different temperatures (40, 50 and 60^0C). During a conducting of the research, we had to find out how the thermal conductivity of a material is changed depending on changing of volume weight of specimens at different temperatures.

Diagram of changing of coefficient of thermal conductivity of specimens depending on changing of volume weight at temperature of heat flow meter equal 40^0C is presented on fig.2.

From the presented diagram one can see that an increasing of volume weight of foamed concrete leads to sharp increasing of coefficient of thermal conductivity. Herewith, an increasing of volume weight from 558 up to 1656 kg/m^3 leads to increasing of coefficient of thermal conductivity from 0.08 up to 0.21 W/(mK), that is, in 2.6 times. The reason of such increasing of thermal conductivity can be explained as follows. It is known that increasing of volume weight of specimens with equal weight leads to decreasing of porosity of a material, that is, to decreasing its free volume. Herewith, material is compacted and sizes of its pores are also decreased. It is known that air is a poor conductor of heat. At decreasing of diameter of pores and free volume, quantity of air filling this volume is also decreased. Besides that, size of air layers filling these pores becomes considerably thinner. As air is a natural heat insulator, the decreasing its quantity in volume of material inevitably leads to deterioration of its heat-insulating properties and to increasing of coefficient of thermal conductivity.

Besides that, it should be taken into account the presence of hydrogen which is gasifier at forming of the porous or foamed structures. Hydrogen can be contained in some closed cells or pores of material. Its quantity also tends to zero at increasing of volume weight of a material. Compaction of material leads to prevalence of mechanism of lattice conductivity, that is, heat oscillations in the knots of crystal lattice can be transferred at long range in all volume of material. Sufficiently low values of coefficient of thermal conductivity of initial monolithic specimen can be explained by its structural inhomogeneity, that is, by alternation of different crystal structures in it which are located neighborly. This is three-dimensional lattice structure of binder and crystal structure of brick wastes.

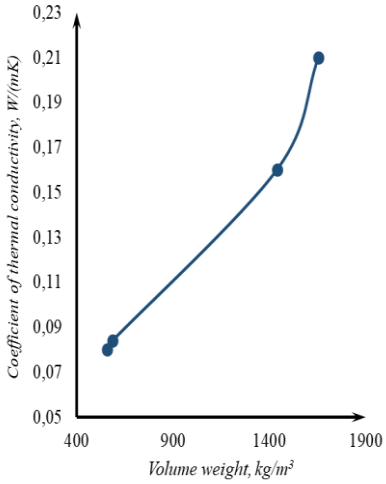

Fig.2. Dependence of changing of coefficient of thermal conductivity of foamed concretes from volume weight at temperature of heat flow meter equal 40^0C

Besides that, presence of rather inhomogeneous impurities in the structure of

ISNN: print 2663-7006; online 2709-2666

foamed concrete also prevents the spreading of heat waves in volume of material. This circumstance can lead to local overheating in the material. It must be taken into account at creating of materials on basis of various wastes.

Then researches of thermal conductivity of foamed concretes at 50^0C were conducted. The results of the conducted experiments are shown on fig.3. From the represented diagram one can see

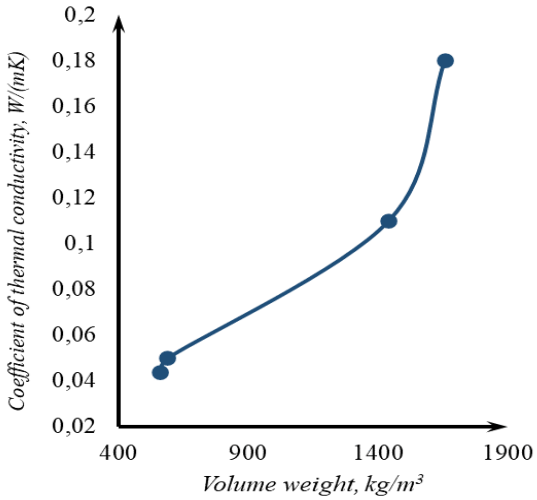

Fig.3. Dependence of changing of coefficient of thermal conductivity of foamed concretes from volume weight at temperature of heat flow meter equal 50^0C

that increasing of volume weight also promotes rapid increasing of coefficient of thermal conductivity of specimens. Herewith, increasing of volume weight from 558 up to 1656 kg/m^3 leads to increasing of coefficient of thermal conductivity from 0.044 up to 0.18 W/(mK), that is, in 4.1 times. Besides that, increasing of temperature gradient on the opposite sides of the specimen leads to sharp decreasing of thermal conductivity over the range 1450-1600 kg/m^3. It is represented by characteristic inflection of curve in the given diapason. The mechanism of changing of coefficient of thermal conductivity is the same as on fig.2. It was explained above. The difference is that higher temperatures create more gradient of temperatures on the opposite sides of specimen. This circumstance leads to relatively low values of coefficient of thermal conductivity in comparison with abovementioned case presented on fig.2.

Researches of coefficient of thermal conductivity were also conducted at temperature of heat flow meter equal 60^0C. The results of the conducted experiments are presented on fig.4.

One can see from the figure that increasing of volume weight of specimens promotes the rising of coefficient of thermal conductivity. Herewith, increasing of volume weight from 558 up to 1656 kg/m^3 leads to increasing of coefficient of thermal conductivity from 0.034 up to 0.16 W/(mK), that is, approximately in 4.7 times. The more characteristic inflection of the curve in diapason 1450-1600 kg/m^3 and relatively low values of coefficient of thermal conductivity are also observed in this case. It is explained by the more gradient of temperatures on the opposite sides of the specimen. Herewith, the sharper decreasing of coefficient of thermal conductivity is observed on the given diapason.

At comparative considering of the curves presented on fig.2, 3 and 4 one can notice that at increasing of volume weight of specimens more than 1400 kg/m^3 the sharp rising of coefficient of

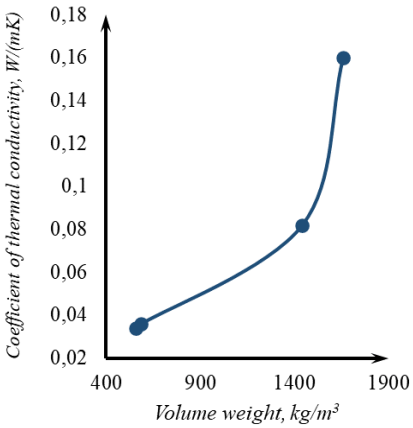

Fig.4. Dependence of changing of coefficient of thermal conductivity of foamed concretes from volume weight at temperature of heat flow meter equal 60^{0}C.

thermal conductivity is observed in all cases. This fact has got the following explanation. At increasing of volume weight a portion of free, unoccupied volume is decreased. Herewith, size of pores is also decreased. They become more narrow and smaller. At decreasing of size of pores, the volume of air interlayer in them is also decreased. But decreasing of volume of air interlayer in each certain pore and in the volume of material as a whole leads to deterioration of heat-insulating properties. This circumstance is a reason of increasing of coefficient of thermal conductivity. Thus, some critical value of volume weight is observed in diapason of values of volume weight 1400-1500 kg/m^3. At this critical value, the material structure turns into the monolithic structure with lowest content of free volume. That is, if value of volume weight is higher than that critical value, then material mainly will be non-porous and monolithic. It should be noted that at increasing of temperature of specimens testing from 40^{0}C up to 60^{0}C the abovementioned transition is observed more clearly.

Thus, the conducted researches of volume weight of foamed concretes make it possible to assert that changing of coefficient of thermal conductivity of specimens correlates with changing of their volume weight and has a scientific explanation. Besides that, specimens of foamed concretes with volume weight 558-900 kg/m^3 in accordance with values of their coefficient of thermal conductivity can be considered as heat-insulating materials. Herewith, values of coefficient of thermal conductivity correspond to values for foamed concretes which make up 0.05-0.3 W/(mK). In some cases, these values even surpass the given indices.

Coefficients of thermal conductivity of some wide-spread materials are presented below in table 1. At considering of the given table one can make a conclusion that the foamed materials obtained on basis of brick wastes have got heat-insulating properties which quite correspond to properties of conventional foamed concretes and even to properties of such materials as glass wool and foamed polyurethane. This circumstance argues about high heat-insulating properties of the obtained materials.

ISNN: print 2663-7006; online 2709-2666

Table 1

Coefficients of thermal conductivity of some materials

Material	Coefficient of thermal conductivity, W/mK
Amianthus	0,15
asbestos-cement plate	0,35
porous concrete	1,4
monolithic concrete	1,75
thermo-insulating concrete	0,18
Paper	0,14
light mineral wool	0,045
woolen felt	0,045
gypsum plaster	0,35
Wood	0,15
reinforced concrete	1,7
Limestone	1,7
Stone	1,4
foamed rubber	0,03
natural rubber	0,042
ceramsite concrete	0,2
clay brick	0,15
cavity brick	0,44
lime-and-sand brick	0,81
solid brick	0,67
slag brick	0,58
foamed concrete	0,3
foamed plastic PS-4	0,04
foamed plastic PVC-1	0,05
foamed polystyrene PS-B	0,04
foamed polyurethane	0,035
light foamed glass	0,06
Polystyrene	0,082
Ruberoid	0,17
glass wool	0,05
glass fiber	0,036
expanded ebonite	0,03

CONCLUSION

1. The increasing of volume weight of specimens from 558 kg/m^3 up to 1656 kg/m^3 at temperature of heat flow meter 40^{0}C leads to increasing of coefficient of thermal conductivity from 0.08 W/(mk) up to 0.21 W/(mk), that is, in 2.6 times.
2. The increasing of volume weight of specimens from 558 kg/m^3 up to 1656 kg/m^3 at temperature of heat flow meter 50^{0}C leads to increasing of coefficient of thermal conductivity from 0.044 W/(mk) up to 0.18 W/(mk), that is, in 4.1 times.
3. The increasing of volume weight of specimens from 558 kg/m^3 up to 1656 kg/m^3 at temperature of heat flow meter 60^{0}C leads to increasing of coefficient of thermal

conductivity from 0.034 W/(mk) up to 0.16 W/(mk), that is, in 4.7 times.

4. Heat-insulating properties of materials become more strongly pronounced at higher temperatures of heat flow meter.
5. The obtained specimens of geopolymeric foamed concrete can be used as heat-insulating materials.

REFERENCES

1. Hussam Alghamdi, Narayanan Neithalath. Synthesis and characterization of 3D-printable geopolymeric foams for thermally efficient building envelope materials. Cement and Concrete Composites**.** 2019, Vol.104, 103377 p
2. Chengying Bai, TaoNi, Qiaoling Wang, Hongqiang Li, Paolo Colombo. Porosity, mechanical and insulating properties of geopolymer foams using vegetable oil as the stabilizing agent. Journal of the European Ceramic Society**.** 2018,Vol.38, Issue 2, February , pp.799-805
3. Rui M.Novais LucianoSenff, João Carvalheiras, Maria P.Seabra, Robert C.Pullar, João A.Labrincha. Sustainable and efficient cork - inorganic polymer composites: An innovative and eco-friendly approach to produce ultra-lightweight and low thermal conductivity materials. Cement and Concrete Composites**.** 2019, Vol. 97, pp.107-117
4. El-Naggar K.A.M., Amin Sh.K., El-Sherbiny S.A, .Abadir M.F. Preparation of geopolymer insulating bricks from waste raw materials. Construction and Building Materials**.** 20 October 2019, Vol. 222, pp. 699-705
5. Nur Ain Jaya, Liew Yun-Ming, Heah Cheng-Yong, Mohd Mustafa Al Bakri Abdullah, Low Foo Wah, Ooi Wan-En, Ilham Mukriz Zainal Abidin, Noorhazleena Azaman. Effect of anisotropic pores on the material properties of metakaolin geopolymer composites incorporated with corrugated fiberboard and rubber. Journal of Materials Research and Technology. September-October 2021, Vol. 14, pp. 822-834
6. Buruberri L.H., .Senff L., .Seabra M.P., .Labrincha J.A. Effect of Al anodizing waste on the final properties of porous geopolymers. Construction and Building Materials**.** 10 December 2020, Vol. 263, 2020, 120-160
7. Hassan Soltan Hassan., .Abdel-Gawwad H.A., . Vásquez García S.R., Isabel Israde-Alcántara. Fabrication and characterization of thermally-insulating coconut ash-based geopolymer foam. Waste Management**.** Vol.80, October 2018, pp. 235-240
8. Gahramanli Y.N.,Hajiyeva R.Sh.,Hasanova M.B.,Samedzadeh B.A. An obtaining of foamed composites on basis of ceramic wastes and research their volume weight. Azerbaijan journal of chemical news. 2020, Vol.1, № 1, pp. 4-13

ISNN: print 2663-7006; online 2709-2666

ИССЛЕДОВАНИЕ ТЕПЛОИЗОЛЯЦИОННЫХ СВОЙСТВ ПЕНОБЕТОНОВ НА ОСНОВЕ КИРПИЧНЫХ ОТХОДОВ

Ю.Н.Кахраманлы, Р.В.Гурбанова, Б.А.Самедзаде
Азербайджанский Государственный Университет Нефти и Промышленности
y.gahramanli@asoiu.edu.az

Проведены исследования по изучению теплоизоляционных свойств полученных вспененных геополимерных бетонов на основе кирпичных отходов. В исходной композиции содержание раствора щелочи составляло 20%масс. Для исследований была взята композиция с соотношением кирпичный отход:связующее = 80:20. Объемная масса исследуемых образцов варьировалась от 558 до 1656 кг/м^3. Температура тепломера поддерживалась на уровне 40, 50 и 60^{0}C. Было установлено, что образцы с объемной массой 558 кг/м^3 при температуре тепломера 60^{0}C имеет наименьший коэффициент теплопроводности 0,03 Вт/(мК). Полученные образцы геополимерного пенобетона могут быть рекомендованы к использованию в качестве теплоизоляционных материалов.
***Ключевые слова**: геополимер, пенобетон, коэффициент теплопроводности, кирпичные отходы.*

KƏRPİC TULLANTILARI ƏSASINDA KÖPÜKLƏNMİŞ BETONLARIN İSTİLİK İZOLYASİYA XASSƏLƏRİNİN TƏDQİQİ

Y.N.Qəhrəmanlı, R.V.Qurbanova, B.Ə.Səmədzadə
Azərbaycan Dövlət Neft və Sənaye Universiteti
y.gahramanli@asoiu.edu.az

Kərpic tullantıları əsasında alınmış köpüklənmiş geopolimer betonlarının istilik izolyasiya xassələrinin öyrənilməsi üzrə tədqiqatlar aparılmışdır. İlkin kompozisiyada qələvi məhlulunun miqdarı 20%küt. səviyyəsində saxlanılırdı. Tədqiqatların aparılması üçün tərkibində kərpic tullantıların əlaqələndiriciyə nisbəti 80:20 olan kompozisiya götürülmüşdür. Tədqiq olunan nümunələrin həcm kütləsi 558-dən 1656 kq/m^3 kimi dəyişirdi. İstilik ölçənin temperaturu 40, 50 və 60^{0}C səviyyəsində saxlanılırdı. Müəyyən edilmişdir ki, istilik ölçənin temperaturu 60^{0}C olduqda həcm kütləsi 558 kq/m^3 olan nümunələrin istilikkeçirmə əmsalı minimal olur və 0,03 Vt/(mK) təşkil edir. Köpüklənmiş geopolimer betonunun alınmış nümunələri istilik izolyasiya materialları kimi istifadə üçün tövsiyə edilə bilər.
***Açar sözlər:** geopolimer, köpüklənmiş beton, istilikkeçirmə əmsalı, kərpic tullantıları.*

AJCN, Vol 3, No. 3, 2021, pp. 73-76

UOT 544.478.1

THE ACTIVITY OF MOLYBDENE-VANADIUM OXIDE CATALYSTS IN THE ISOPROPYL ALCOHOL CONVERSION REACTION

N.I.Dushdurova
Azerbaijan State Oil and Industry University
nurlana.dushdurova@mail.ru

The activity of molybdenum-vanadium oxide catalysts in the conversion of isopropyl alcohol has been studied. It was found that acetone and propylene are the main products of the isopropyl alcohol conversion reaction. Studies have shown that the activity of binary molybdenum-vanadium oxide catalysts depends both on the reaction conditions and on the atomic ratio of molybdenum to vanadium. It has been shown that molybdenum-vanadium oxide catalysts have a sufficiently high activity in the reaction of propylene and acetone formation and can be used for further modification in order to increase their catalytic activity.
Keywords: *isopropyl alcohol, acetone, propylene, binary catalysts, molybdenum oxide, vanadium oxide.*

INTRODUCTION

For sustainable development in recent years, more and more attention of scientists is turned to obtaining valuable chemical products from renewable raw materials. This is because the use of renewable resources in industry leads to a decrease in emissions of greenhouse gases and toxic substances into the environment, which helps to reduce the negative impact of industry on the environment. It is known from the periodical literature that the most promising renewable resources are ethanol, isopropanol and butanol [1]. Isopropanol is an important feedstock for various chemicals and is used in many industrial processes as solvents, oils, varnishes and cosmetics, or as an antiseptic and disinfectant [2]. The conversion reaction of isopropyl alcohol can produce such valuable compounds as propylene, acetone, etc. [3].

It is known from the periodical literature that binary and complex catalysts based on vanadium and molybdenum oxides exhibit a high selectivity in the reactions of conversion of organic compounds [4,5,6]. In this regard, in this work, we investigated the activities of vanadium-molybdenum oxide catalysts of various compositions in the conversion of isopropyl alcohol.

EXPERIMENTAL PART

Molybdenum-vanadium oxide catalysts of various compositions were prepared by precipitation of aqueous solutions of ammonium molybdenum acid and ammonium metavanadate. The resulting mixture was evaporated and dried at a temperature of 100-110°C, then calcined at a temperature of 200-250°C until the complete release of nitrogen oxides. After that, the obtained samples were calcined at a temperature of 600° C for 10 hours. The catalytic activity of the synthesized samples was studied on a flow-through unit with a tubular reactor in the temperature range 150-450°C. For this purpose, 5 ml of catalyst with a grain size of 1-2 mm was loaded into the reactor and a reaction mixture consisting of a mixture of isopropyl alcohol and water and nitrogen was passed through the catalyst. The volumetric feed rate of the raw material was 1200 h^{-1}. The ratio of the starting reagents was alcohol: nitrogen: H_2O = 1: 5: 4. Analysis of

ISNN: print 2663-7006; online 2709-2666

raw materials and reaction products was carried out by chromatographic method. The analysis of condensed propylene, acetone, and isopropyl alcohol was carried out by chromatography with a flame ionization detector using a column filled with a Celite sorbent with 15000 polyethylene glycol phases deposited on its surface in an amount of 15%. C_1 -C_3 hydrocarbons and carbon dioxide were analyzed on a chromatograph with a thermal conductivity detector and a column length of 5 m. The stationary phase was an ester of diethylene glycol and n-butyric acid deposited on an INZ-600 Insensky brick.

RESULTS AND DISCUSSION

Studies have shown that the products of isopropyl alcohol conversion are acetone and propylene. At high temperatures, a small amount of isopropyl alcohol decomposition products is also observed. As an example, Figure 1 shows the results of a study of the conversion of isopropyl alcohol on a catalyst Mo-V=1-9. As can be seen from fig.1 the conversion of isopropyl alcohol on the studied catalyst begins at a temperature of 150°C with the formation of 11.5% propylene. As the obtained data show, the yield of the dehydration product of isopropyl alcohol, namely propylene, passes through a maximum with an increase in the reaction temperature. Thus, the highest propylene yield is observed at a temperature of 300°C and reaches 70.5%. The formation of acetone on the studied sample begins at a temperature of 200°C (1.7%). With an increase in the reaction temperature, the yield of acetone passes through a maximum at 350°C.

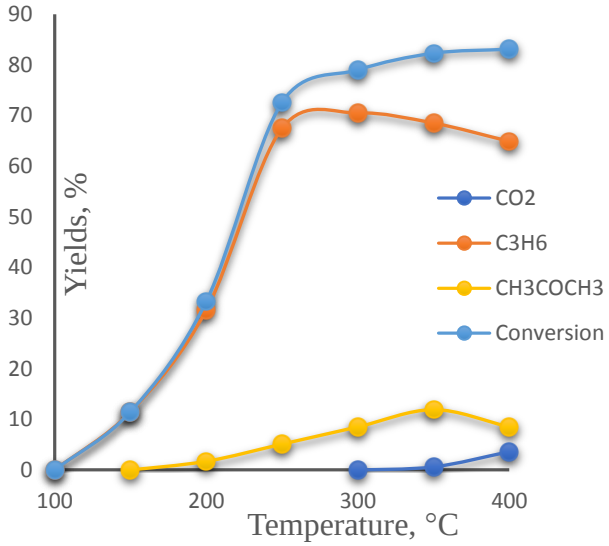

Fig.1. Influence of temperature on the yields of isopropyl alcohol conversion products on the catalyst Mo-V = 1-9

As can be seen at this temperature, the acetone yield reaches 11.9%. The formation of carbon dioxide, as seen from Figure 1, is observed at temperatures above 350°C and does not exceed 3.6%. The formation of carbon dioxide at high temperatures is apparently due to oxygen oxidation of the catalyst lattice of the feedstock and or reaction products. As can be seen from fig.1, the conversion of isopropyl alcohol on the catalyst Mo-V = 1-9 reaches about 83.1%.

Experiments have shown that the activity of molybdenum-vanadium oxide catalysts in the conversion of isopropyl alcohol also strongly depends on the atomic ratio of molybdenum to vanadium. Figure 2 shows the dependences of the yields of isopropyl alcohol conversion products on the atomic ratio of molybdenum to vanadium at a temperature of 250°C.

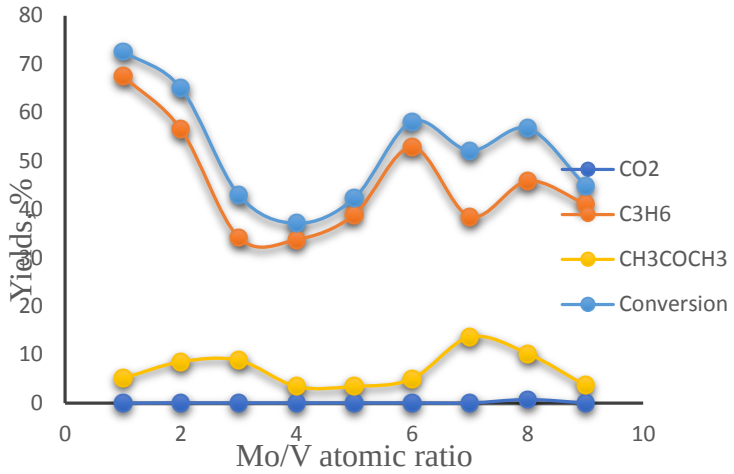

Fig.2. Dependences of the yields of isopropyl alcohol conversion products on the atomic ratio of molybdenum to vanadium. T = 250°C

As can be seen from Fig. 2, with an increase in the atomic ratio of molybdenum to vanadium, the propylene yield first decreases, reaching a minimum on the Mo-V = 3-7 sample and then begins to increase to 52.8% on the Mo-V = 6-4 sample, after which it decreases again. As can be seen from Fig. 2, the dependence of the acetone yield with an increase in the atomic ratio of molybdenum to vanadium has the form of a curve with two maxima on the catalysts Mo-V = 3-7 and Mo-V = 7-3. Figure 2 also shows that the dependence of the conversion of isopropyl alcohol on the atomic ratio of molybdenum to vanadium has the same character as for the yield.

CONCLUSION

Studies have shown that propylene and acetone are the main products of the isopropyl alcohol conversion reaction.

Molybdenum-vanadium oxide catalysts have a high activity in the reaction of partial conversion of isopropyl alcohol, and they are promising for further modification in order to increase their catalytic activity.

REFERENCES

1. Yuki Soma, Kentaro Inokuma, Tsutomu Tanaka, Chiaki Ogino, Akihiko Kondo, Masahiro Okamoto, Taizo Hanai. Direct isopropanol production from cellobiose by engineered Escherichia coli using a synthetic pathway and a cell surface display system. Journal of Bioscience and Bioengineering. 2012, Vol.114, Issue1, July, pp. 80-85
2. El-Molla S.A,.Hammed M.N,.El-Shobaky G.A. Catalytic conversion of isopropanol over NiO/MgO system doped with Li2O. Materials Letters. 2004,Vol.58, Issue 6, pp.1003-1011

ISNN: print 2663-7006; online 2709-2666

3. Anas Benyounes, Mohamed Kacimi, Mahfoud Ziyad, Philippe Serp. Conversion of isopropyl alcohol over Ru and Pd loaded N-doped carbon nanotubes. Chinese Journal of Catalysis.Vol.35, Issue 6, 2014, pp. 970-978
4. Mamoru Ai, Partial oxidation of propylene on V2O5, P2O5-based catalysts, Journal of Catalysis. Vol.101, Issue 2, October 1986, pp 473–483
5. .Concepción P,. Botella P,. López J.M Nieto, Catalytic and FT-IR study on the reaction pathway for oxidation of propane and propylene on V- or Mo–V-based catalysts, Applied Catalysis A: General.Vol.278, Issue 1, 28 December, 2004,pp. 45–56
6. Abd El-Salaam K.M , Hassan E.A, Studies on the heterogeneous oxidation of 1-butene over V_2O_5-MoO_3 catalysts, Surface Technology.Vol.l9, Issue 3, September 1979, pp. 195–202

АКТИВНОСТЬ МОЛИБДЕН-ВАНАДИЙ ОКСИДНЫХ КАТАЛИЗАТОРОВ В РЕАКЦИИ ПРЕВРАЩЕНИЯ ИЗОПРОПИЛОВОГО СПИРТА

Н.И.Душдурова
Азербайджанский Государственный Университет Нефти и Промышленности
nurlana.dushdurova@mail.ru

Изучена активность катализаторов на основе оксида молибдена и ванадия в превращении изопропилового спирта. Установлено, что основными продуктами реакции превращения изопропилового спирта являются ацетон и пропилен. Исследования показали, что активность бинарных катализаторов на основе оксида молибдена и ванадия зависит как от условий реакции, так и от атомного отношения молибдена к ванадию. Показано, что катализаторы на основе оксида молибдена-ванадия обладают достаточно высокой активностью в реакции образования пропилена и ацетона и могут быть использованы для дальнейшей модификации с целью повышения их каталитической активности .
Ключевые слова: *изопропиловый спирт, ацетон, пропилен, бинарные катализаторы, оксид молибдена, оксид ванадия.*

MOLİBDEN-VANADIUM OKSID KATALİZATORLARIN İZOPROPİL SPİRTİN ÇEVRİLMƏSİ REAKSİYASINDA AKTİVLİYİ

N.I.Duşdurova
Azərbaycan Dövlət Neft və Sənaye Universiteti
nurlana.dushdurova@mail.ru

Molibden-vanadium oksid katalizatorlarının izopropil spirtinin çevrilməsi reaksiyasında aktivliyi öyrənilmişdir. Müəyyən edilmişdir ki izopropil spirtin çevrilmə reaksiyasının əsas məhsulları aseton və propilendir. Aparılmış tədqiqatlar göstərmişdir ki binar molibden-vanadium oksid katalizatorlarının aktivliyi həm reaksiya şəraitindən, həm də molibdenin vanadiuma atom nisbətindən asılıdırlar. Müəyyən edilmişdir ki Molibden-vanadium oksid katalizatorları propilen və aseton əmələ gəlməsi reaksiyasında kifayət qədər yüksək aktivliyə malikdirlər və onların katalitik aktivliyini artırmaq üçün əlavə modifikasiya üçün istifadə oluna bilər.
Açar sözlər: *izopropil spirti, aseton, propilen, binar katalizatorlar, molibden oksidi, vanadium oksidi.*

AJCN, Vol 3, No. 3, 2021, pp. 77-84

UOT: 54-76; 543.51; 543.06

SORPTION PROPERTIES OF RUTILE PHASE TiO_2 NANOPARTICLES

S.R. Hajiyeva, E.M. Gadirova
Baku State University
elmina2010@mail.ru

There are many scientific studies on phenol adsorption. Sorption of phenol in the presence of activated carbon, graphite oxide and other adsorbents is very common. This article is the first to study the sorption properties of TiO_2nanoparticles with a rutile phase; TiO_2 nanoparticles with a rutile phase were synthesized by the sol-gel method and used as an adsorbent. Later the process of adsorption of a 1 mgL^{-1} phenol solution in the presence of rutile TiO_2 nanoparticles was studied. The adsorption process lasted 2 hours at a temperature of 25°C.Although the rutile TiO_2 phase is a very good photocatalyst it has been shown to be a weak adsorbent. Nano crystalline TiO_2 particles of the rutile phase were characterized by powder X-ray diffraction (XRD).The course of adsorption was studied on the device "Varian Cary 50". Based on the curves plotted on the "Varian Cary 50" it was determined that adsorption was incomplete. At the end of the process judging by the graph we can say that the amount of phenol in the solution decreased but phenol still remained which indicates incomplete adsorption. Mathematical modeling of the process has been developed using both logistic and exponential methods.
***Keywords**: nano-TiO_2, phenol, adsorption, XRD, TEM.*

INTRODUCTION

Phenol adsorption purification is one of the studies aimed at solving environmental problems. Adsorption purification of water from phenol is the most important chemical direction, since sorption purification is widespread. According to the literature adsorption processes in the presence of TiO_2 are known [1].Sources also contain information on adsorption by titanium oxide. The use of TiO_2 as an adsorbent with photocatalytic properties offers many advantages: TiO_2 is chemically and thermally stable. TiO_2 which has a photocatalytic effect is widely used to remove toxic substances from various materials. For example, in countries such as Japan and China TiO_2 is added to concrete reinforcement and wall masonry in closed tunnels to purify the air from nitrogen gases [2].

The use of photocatalysis for the purification of waste water from organic micropollutants is an interesting alternative and in recent years has attracted great interest from many researchers. The stage of adsorption of micropollutants on a photocatalyst, mainly of the anatase form of titanium oxide is a decisive stage in the photodegradation process.An experimental study of the adsorption of phenol selected as a model pollutant on a photocatalyst titanium oxide anatase (Degussa P25) is presented. The amount of adsorbed phenol was measured by UV spectroscopy. The equilibrium of adsorption was reached after 1 h; the adsorption kinetics was slow and obeyed the Lagergren model. Adsorption is a single layer chemisorption and follows the Langmuir model. The study also showed the advantage of operating at high stirring speeds and natural pH. Stirring with ultrasound leads to a slight increase in the amount of adsorbed phenol (5%) since this mixing mode reduces the phenomenon of agglomeration of titanium oxide particles and, therefore, increases the catalyst interface area [3].

There are various methods of phenol adsorption[4-7].New composite materials have been developed by impregnating Al_2O_3/TiO_2 cellulose cotton materials and these

ISNN: print 2663-7006; online 2709-2666

composites are widely used for the treatment of toxic solutions[8,9].Cotton is a very good absorbent and absorbs the solution therefore toxic substances in the solution are absorbed together with the solution [10-12]. It has been found that this method can remove any toxic substance from the system. The adsorption of phenol by graphite oxide nanoparticles and activated carbon was also studied [13]. For this purpose, graphite oxide (GO) has recently been used. GO is a graphite oxidation product having a group of carbonyl and carboxyl groups. as well as epoxy and hydroxyl groups at the edges of its layers [14-16].GO is a very valuable membrane material due to its low cost and ease of production, good chemical stability, mechanical strength, and high ability to remove pollutants [17,18].Studies have shown that GO membrane has very good ionic and molecular selectivity and water permeability[19].The use of GO/Al_2O_3 composite membranes for water purification is a subject of growing research interest due to the simple and effective approach they support. On this composite obtained, it was possible to purify phenol from wastewater to 99.9% .There are also articles on the role of TiO_2 in wastewater treatment [20].

EXPERIMENTAL PART

The process was carried out at room temperature and used TiO_2 with the modification of rutile. The adsorption process continued for two hours with periodic stirring. In this case, 0.05 g of TiO_2 and 20 ml of a 1 mgL^{-1} phenol solution were taken and the process was carried out at a temperature of 25^0C.We studied the adsorption properties of TiO_2 nanoparticles with a complete rutile phase. TiO_2 nanoparticles were obtained by the sol-gel method. TiO_2 nanoparticles were analyzed by TEM, SEM, XRD methods (fig.1,2).TiO_2 nanoparticles are spherical with sizes ranging from 10 to 30 nm. SEM and TEM analysis data correlate well with the results obtained by X-ray diffraction (XRD)analysis.

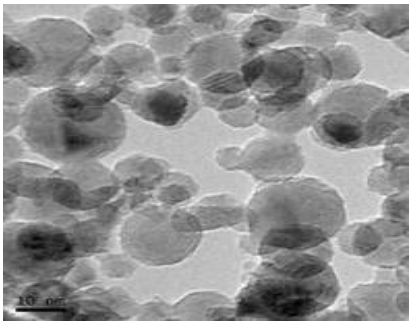

Fig.1. TEM analysis of TiO_2 nanoparticles

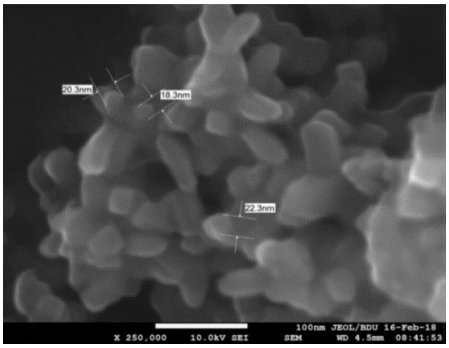

Fig.2. SEM analysis of TiO_2 nanoparticles

The purity and crystalline properties of TiO_2 nanoparticles were studied by powder X-ray diffraction. The graphs of X-ray structural analysis of the studied nanocomposite materials were recorded on a Rigaku Mini Flex 600 powder diffractometer. An X-ray tube with a copper anode (Cu-K α-radiation, 30 kV and mA) was used to draw diffraction spectra at room temperature. At 2θ = 20 ° -80 ° with a discrete growth mode, these spectra were obtained as 2θ = 0.05 ° and the exposure time was τ = 5 seconds.

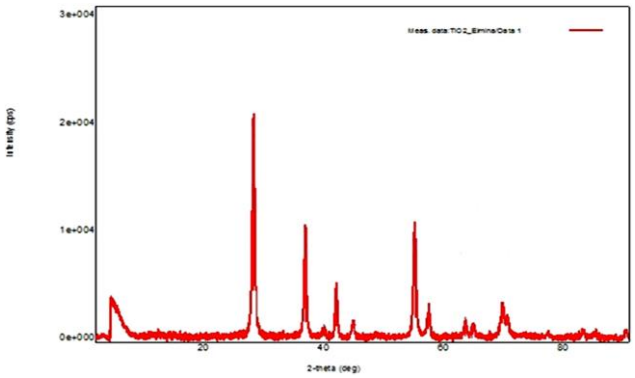

Fig. 3. XRD analysis of TiO_2 nanoparticles

In this work, TiO_2 nanoparticles were used to remove phenol from waste water. For this a solution (5 ml) of 0.05 g of TiO_2 in 10 ml of distilled water was prepared. The nanoparticles were completely mixed in the presence of X-ray radiation for a uniform discharge in distilled water. The resulting TiO_2 was used to absorb a phenol solution with a concentration of 1 mgL^{-1}. A mixture of 5 ml of a rutile TiO_2 composite with 20 ml of a 1 mgL^{-1} phenol solution was absorbed for 2 hours at a temperature of 25°C. Based on the curves obtained, it was established that adsorption is slow. The process was investigated on a "Varian Cary 50" device.

RESULTS AND DISCUSSION

The graph below shows the dependence of the absorption coefficient of a solution of phenol with a concentration of 1 mgL^{-1}on the wavelength (fig.4). No adsorption occurred during the process; therefore curves compatible with phenol were obtained in the 270 nm area.

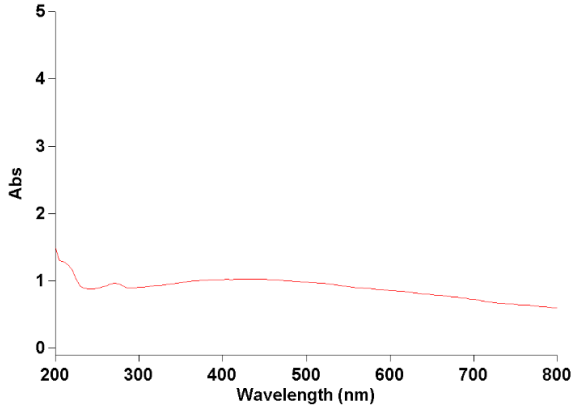

Fig.4. Graph before adsorption of phenol solution 1 mgL^{-1}

ISNN: print 2663-7006; online 2709-2666

As can be seen in Graph 1 the curves obtained for phenol were recorded at 200-300 nm. It is also known from the literature that the curve obtained at a wavelength of 270 nanometers corresponds to the curve of phenol.

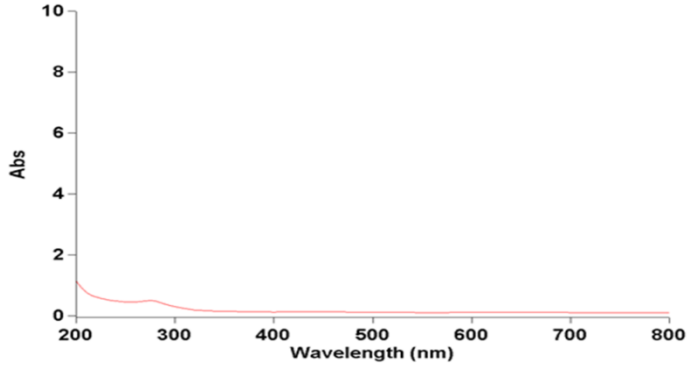

Fig.5. After absorption of phenol nanoparticles 1 mgL^{-1} + TiO_2

After two hours of adsorption, the phenol solution was filtered. This solution was then transferred to a "Varian Cary 50" spectrophotometer. In this case, the curves corresponding to phenol (270 nm) were again observed, however, according to the measurements in the graph a decrease in the degree of phenol (30%) in the solution was observed which indicates a weak adsorption. After 60 minutes of the process the adsorption curves practically do not change which is associated with the capture of the surface of TiO_2 nanoparticles due to chemisorption. Consequently adsorption occurs over a period of time and then stops. The following graph compares the adsorption curves for 30, 60, 90 and 120 minutes (fig.6).

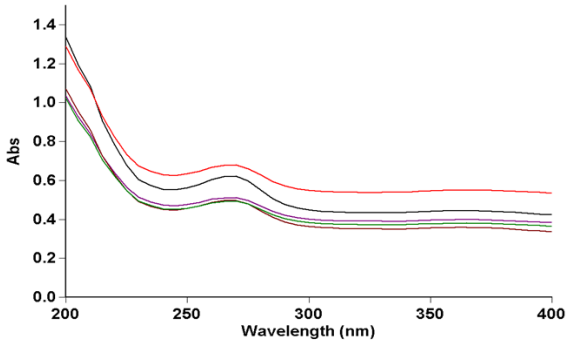

Fig.6. Comparison of phenol adsorption curves in the presence of TiO_2

As can be seen from fiq.3 the curve for phenol declined from top to bottom but was still observed. This indicates that the adsorption started within a certain period of time after which the adsorption stopped. It is believed that this is accompanied by chemisorption and aggregation of nanoparticles.

The mathematical model of the adsorption process is based on two methods: exponential and logistic. In both models a relationship was found between the amount of adsorbent and the total duration of the adsorption process.

I. Exponential model:

The following table is calculated by adding various amounts of nanoparticles with a TiO_2 concentration (0.02; 0.03; 0.05 grams) to a 1 mgL^{-1} phenol solution and the time required for complete adsorption of phenol in the process.

Table1

Changes of the amount of TiO_2 over time

Time(hour)	TiO_2(gr)
2.58	0.02
2.17	0.03
2	0.05

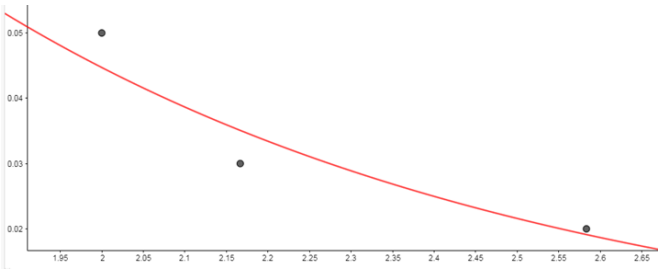

Fig.7. Dependence of phenol adsorption time on the amount of TiO_2 nanoparticles(I model**)**

The resulting geometric formula between the amount of adsorbent and the duration of the process is as follows:

$$(TiO_2+\ldots) = Y=0.82e^{-1.46t}$$

II. Logistic model:

The time required to completely remove phenol from a 1 mgL^{-1} solution with added TiO_2 is shown in the table below.

Table 2

Changes of the amount of TiO_2 over time

Time(hour)	TiO_2(gr)
2.58	0.02
2.17	0.03
2	0.05

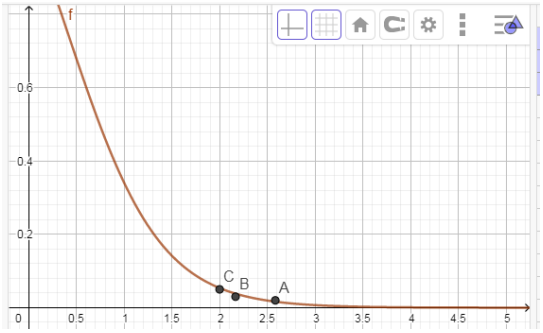

Fig.8. Dependence of phenol adsorption time on the amount of TiO_2 nanoparticles (IImodel**)**

According to the model the following formula shows the relationship between the amount of adsorbent and the duration of the adsorption process:

$$(TiO_2+\ldots)=Y=1.5 \,/\, 1+0.43e^{2.07t}$$

Thus both models of the adsorption process under consideration make it possible to determine in advance the duration of phenol adsorption with various amounts of TiO_2 adsorbent.

ISNN: print 2663-7006; online 2709-2666

CONCLUSION

1. Crystalline TiO_2 nanoparticles of the rutile phase were characterized by XRD.
2. The size of the nanoparticles determined by TEM, SEM analysis, was about 10-30 nm.
3. Experiments have shown that TiO_2 nanoparticles with a rutile phase are a weak adsorbent.
4. The course of adsorption was studied on the device "Varian Cary 50".
5. Mathematical models of the adsorption process are based on two methods: exponential and logistic models.

REFERENCES

1. Anirudhan T. S., Sreekumari S. S., & Bringle C. D. Removal of phenols from water and petroleum industry refinery effluents by activated carbon obtained from coconut coir pith. Adsorption. 2009,Vol.15, pp.439-451
2. Ghafari M., Cui Y., Alali A. & Atkinson J. D. Phenol adsorption and desorption with physically and chemically tailored porous polymers: Mechanistic variability associated with hyper-cross-linking and amination. J. Hazard. Mater. 2019,Vol.361, pp.162-168
3. Gundogdu A. et al. Adsorption of phenol from aqueous solution on a low-cost activated carbon produced from tea industry waste: equilibri,m, kinetic, and thermodynamic study. J. Chem. Eng. Data. 2012,Vol.57, pp.2733-274
4. Goto M., Hayashi N. & Goto S. Adsorption and desorption of phenol on anion-exchange resin and activated carbon. Environ. Sci. Techno.1986, Vol.20, pp.463-467
5. Caturla F., Martin-Martinez J., Molina-Sabio M., Rodriguez-Reinoso F. & Torregrosa, R. Adsorption of substituted phenols on activated carbon. J. Colloid. Interface. 1988, Sci.124, pp.528-534
6. Alam M. Z., Ameem E. S.,Muyibi S. A., Kabbashi N. A. The factors affecting the performance of activated carbon prepared from oil palm empty fruit bunches for adsorption of phenol. Chem. Eng. 2009,Vol,155, pp.191-198
7. Issabayeva G., Hang S.Y.,Wong M.C., Aroua M. K. A review on the adsorption of phenols from wastewater onto diverse groups of adsorbents. Rev. Chem. Eng. 2018, Vol.34, pp.855-873
8. Miao Q. et al. Activated carbon prepared from soybean straw for phenol adsorption. J. Taiwan Inst. 2013, Chem. Eng.Vol. 44, pp.458-465
9. TranV. S. et al.Typical low cost biosorbents for adsorptive removal of specific organic pollutants from water. Biores. Technol. 2015,Vol.182, pp.353-363
10. Salari M. et al. High performance removal of phenol from aqueous solution by magnetic chitosan based on response surface methodology and genetic algorithm. J. Mol. Liqs. 2019,Vol.285, pp.146-157
11. Salyakhova M.A. Filtering-sorbing material with an embedded photocatalyst. Bulletin of Kazan Technological University. 2013, Vol.16, №23, pp.52-53
12. Shabanova N.A.Chemistry and technology of nanodispersed oxides. N.A. Shabanova V.V., Popov P.D., Sarkisov. M. ICC "Akademkniga". 2007, 309 p
13. Gadirova E M. Adsorption of phenol in the presence of graphine oxide nanoparticles. Az.TU.Scientific works. Fundamental Sciences, ISSN 1815-1779.

2019, № 1, pp.166-171
14. Fabing Su, Lu Lv, Tee Meng Hui, Zhao X.S. Phenol adsorption on zeolite-templated carbons with different structural and surface properties.Carbon. 2005,Vol.43,№6, pp.1156-1164
15. Honcharuk V.V.Environmental aspects of modern technologies for the protection of the aquatic environment.Kiev: Naukova Dumka. 2005,324 p
16. Butyrin G.M. Highly porous carbon materials. Moscow: Chemistry. 1976,192 p
17. Piseopo A. D. Robert and J.V. Weber, App. Cata.B.35,2001, pp.117-124
18. Abussaud B., Asmaly H.A., Ihsanullah Saleh T.A., Gupta V.K., Taharlaoui, Atieh M.A. Sorption of phenol from waters on activated carbon impregnated with iron oxide, aluminum oxide and titanium oxide. Journal of Molecular Liquids.2016, Vol.213, pp.351-359
19. Shang R., Goulas A.,Tang C.Y.,Serra X.F., Rietveld L.C.,Heijman S.G.J. Atmospheric pressure atomic layer deposition for tight ceramic nanofiltration membranes:synthesis and application in water purification. Journal of Membrane Science.Vol.528,2017,pp.163-170
20. Hu X., Yu Y., Ren S., Lin Na., Wang Y., Zhou J. Highly efficient removal of phenol from aqueous solutions using graphene oxide/Al_2O_3 composite membrane. Journal of Porous Materials. 2018, Vol.25, İssue 3, pp.719-726

СОРБЦИОННЫЕ СВОЙСТВА НАНОЧАСТИЦ TiO_2 РУТИЛЬНОЙ ФАЗЫ

С.Р. Гаджиева,Э.М.Кадырова
Бакинский Государственный Университет
elmina2010@mail.ru

Существует множество научных исследований по адсорбции фенола. Процессы сорбции фенола в присутствии активированного угля, оксида графита и других адсорбентов очень распространены. В нашей статье впервые исследованы сорбционные свойства наночастиц TiO_2 с рутиловой фазой; наночастицы TiO_2 с фазой рутила были синтезированы золь-гелевым методом и использованы в качестве адсорбента. Изучен процесс адсорбции раствора фенола 1 мг/л в присутствии наночастиц TiO_2. Процесс адсорбции длился 2 часа при температуре 25°C. Хотя рутиловая фаза TiO_2 является очень хорошим фотокатализатором, было показано, что она является слабым адсорбентом.Нанокристаллические частицы TiO_2 рутиловой фазы охарактеризованы методом порошковой рентгеновской дифракции (XRD). На приборе «Varian Cary 50» изучен ход адсорбции. На основании кривых, построенных на приборе «Varian Cary 50» было определено, что адсорбция была неполной. По окончании процесса судя по графику, можно сказать, что количество фенола в растворе уменьшилось,но фенол еще остался, что свидетельствует о неполной адсорбции. Разработано математическое моделирование процесса как логистическим, так и экспоненциальным методами.
***Ключевые слова**: нано-TiO_2, фенол, адсорбция, ДРИ, ТЭМ.*

RUTİL FAZALI TiO_2 NANOHİSSƏCİKLƏRİN SORBSİYA XÜSUSİYYƏTLƏRİ

S.R. Hacıyeva, E. M. Qədirova
Bakı Dövlət Universiteti
elmina2010@mail.ru

Fenolun adsorbsiyası ilə bağlı bir çox elmi işlər vardır. Aktivləşdirilmiş karbon, qrafit oksid və

ISNN: print 2663-7006; online 2709-2666

digər adsorbentlərin iştirakında fenolun sorbsiyası ilə bağlı elmi işlər çox yayılmışdır. Məqalədə ilk dəfə rutil fazalı TiO_2 nanohissəciklərin sorbsiya xüsusiyyətlərinə baxılmışdır. Rutil fazalı TiO_2 nanohissəciklər sol-gel üsulu ilə sintez edilmiş və prosesdə adsorbent kimi istifadə edilmişdir.Daha sonra rutil fazalı TiO_2 nanohissəciklərinin iştirakı ilə 1 mgL-1 fenol məhlulunun adsorbsiya prosesi öyrənilmişdir. Adsorbsiya prosesi 25°C temperaturda 2 saat davam etmişdir.Rutil fazaya malik TiO_2-nin çox yaxşı fotokatalizator olmasına baxmayaraq,zəif adsorbent olması öyrənilmişdir. Rutil fazalı kristal TiO_2 nanohissəciklərnin tozu rentgen quruluş difraksiyası metodu ilə(XRD) ilə xarakterizə olunmuş, "Varian Cary 50" cihazında adsorbsiyanın gedişatı öyrənilmişdir."Varian Cary 50" cihazında qurulan əyrilərə əsasən adsorbsiyanın natamam getməsi müəyyən edilmişdir.Alınan qrafikə əsasən demək olar ki,prosesdən sonra məhlulda qalan fenolun miqdarı azalmış, lakin tam yox olmamışdır;bu isə natamam adsorbsiyanın getməsindən xəbər verir.Prosesin riyazi modelləşməsi həm logistik, həm də eksponensial metoddan istifadə etməklə tərtib edilmişdir.

Açar sözlər: *nano-TiO_2, fenol, adsorbsiya, XRD, TEM.*

AJCN, Vol 3, No. 3, 2021, pp. 85-92

UDC: 661.721.4

SYNTHESİS AND STUDY OF MESOPOROUS TİTANİUM-SİLİCATE CATALYSTS

R.O.Majidov, M.M.Agahuseynova
Azerbaijan State Oil and İndustry University
Ramin_86-86@mail.ru

The paper presents the results of studies on the development of synthesis methods and study of the properties of a catalyst based on titanium silicalite for the synthesis of MEK-methylethylketone. Samples of titanium silicalite were synthesized with different ratios of the starting reagents - tetraethoxysilane and tetrabutoxysilane. Tetra-n-propyl ammonium hydroxide was used as a structure-forming agent. The data of IR spectroscopy and powder X-ray diffraction made it possible to establish the effect of the amount of the structure-forming agent on both the structure and morphology of the titanium silicalite obtained. The main product is a mixture of TiO_2 and amorphous SiO_2. The dependence of the average particle size on the initial ratio of the initial reagents is established: with an increase in the initial molar ratio of the reactants, a change in the size of the catalyst particles is observed. The main indicators of the catalytic activity of the catalyst samples obtained at different initial ratios of reagents are compared. The carried out physicochemical studies on the synthesis of titanium silicalite made it possible to establish the composition that provides the maximum selectivity for the formation of methylethylketone.

Keywords: *methylethylketone, mesoporous titanium-silicate catalyst, catalytic activity.*

INTRODUCTION

Methylethylketone (MEK) is a chemical homologue of acetone. Prossessing a number of valuable properties, it is widely used in various fields of industry.

Due to the extremely high dissolving power, methylethylketone-MEK finds wide industrial application [1]. It is used in the production of polyurethane varnishes for covering magnetic tapes of computers, audio and video cassettes, is the best dewaxing agent for lubricating oils, ensuring their frost resistance, is a solvent in the production of foams, various paints, epoxy resins, polyvinyl chloride, artificial leather, serves as the basis for printing inks. It is used to obtain rubber antioxidants, to plasticize nitrocellulose derivatives used in the production of smokeless propellants, and also finds application as a solvent for film coatings of tablets and capsules of drugs, as a reagent and extractant in many pharmaceutical industries.

Annual world production of MEK in 2020 was at the level of 1.8 million tons, with about 30% of production concentrated in Central Europe. At present, the MEK is not produced in Azerbaijan and all the need for it is satisfied by imports. The lack of own production of MEK is explained by the lack of an effective way to obtain it. The importance of MEK as a solvent, given its widespread use in various industries, does not raise any questions, and the development of effective methods for its preparation is a very urgent task.

Analysis of the data on the use of MEK showed that each area of use of the MEK presents specific requirements for the quality of the product. So in the production of audio, video cassettes, in the perfume industry, high purity MEK is required.

When MEK is used in the oil refining and petrochemical industry at oil dewaxing and paraffin deoiling units, the requirements for product purity are somewhat lower.

ISNN: print 2663-7006; online 2709-2666

Titanium silicalite (TS-1) is of particular interest as a possible catalyst for the MEK synthesis. The promising nature of its use is evidenced, in particular, by the development and industrial implementation in recent years of a number of new large-scale organic synthesis processes.

This work is devoted to the development of a new method for obtaining MEK by liquid-phase oxidation of n-butane with aqueous solutions of hydrogen peroxide on a heterogeneous titanium-silicalite catalyst.

EXPERIMENTAL PART

Tetraethoxysilane (TEOS) of reagent grade grade, tetrabutoxytitanium (TBOT) of reagent grade grade were used as a starting material for the production of titanium silicalite, and tetra-n-propylammonium hydroxide (TPAG) of reagent grade grade was used as a structuring agent.

Methylethylketone synthesis was carried out on a laboratory setup shown in fig. 1. An empty n-butane dispenser (1) is weighed on an analytical balance. After that, the dispenser (1) is connected to a cylinder with n-butane, it is filled, and weighed again. By the difference in weights, the mass of n-butane in the dispenser is determined. Based on the obtained mass of n-butane, the load of the main components (solvent, hydrogen peroxide and catalyst) is calculated. The solvent, hydrogen peroxide and catalyst are charged into a jacketed batch reactor (8). The reactor is closed with a lid and connected to a pressure gauge (2).

After evacuation, a dispenser (1) is connected to the reactor and n-butane is squeezed into the reactor through a fine adjustment valve (5). The batcher is weighed and the exact weighed portion of n-butane loaded into the reactor is found by the difference in weights.

The magnetic stirrer (3) is turned on and the heat carrier is fed into the jacket from the thermostat. From the moment of the beginning of thermostating, the time of the beginning of the experiment is recorded. At regular intervals, samples are taken for analysis for the content of methyl ethyl ketone and hydrogen peroxide.

Sampling from the reactor is carried out into specially prepared ampoules through a steel capillary. ~ 10 ml of an aqueous solution of methanol is poured into ampoules for analysis for methyl ethyl ketone, and for analysis for hydrogen peroxide - 10 ml of "glacial" acetic acid.

The samples taken are analyzed for methyl ethyl ketone content (chromatographic analysis) and for hydrogen peroxide content (iodometric titration).

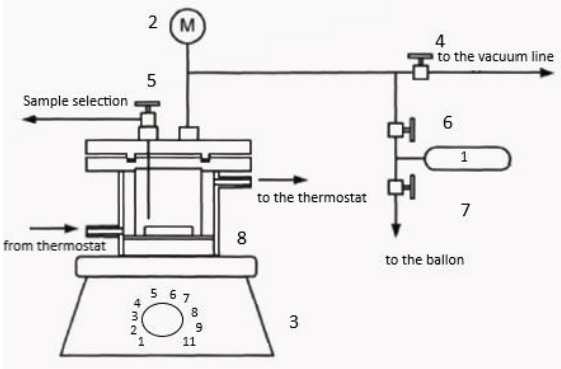

Fig.1. MEK synthesis plant 1 dispenser; 2-pressure gauge; 3-magnetic stirrer; 4,5,6,7-regulating valve; 8-reactor.

Method for the determination of hydrogen peroxide

Determination of hydrogen peroxide is carried out iodometrically using starch as an indicator:

$$H_2O_2 + 2KJ + 2CH_3COOH \text{----->} 2H_2O + J_2 + 2CH_3COOK,$$

$$J_2 + 2Na_2S_2O_3 \text{------>} Na_2S_4O_6 + 2NaJ$$

A sample of the analyte is placed in two flasks with a capacity of 250 ml. The mass of the sample is determined by the difference between the weights of the flask with the sample and the void. Weighing is carried out on an analytical balance with an accuracy of 0.0002 g. 10 ml of glacial acetic acid and 2 ml of a 50% aqueous solution of potassium iodide were added to the weighed portions. The samples are kept in the dark for 20 min and titrated with a standard aqueous solution of sodium thiosulfate (0.1 N) using a freshly prepared starch solution. A blank experiment is carried out in parallel.

The H_2O_2 content (wt.%) is calculated by the formula

$$X_{H2O2} = (1.70\text{-}(V\text{-}Vx)\ K\ C)/g$$

where 1.70 = 34.0-100 / (2-1000) is a complex of constants, including the molecular weight of H_2O_2 (34.0), the equivalence factor (2), the coefficient of reduction of the sample of the analyte to 100 g, and the conversion factor cm^3 to liters (1000), hl / cm^3. From two parallel determinations, the average H_2O_2 content is found.

V - is the volume of sodium thiosulfate used for titration of a sample of the studied mixture, ml.;

V_x is the volume of sodium thiosulfate used for titration of a blank sample, ml;

C-normality of a standard sodium thiosulfate solution, g-eq / l;

K-correction to the normality of sodium thiosulfate solution;

g- is the mass of the analyte, g.

The discrepancy between the results of parallel determinations does not exceed 0.5%.

Gas chromatographic analysis technique

Gas chromatographic analysis was performed on an "ЛХМ-8МД" chromatograph with a stainless steel column (2 m x 3 mm). Polysorb-1 was used as a sorbent. Flame ionization detector. The operating mode of the device and the retention times of substances are shown in table 1.

Table 1

Chromatograph operating mode

Parameter	Parameter value
Column oven temperature,° C	140
Evaporator temperature, °C	170
Carrier gas consumption (N2), cm^3 / min	35
Air consumption, cm^3 / min	300
Hydrogen consumption, cm^3 / min	30
Retention time of substances, s	-
Butane	5
Methanol	50
Methylethylketone	300

Methods for studying the structure and morphology of titanium silicalite

To characterize the structure and morphology of the obtained catalyst samples, we used IR spectroscopy, powder X-ray diffraction, and electron microscopy.

ISNN: print 2663-7006; online 2709-2666

IR spectra of the samples were recorded in air at room temperature on a Perkin-Elmer 221 spectrometer in KBr tablets in the range of 400-4000 cm-1.

X-ray diffraction patterns were taken on a Shimadzu LAB XRD-6000 diffractometer (Cu-Kλ, Ni-filter, voltage 30 kV, current 30 mA) with continuous rotation of the uvette with the sample. The counter movement speed was 2 deg^{-1}, the diffraction patterns were recorded in the angle range 20 = 5-80 °. Compounds were identified using a PDF-4 file.

Examination of the outer surface was carried out using a Hitachi S-2500 electron microscope. A layer of gold was previously deposited on the particles under study using a vacuum setup to eliminate the appearance of a surface charge and protect them from thermal destruction during the scanning process. The range of investigated magnifications is 50-65000 times. Static studies were carried out using the Origin Pro 7.0 software, based on images of at least 250 particles.

Method for determining the titanium content in titanium silicalite

Silicon was removed by treating a titanium silicalite sample with hydrofluoric acid followed by calcining. The residue was taken up in solution by fusion with potassium sulphate and dissolving in water. In the resulting solution, titanium was determined by a method based on the formation of a yellow-colored complex compound of titanium with diantipyrylmethane in a hydrochloric acid medium and measuring the light absorption of the resulting solution at a wavelength λ = 395 nm.

RESULTS AND DISCUSSION

To assess the effect of the TBOT / TEOS ratio, a series of experiments was carried out at different molar ratios of the TEOS: TBOT: TPAG: H_2O = 1: (0.02, 0.04, 0.06, 0.08): 0.5: 25, which corresponds to the theoretical TiO_2 content, wt% ... 2.60, 5.06, 7.41, 9.64 respectively. The reaction takes place with stirring and heating to 170°C. After cooling the resulting titanium silicalite suspension, the solid obtained from the strongly basic mother liquor still containing TPAG was washed with water to pH = 7-8, dried for 12 hours at 120°C, and then calcined in air at 550°C for 6 hours in a muffle furnace.

It should be noted that the initial molar ratio of TBOT-TEOS has a significant effect on the obtained samples of titanium silicalite. At a low initial content of TBOT (TBOT / TEOS = 0.01) in the initial gel, TiO_2 is quantitatively incorporated into the structure in a tetracoordinated state. An increase in the TBOT-TEOS ratio in the gel above 0.02 does not lead to an increase in its content in the crystal lattice of the samples. In fig. 2 shows the dependence of the ratio of the intensities of the bands 960 cm^{-1} (Ti-O-Si) and 550 cm^{-1} (Si-O-Si) on the initial content of TiO_2, showing the degree of inclusion of TiO_2 in the crystal lattice of titanium silicalite.

Excess TiO_2 is not included in the zeolite structure and remains in an amorphous form (anatase). Amorphous TiO_2 (anatase) blocks the pores of titanium silicalite and catalyzes the decomposition reaction of hydrogen peroxide. This theory is in good agreement with the results obtained when testing samples. Thus, the dependence of the selectivity of the formation of MEK on the molar ratio has an extreme character with a maximum at the ratio of TBOT / TEOS = 0.02 (2.60% TiO_2). With an increase in the TBOT / TEOS ratio from 0.04 (5.06% TiO_2) to 0.08 (9.64% TiO_2), a significant decrease in the yield and initial rate of MEK formation is observed. The dependence of

the main parameters of the process is shown in fig. 3

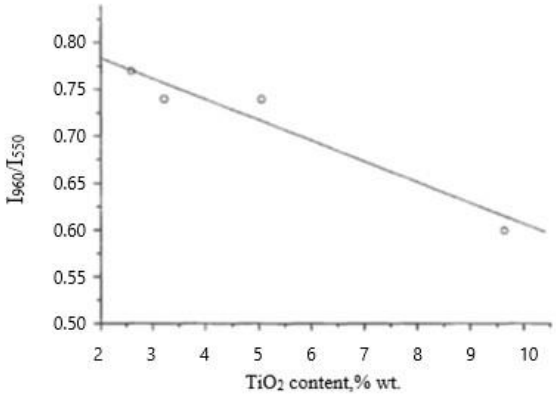

Fig.2. Dependence of the ratio of the integrated intensities of the 960 and 550 cm^{-1} bands on the initial TiO_2 content.

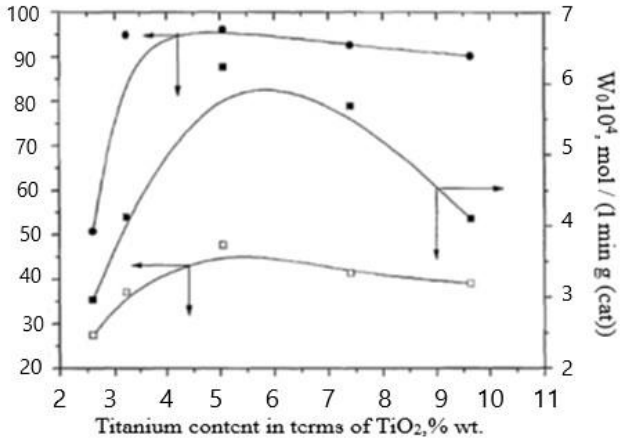

Fig.3. Influence of TiO_2 content% wt. on the main parameters of the process: ■-degree of conversion of hydrogen peroxide; □-yield of methylethylketone; ●-initial rate of methyl ethyl ketone formation

Analysis of kinetic curves for the accumulation of MEK, obtained using samples of titanium silicalite with different titanium content, shows that the optimal molar ratio of TBOT / TEOS = 0.02 provides the maximum selectivity of MEK formation.

Study of the influence of the TPAG / TEOS ratio

As shown by the data of IR spectroscopy and powder X-ray diffraction, the use of different amounts of a structure-forming agent (TPAG) has a key effect on both the structure and morphology of the titanium silicalite obtained. So, when the molar ratio TPAG / TEOS is less than 0.0833, the formation of titanium silicalite is not observed at all. Apparently, at this molar ratio, the minimum concentration of the structure-forming agent is not reached, at which the assembly of the regular structure of the zeolite is possible. According to IR spectroscopy data, when the TPAG / TEOS ratio is less than 0.0833, the main product is a mixture of TiO_2 (anatase) and amorphous SiO_2 (fig. 4)

ISNN: print 2663-7006; online 2709-2666

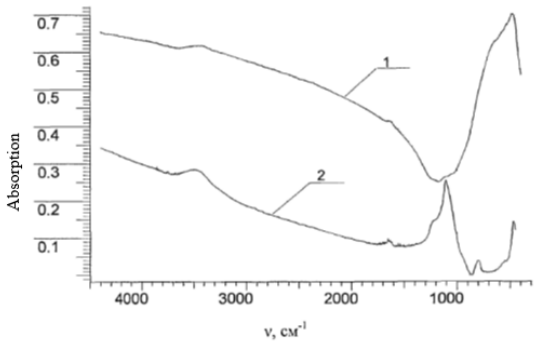

Fig.4. IR spectra of anatase (1) and catalyst samples obtained at an initial molar ratio TPAG / TEOS = 0.0833 (2).

Powder X-ray diffraction of the samples also showed the appearance of anatase peaks on the X-ray diffraction pattern (fig. 5).

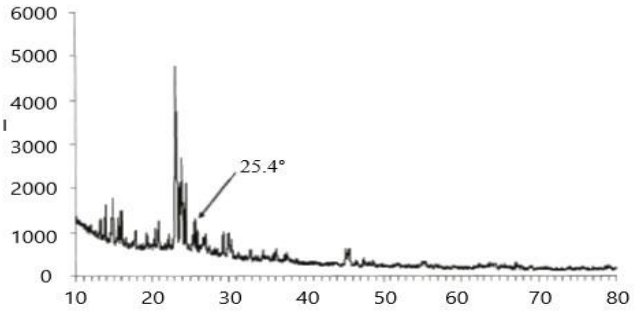

Fig. 5. X-ray diffraction patterns of a catalyst sample obtained with an initial molar ratio TPAG / TEOS = 0.0833

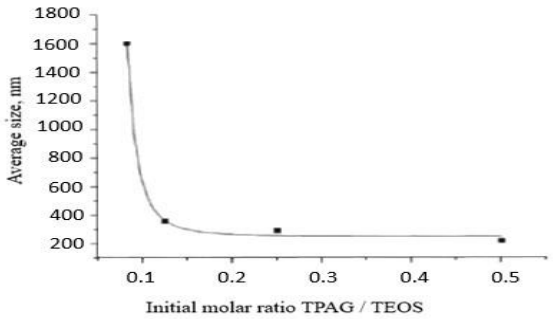

Fig.6. Dependence of the average particle size on the initial TPAG / TEOS ratio

A comparison of the main indicators of the catalytic activity of catalyst samples obtained at different initial molar ratios is shown in fig.6. At the initial molar ratio TPAG / TEOS = 0.083, no MEK formation is observed. The insignificant degree of PV conversion is explained by the formation of a stable complex of anatase with PV. With a further increase in the ratio from 0.125 to 0.5, the MEK yield and the degree of PV conversion remain practically constant (40 and 93%, respectively). An increase in the initial rate of formation of MEK is explained by an increase in the total specific surface area of the catalyst.

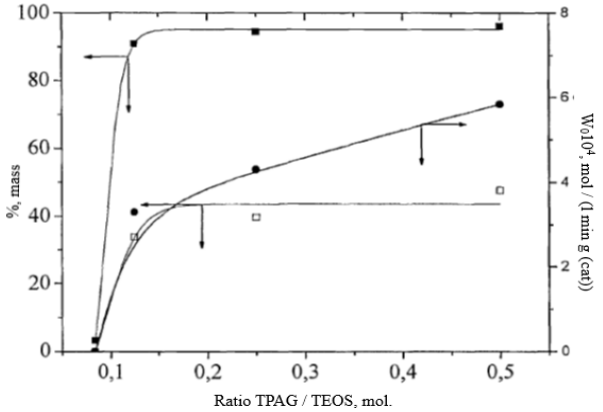

Fig.7. Influence of the initial molar ratio TPAG / TEOS on the main parameters of the process:
■ – hydrogen peroxide conversion; □ – methylethylketone yield; •- initial rate of methylethylketone formation

Thus, the studies carried out on the synthesis of titanium silicalite with different molar ratios TPAG / TEOS show that the TPAG / TEOS ratio = 0.5 provides the maximum selectivity of the formation of MEK.

CONCLUSION

A procedure has been developed for the synthesis of a mesoporous catalyst based on titanium silicalite for the production of methylethylketone by liquid-phase oxidation of N-butane with hydrogen peroxide

The physicochemical and catalytic properties of the synthesized catalyst have been studied. The optimal ratio of the initial reagents and the structuring agent was chosen, which ensure the maximum selectivity of the formation of MEK.

REFERENCES

1. Gushchevsky A.B., Kolesov M.L. and others. Current state and prospects of the production of methyl ethyl ketone. Modern problems of chemistry and chemical industry. - M .: NIITEKHIM. 1987, Issue 8, 211 p
2. Pat. I 20090088. Azerbaijan. Catalyst for obtaining methyletilketone. 2008
3. Danov S.M., Sulimov A.B., Fedosov A.E. Methods for preparing catalysts based on titanium silicalite for selective liquid-phase oxidation of organic compounds with hydrogen peroxide. Catalysis in industry. 2007, № 2, pp. 33-36
4. Pat. 6121497 USA. Process of recovering methylethylketone from an aqueous mixture of methylethylketone and ethanol. 2000
5. Agaguseynova M.M., Amanulayeva G.İ., Bayramova Z.E. Catalysts for oxidation buten-1 to methyletilketone. Russian Journal of Chemistry and Chemical Technology. 2018, (61), Vol. 2, pp. 53-57
6. Bonino F.,.Damin A., Ricchiardi G., Ricci M., Spano G., Aloisio R.D., Zecchina A., Lamberti C., Prestipino C., Bordiga S. J. Phys. Chem. B, 2004, 108, pp.35-73
7. Chaudhari K.,.Bal R.,.Srinivas D., Chandwadkar A.J., Sivasanker S. Microporous Mesoporous Mater. 2001, 50, 209 p
8. Noda C.,Perez, Moreno E., Henriques C.A., Valange S.,Gabelic Z. J.L.F.Monteiro.

ISNN: print 2663-7006; online 2709-2666

Microporous Mesoporous Mater. 2000, 41, 137 p
9. Chiker F., Lapisardi G.,.Launay F.,.Nogier J.-F., Bonardet J.-L. Catal. Commun. 2004, 5, 247 p
10. Dusi M., Mallat T., Baiker A. Catal. Rev. Sci. Eng.2000, 42, 213 p

СИНТЕЗ И ИССЛЕДОВАНИЕ МЕЗОПОРИСТЫХ ТИТАН-СИЛИКАТНЫХ КАТАЛИЗАТОРОВ

Р. О. Маджидов, М. М. Агагусейнова
Азербайджанский Государственный Университет Нефти и Промышленности
Ramin_86-86@mail.ru

В работе приведены результаты исследований по разработке методов синтеза и изучения свойств катализатора на основе силикалита титана для процесса синтеза МЭК-метилэтилкетона. Синтезированы образцы силикалитов титана с различным соотношением исходных реагентов - тетраэтоксисилана и тетрабутоксисилана. В качестве структурообразующего агента использовали гидроксид тетра-н-пропиламмония. Данные ИК-спектроскопии и порошковой рентгенографии позволили установить влияние количества структурообразующего агента как на структуру, так и на морфологию получаемого силикалита титана. Основным продуктом является смесь TiO_2 и аморфного SiO_2. Установлена зависимость среднего размера частиц от начального соотношения исходных реагентов: с увеличением начального мольного соотношения реагенты наблюдается изменение размеров частиц катализатора. Сравнены основные показатели каталитической активности образцов катализатора, полученного при различном начальном соотношении реагентов. Проведенные физико-химические исследования по синтезу силикалита титана позволили установить состав, обеспечивающий максимальную селективность образования метилэтилкетона.
Ключевые слова: *метилэтилкетон, мезопористый титан-силикатный катализатор, каталитическая активность.*

MEZOMƏSƏMƏLİ TİTAN-SİLİKAT KATALİZATORLARIN SİNTEZİ VƏ TƏDQİQİ

R.O. Məcidov, M.M.Ağahüseynova
Azərbaycan Dövlət Neft və Sənaye Universiteti
Ramin_86-86@mail.ru

Məqalədə sintez metodlarının inkişafı və MEK-metiletilketonun sintezi üçün titan silikalitə əsaslanan katalizatorun xüsusiyyətlərinin öyrənilməsi üzrə tədqiqatların nəticələri təqdim olunur. Titan silikalit nümunələri başlanğıc reaktivlərin - tetraetoksisilan və tetrabutoksisilanın müxtəlif nisbətləri ilə sintez edilmişdir. Struktur əmələgətirici kimi tetra-n-propilammonium hidroksid agentindən istifadə edilmişdir. İK spektroskopiya və toz rentgenoqrafiyasının məlumatları, struktur əmələgətirici agentin miqdarının həm alınan titan silikalitin quruluşuna, həm də morfologiyasına təsirini təyin etməyə imkan verdi. Əsas məhsul TiO_2 və amorf SiO_2 qarışığıdır. Orta hissəciklərin ölçüsünün ilkin reaktivlərin ilkin nisbətindən asılılığı müəyyən edilmişdir: reaktivlərin ilkin molar nisbətinin artması ilə katalizator hissəciklərinin ölçüsündə dəyişiklik müşahidə olunur. Reaktivlərin müxtəlif ilkin nisbətində alınmış katalizator nümunələrinin katalitik aktivliyinin əsas göstəriciləri müqayisə olunmuşdur. Titan silikalitinin sintezi üzrə aparılmış fiziki-kimyəvi tədqiqatlar, metiletilketonun formalaşmasının maksimal selektivliyini təmin edən tərkibin yaradılmasına imkan vermişdir.
Açar sözlər*: metiletilketon, mezo məsaməli titan-silikat katalizatoru, katalitik aktivlik.*

AJCN, Vol 3, No. 3, 2021, pp. 93-100

UDC: 541.15

CALCULATION PERCENTAGE OF ELECTRONS EMISSION FROM BERYLLIUM OXIDE SURFACE INTO WATER, IN BEO/H_2O SYSTEM UNDER THE EFFECT OF IONIZING RADIATION

N.K. Abbasova
Baku State University
ramazanova.abbasova.nermin@gmail.com

Influence of γ-quanta through BeO/H_2O system formed unbalanced energy carries: electron-positive ion pairs, electron- excitement situation, various radiation defects. The used of onefold collision methods and stepping Monte-Karlo, a base of Mathcad programs physical (10^{-15}-10^{-12} sec) and physicochemical (10^{-11}-10^{-6} sec) stages ,calculated formation of radiation-chemical yields of electron-positive ion pairs and electron- ecxitement situation. Formation of Solid/liquid systems energy carriers inside of solids, between solids and the liquid, inside of a liquid, plays an important role occurring physical, physicochemical, and chemical process. Observed formation of a hole inside of solids and emission to the surface, electrons to the surface, and from the surface to the inside of the liquid. Electrons that influenced emission inside of a liquid gradually lost kinetics energy to transform thermal electrons occurs in solvation and radioliz of water.

***Keywords**: γ-quanta, energy carries, BeO/H_2O system, radioliz of water, radiation-chemical yield.*

INTRODUCTION

Recently, in various research studies, the action of ionizing radiation (γ-quants, electrons, protons, neutrons, α-particles, high-energy ions, etc.) in contact with metal or metal oxides of different particle sizes of liquids, especially water-borne products the sharp dependence of radiation-chemical emission on particle size was observed [1-11]. This effect is especially pronounced in nano- and micro-sized substances. For example, the radiochemical yield of molecular hydrogen from the radiolysis of water adsorbed on the surface of nano-ZrO_2 is higher than that of other metal oxides [1,2]. On the other hand, H_2-radiation-chemical output was obtained greater. It has been suggested that this increase in molecular hydrogen obtained from the radiolysis of water in suspension systems may be due to the emission of energy-carrying electrons inside the silicate [3,4] into the liquid phase, water under the influence of radiation [3]. During the radiolysis process on the nano-sized silicate surface of water, as the pores shrink, the OH output [5] decreases, while the H_2 and H_2O_2 emissions [6] increase.

Ouerdane H. [7] and other authors using the Monte Carlo method to model holes in the amorphous nano-BeO system suspended in water under the influence of ionizing radiation, holes migrating to the interfacial boundary in the physical and physicochemical stages of the process, and radiation-chemical emissions of electrons emitted into the water, made calculations. It was found that the emission of electrons emitted into water varies depending on the size of the nanoparticle and the degree of porosity [7]. These results coincide with the results obtained from experiments [8].

Electron emission from oxides into water under the influence of ionizing radiation in the system of various nano-sized oxides (SiO_2, ZnO, Al_2O_3, Nd_2O_3, Sm_2O_3) suspended in water has been determined [9]. The spectrum of electrons oscillating in water proves that it does not change in the picosecond-nanosecond range, and a strong difference is obtained in the nanosecond-microsecond range.

ISNN: print 2663-7006; online 2709-2666

Obtaining molecular hydrogen from the transformation of water under the influence of γ-quanta and ^{4}He ions with an energy of 5 MeV in the SiC (α-phase, β-phase) nanoparticle / water system has been studied [10]. The research was carried out in two ways: 1) adsorption of water, 2) suspension of SiC in water. Spectroscopic analysis has shown that under the influence of radiation, the α-phase changes to the β-phase, and on the surface of SiC occurs the oxidation of silicon, ie SiO_2, and the release of hydrogen in the suspension system is large.

The time-dependent release of electrons liberated under the influence of γ-quanta with a pulse of 20 ns on the suspension of glass nanoparticles of different porosity (1-57 nm) [11]. It has been found that the emission of electrons in the pores of a 1 nm particle is twice as high as that of pure water. This proves that some of the electrons formed inside the solid under the influence of radiation are emitted from the surface of the solid into the liquid phase.

Unbalanced energy carriers formed under the influence of γ-quanta: electron-positive ion pairs and electron-excitation states (excitons) occur with equal probability in the whole volume within a homogeneous medium. In the absence of an external electric field, energy carriers are transported with the same probability in all directions. Some of the electrons migrating to the surface are also emitted from the surface into the liquid phase.

Given the above, the process of radiolysis of water in suspended heterogeneous systems can be divided into three parts:

• Homogeneous radiolysis of pure water;

• Heterogeneous radiolysis of water adsorbed on the surface of a solid;

• The surface of a nanoparticle depends on the volume of the working phase, where energy carriers (electrons, ions and excitons) formed by radiation can diffuse and pass through the surface to the water and participate in the decomposition of water.

EXPERIMENTAL PART

For the experiment, distilled water was used as the objects of study, and the BeO catalyst was used as a solid for the radiation-catalytic processes of water decomposition.We took high-purity beryllium oxide. Pre-heat treated and purified from impurities Then it was added to ampoules with a volume of 19 ml, then 5 ml of water was added thereto. We cleaned the water from the air. After which beryllium oxide of various weights and sizes was added here. Then the ampoule was sealed. This entire process was carried out in a vacuum adsorption unit. Then these ampoules were subjected to γ-radiation (^{60}Co, P = 19.05 rad / san, T = 300K). Then the composition of this ampoule after irradiation was studied. The effect of mass and measurement effects on the amount, rate of formation and radiation-chemical output of molecular hydrogen formed by the process of radiolysis of water under the influence of γ-quanta (^{60}Co, P = 19.05 rad / sec, T = 300K) was studied. The results of the presented work were obtained using high-precision and sensitive gas chromatographs "Agilent-7890" and "Color-102", IR-spectrophotometer, EPR-spectrometer, physicochemical and chemical analysis methods. Theoretical studies using Monte Carlo, step, single-collision methods, the trajectories of electrons formed under the influence of ionizing radiation on the basis of Mathcad program were observed in the physical and physicochemical stages of the process (10^{-15}-10^{-12} seconds) and the emission percentage of electrons emitted from the surface ratio was calculated. The emitted electrons gradually lose their kinetic energy in

liquid water, turn into thermal electrons, become salvageable and participate in the radiolysis of water**.**

The purpose of this work is to identify the regularities of obtaining molecular hydrogen as an environmentally friendly type of alternative fuel. To achieve this goal, we have set ourselves some tasks, one of which is to identify the mechanism of what is happening inside the BeO + H_2O system.

As we know, beryllium oxide has a hexagonal structure. From geometry it is known to calculate the volume of other spatial bodies formed by an arbitrary vertical displacement of a flat surface, we use the formula V = Sd, it is also known from physics that V = m / ρ. If the surface area of a porous body of mass m is -S and the density is -ρ, then the average thickness of the porous walls of the body (d) is given by:

$$d = \frac{V}{S} = \frac{\frac{m}{\rho}}{S} = \frac{m}{\rho S} \qquad (1)$$

can be determined on the basis of expression (1). If in expression (1) m = 1 g, the surface area of the object is equal to the area of a particular surface. The average thickness is equal to the numerical value. If we take ρ = 2.33 g /sm^3, S_x = 60 m^2 / gr for BeO, then the average thickness d = 71.5 nm is obtained.

Assuming that the concentration of energy carriers (electron-positive ion pairs, excitons, different types of radiation defects, etc.) formed inside a solid under the influence of ionizing radiation (γ-quanta) is the same throughout the volume, and the free distance of each energy carrier is λ_i, A model has been developed for the surface diffusion of electron and positive ion pairs, which are energy carriers of the same probability in all directions at any point dV→0 (Figure 1)

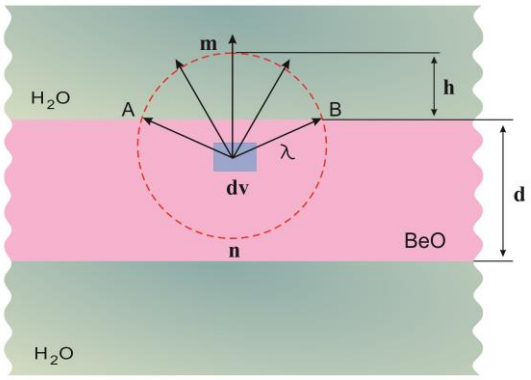

Fig.1. Free escape distances of energy carriers within BeO with average thickness of pores suspended in water-λ, conditional separation of energy carriers according to free escape distances (λ).

If both, the mass and the size of the substance suspended in water change, the energy carriers transferred to the water, as well as the radiation-chemical output of the corresponding molecular hydrogen, change. However, after a certain concentration of particles of each size in the environment, a balance is established between the energy carriers and the processes of formation of intermediate products. If the electrons, which are energy carriers in the amount of dV (fig.1), are radiated in all directions with equal probability of average escape distance λ, then the AmB part of the spherical segment characterizes the emission, and the AnB part characterizes the rest of the matter. If the density of electrons formed within a single particle by the action of radiation is a, then

ISNN: print 2663-7006; online 2709-2666

the number of electrons will be emitted from the corresponding particle surface into the liquid phase (into water), and will probably remain in the particle volume corresponding to the remaining spherical segment of the particle. Percentage of electrons emitted from the surface [12]:

$$\phi_i = \frac{N_{emis}}{N_{gen}} = \frac{aV_{seg.AmB}}{aV} = \frac{V_{seg.AmB}}{V} = \frac{\frac{2}{3}\pi\lambda^2 h}{\frac{4}{3}\pi\lambda^3} = \frac{h}{2\lambda} \qquad (2)$$

is calculated as the number of electrons emitted by the N_{gen} radiation inside the particle, N_{emis} emitted from the surface into the water.

RESULTS AND DISCUSSION

Calculations were made using simple geometric constructions and calculations in the range 0-R of h and the values-λ=md of the average running distance, which are the values m=0,1-4 of, and the results obtained are given in Figure 2. As can be seen in the figure, electrons, which are energy carriers formed inside the particle, migrate to a particle surface depending on the particle size and are emitted into the water. The electrons emitted into the water lose their kinetic energy as a result of the collision with water molecules and are converted first into heat and then into solvation electrons. This means that the electrons emitted into the water and solvation in the water are involved in the formation of molecular hydrogen. The calculation was performed using the stepping method.

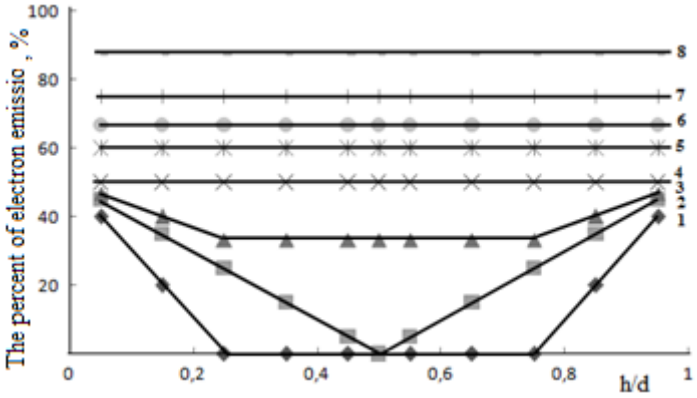

Fig.2. Distribution of electrons emitted from the surface by the distance of the nanoparticle from the center (λ/d=0,25 (1); 0,5 (2); 0,75 (3); 1 (4); 1,25 (5); 1,5 (6); 2 (7); 4(8)).

The average running distance of an electron

$$\lambda = \frac{1}{\sigma_{tot}(E) \cdot n} \qquad (3)$$

Where $\sigma_{tot}(E)=\sigma_j(E)+\sigma_i(E)$ (E) is the full effective cross-section of the collision [13], where electron-excitation-$\sigma_j(E)$ and ionization-$\sigma_i(E)$ is equal to the sum of the effective cross sections of the processes. n is the number of atoms or molecules per unit volume of matter, [13] which can be calculated as follows:

$$n=\frac{N}{V}=\frac{\nu N_A}{V}=\frac{\frac{m}{M_{BeO}}N_A}{V}=\frac{m}{V}\frac{N_A}{M_{BeO}}=\frac{\rho N_A}{M_{BeO}} \qquad (4)$$

where N_A-Avagadro is the molar mass of M_{BeO} = 25 g / mol-beryllium oxide. Given the data, the average running distance can be determined based on the expression.

$$\lambda=\frac{M_{BeO}}{\sigma_{tot}\cdot\rho\cdot N_A} \qquad (5)$$

Figure 3 shows a graph of the average escape distance of an electron inside BeO as a function of its kinetic energy. As can be seen, in electrons with kinetic energy E = 0.01-10 keV, the average escape distance within BeO varies in the range of 3.5-161 nm.

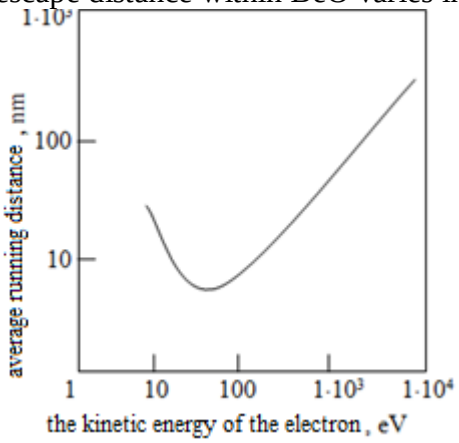

Fig 3. The dependence of the average escape distance of an electron inside BeO on its kinetic energy.

Then, on the basis of these values, the percentage of migration of energy carriers to the surface formed within the particle under the influence of ionizing radiation corresponding to each value of m:

$$\phi=\frac{\sum_n \phi_i V_i}{\frac{4\pi R^3}{3}}=\frac{\sum_n \phi_i 4\pi r_i^2 \Delta r_i}{\frac{4\pi R^3}{3}}=\frac{3\sum_n \phi_i r_i^2 \Delta r_i}{R^3} \qquad (6)$$

Calculated, based on the expression. Here, n- the number of steps, the emission percentage corresponding to step φ_i-i, r_i, Δr_i and $V_i = 4\pi r_i^2 \Delta r_i$ and the radius, thickness, and volume of the i-the sphere, respectively. The dependence of the emission percentage of electrons emitted from the surface of the nano-particles on the average free escape distance of the particle is given in fig.4.

In a suspended system (BeO / H_2O), the concentration of electrons of a certain thickness around a solid particle is greater than that other particles due to the electrons emitted from the solid to the liquid phase. Electrons emitted into a liquid gradually lose their kinetic energy as a result of an inelastic collision and are first converted into thermal electrons, which can then be trapped or solvated in traps inside the water. The formation reactions (1-3) of molecular and atomic hydrogen obtained from radiolytic decomposition between solvated electrons and water molecules and protonated water molecules (H_2O^+) can be described as follows:

ISNN: print 2663-7006; online 2709-2666

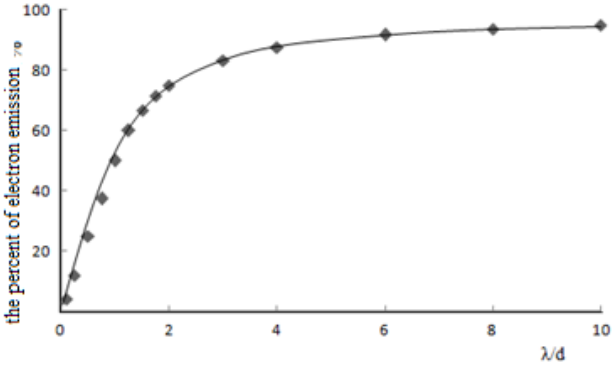

Fig.4. Dependence of the emission percentage of electrons emitted from the BeO surface on the average free escape distance of the particle (abscissa λ/d).

$$2e^{-}_{aq} + 2H_2O \rightarrow H_2 + 2OH^{-} \quad (7)$$

$$e^{-}_{aq} + H + H_2O \rightarrow H_2 + OH^{-} \quad (8)$$

$$e^{-}_{aq} + H_3O^{+} \rightarrow H + H_2O \quad (9)$$

Due to the electrons emitted and liberated in the liquid phase (water), reactions with a high velocity constant (7-9) take place, which also increases the radiation-chemical output of molecular hydrogen.

CONCLUSION

The percentage of electron emissions from the surface of a solid into water varies depending on the average thickness of the pores of the porous body and the energy of the electrons;

The concentration of electrons released into the water due to the electrons emitted from the surface of the solid into the water varies depending on the average pore thickness of the porous body, which means a change in the radiation-chemical output of molecular hydrogen.

REFERENCES

1. LaVerne J. A. and Tandon L. J., Phys. Chem. B 106, 2002, 380 p
2. Petrik. N.G., Alexandrov A.B., and Vall I., J. Phys. Chem. B 105, 2001,5935 p
3. Schatz T., Cook A.R. and Meisel D., J. Phys. Chem. B 102, 1998,7225 p
4. LaVerne J. A. and Tonnies S.E., J. Phys. Chem. B 107, 2002, 7277 p
5. Foley S., Rotureau P., Pin S., Baldacchino G., Renault J.P. and Mialocq J.C., Angew. Chem., Int. Ed. 44, 2005, 110 p
6. Rotureau P., Renault J.P., Lebeau B., Patarin J. and Mialocq J.C. Chem.Phys. Chem 6, 2005, 1316 p
7. Ouerdane H., Gervais B., Zhou H., Beuve M., Renault J.P. Radiolysis of water confined in porous silica: a simulation study of the physicochemical yields. J. Phys. Chem. 2010, 114, pp.12667-12674
8. Dimitrijevic N.M., Henglein A., Meisel D. Charge separation across the silica nanoparticle/water interface. J. Phys. Chem. B 1999, 103, pp. 7073-7076
9. Chelnokov E., Cuba V., Simeone D., Guigner J.M., Schmidhammer U., Mostafavi

M., Caër S.Le. Induced by Ionizing Radiation Electron Transfer at Oxide/Water Interfaces, J. Phys. Chem. C, 2014, 118 (15), pp. 7865–7873
10. Schofield J., Reiff S.C., Pimblott S.M., LaVerne J.A. Radiolytic hydrogen generation at silicon carbide–water interfaces.Journal of Nuclear Materials, Vol 469, February 2016,pp. 43-50
11. Raluca M. Musat, Andrew R. Cook, Jean-Philippe Renault, and Robert A. Crowell, Nanosecond Pulse Radiolysis of Nanoconfined Water, J. Phys. Chem. C, 2012, 116 (24), pp.13104–13110
12. Aleshkevich V.A. Course of general physics. Molecular physics. M.: FIZMATLIT 2016, 281—283,312 p
13. Jafarov Y.D., Ramazanova N.K. Calculation of deqradation spectrum of low energy electrons within infinite homoqeneuus Beryllium Oxide on the basis of Mathematical ModellinqJournal of Radiation Researches, Baku Vol.5, №1, 2018, pp.5-11

РАСЧЕТ ПРОЦЕНТА ВЫБРОСА ЭЛЕКТРОНОВ, ЭМИССИРУЕМЫХ С ПОВЕРХНОСТИ ОКСИДА БЕРИЛЛИЯ В ВОДУ, В СИСТЕМЕ BEO / H_2O ПОД ДЕЙСТВИЕМ ИОНИЗИРУЮЩЕГО ИЗЛУЧЕНИЯ

Н.К. Аббасова
Бакинский Государственный Университет
ramazanova.abbasova.nermin@gmail.com

Под действием γ-квантов в системе BeO/H_2O образуются такие несбалансированные энергоносители, как: электронно-положительные ионные пары, состояния электронного возбуждения, различные радиационные дефекты и т.д. Используя пошаговые методы Монте-Карло, однократное столкновение, на основе программы Mathcad были вычислены радиационно-химические выходы электрон-положительной ионной пары и электрон-возбуждения, образующихся в физическом (10^{-15}-10^{-12} секунд) и физико-химическом (10^{-11}-10^{-6} сек) этапах процесса. Энергоносители, образующиеся в системе твердое тело / жидкость, играют важную роль в физических, физико-химических и химических процессах, происходящих в твердом теле, на границе твердое тело-жидкость и внутри жидкости. Наблюдались выбросы дырок и электронов на поверхность и с поверхности в жидкость (воду). Эмиссируемые электроны внутри жидкости (воде) постепенно теряя свою кинетическую энергию, превращаются в тепловые, а затем и вовсе сольватируясь принимают участие в процессе радиолиза воды.

Ключевые слова: *γ-кванты, переносчики энергии, система BeO / H_2O, радиолиз воды, радиационно-химический выход.*

İONLAŞDIRICI ŞÜALARIN TƏSİRİ İLƏ BeO/H_2O SİSTEMİNDƏ BERİLLİUM OKSİD SƏTHİNDƏN SU DAXİLİNƏ EMİSSİYA OLUNAN ELEKTRONLARIN FAİZ NİSBƏTİNİN HESABLANMASI

N.K. Abbasova
Bakı Dövlət Universiteti
ramazanova.abbasova.nermin@gmail.com

γ-kvantların təsiriləBeO/H_2O sistemi daxilində əmələ gələn qeyri-tarazlıqlı enerji daıyıcıları: -elektron-müsbət ion cütü, elektron-həyacanlanma halları, müxtəlif cür

ISNN: print 2663-7006; online 2709-2666

radiasiya defektləri və s. əmələ gəlir. Monte-Karlo, addımlama, birqat toqquşma metodlarından istifadə edərək, Mathcad proqramı əsasında prosesin fiziki(10^{-15}-10^{-12} san) və fiziki-kimyəvi (10^{-11}-10^{-6} san) mərhələlərində əmələ gələn elektron-müsbət ion cütünün və elektron-həyacanlanma hallarının radiasiya-kinyəvi çıxımları hesablanmışdır. Bərk cisim/maye sistemində əmələ gələn enerji daşıyıcıları bərk cisim daxilində, bərk cisim maye sərhəddində və maye daxilində gedən fiziki, fiziki-kimyəvi və kimyəvi proseslərdə mühüm rol oynayırlar. Bərk cisim daxilində əmələ gələn deşiklərin və elektronların səthə qədər və səthdən maye (su) daxilinə emissiyası izlənilmişdir. Emissiya olunan elektronlar maye (su) daxilində öz kinetik enerjisini tədricən itirərək istilik elektonlarına çevrilirlərək salvatlaşırlar və suyun radiolizi prosesində iştirak edirlər.

Açar sözlər: *γ-kvant, enerji daşıyıcısı, BeO/H_2O sistemi, suyun radiolizi, radiasiya-kimyəvi çıxım.*

AJCN, Vol 3, No. 3, 2021, pp. 101-109

UOT: 541.128.13:524.941. 547.211:542.943

OXİDATİVE CONVERSİON OF METHANE. EFFECT OF CATALYST AND PERSPECTİVE DİRECTİONS OF REACTİON

[1] E.H. Ismailov, [1] D.B.Taghiyev, [1] S.M. Zulfugarova, [1] G.R. Azimova, [1] S.N. Osmanova, [2] J.W. Thybaut
[1]Institute of Catalysis and Inorganic Chemistry named after acad. M.Naghiyev ANAS,
[2] Ghent University, B-9052 Gent, Belgium
etibar.ismailov@gmail.com

The well-known MnNaW catalysts based on SiO_2 for oxidative condensation of methane (OCM) were synthesized by various methods, characterized by X-ray diffractometry (XRD), scanning electron microscopy with energy dispersive elemental analysis (SEM/EDX), electron magnetic resonance (EMR) spectroscopy, N_2 adsorption-desorption measurements, and tested as OCM catalysts at atmospheric pressure to convert into a mixture of ethylene + carbon oxides for further hydroformylation to propylene. The structural and catalytic features of the synthesized systems are discussed. The necessity of using mainly X-ray diffraction, Raman, and EMR methods for studying catalysts in situ mode in combination with online MS analysis of gas-phase reaction products to establish the nature of catalytically active phases, centers, their mechanism of functioning, activation of CH_4 with the formation of C-C bond for the synthesis of hydrocarbons C_2 and C_{2+} is considered.

Keywords: *oxidative conversion of methane, $NaMnW/SiO_2$ catalyst, ethylene-carbon monoxide mixture, magnetic, texture properties*

INTRODUCTİON

Oxidative condensation of methane (OCM) is one of the promising methods for processing natural gas into an ethane-ethylene mixture. A limiting factor in the practical implementation of the process is the low yield of target products. The best catalysts make it possible to obtain selectivity for C_2-products up to 70-80% at a methane conversion of 25-30 % [1, 2]. A tempting approach based on a combination of the OCM reaction to produce ethylene and carbon monoxide in the reaction products with the required CO/C_2H_4 ratio with the hydroformylation reaction of this mixture to propylene is used in project C123 of the EU Horizon2020 program. This work presents the results of testing nanostructured oxide systems $MnNaW/SiO_2$ as catalysts for the OCM reaction to obtain gas-phase mixtures with an equimolar ratio C_2H_4/CO, and discusses the structural and catalytic features of the synthesized systems.

EXPERİMENTAL PART

Catalysts preparation

To prepare the catalysts, mesoporous silica matrices preliminarily were synthesized, using tetraethoxysilane, TEOS, cetyl-tri-methyl-ammonium bromide, CTAB (samples 1), TEOS, triethanolamine, TEA (samples 2) TEOS, citric acid, CA (samples 3) as precursors. Further, the reaction mixture containing an aqueous solution of surfactant, TEOS and ammonia was kept in a thermostat for several hours at room temperature until mesoporous silica was formed. Then the solution was filtered, the resulting precipitate was washed with distilled water and dried in air at room

ISNN: print 2663-7006; online 2709-2666

temperature. Salts of the corresponding metals were introduced into the hydrophobic part of the "template/silicon dioxide" composite by impregnating them with aqueous solutions of samples of 1,2,3 mesoporous silicon dioxide. The resulting gel after drying at room temperature is placed in a drying oven and kept at 80-100 °C for 3-4 hours until completely dry. The final heat treatment of the obtained sample is carried out in a muffle furnace at 850 °C for 4 hours.

Catalysts characterization

The catalysts were characterized by scanning electron microscopy (SEM; Hitachi S-3400N) equipped with an energy-dispersive X-ray fluorescence spectrometer (EDX; Oxford), X-ray diffractometers XRD D2, Bruker, Germany and XRD TD3500, China; Atomic Absorption Spectrometer, iC3000, Thermo Scientific, USA; EPR spectrometer EMX_micro, Bruker, Germany; the specific surface area and total pore volume of the samples was determined by low-temperature adsorption of nitrogen using SORBI-MS (Russia) and Belsorp Mini II, BEL Japan Inc. instruments. The powders were activated for 18 hours under vacuum at 90°C to remove moisture before measuring the texture values. Radical freezing system in combi- nation with JES-PE-3X, Jeol EPR spectrometer and home made quartz flow reactor connected with radicals freezing system for registration of hydro- carbon and peroxide radicals and investigation of their concentration as a function of reaction condition and type of catalyst. The reactions were carried out at temperatures 550 -850°C. The synthesized samples as catalysts for the OCM reaction were tested using a flow-through setup with a fixed catalyst bed. Gas-phase producns of the reaction after the reactor were analyzed using Agilent 7280A (USA) and LXM 80 (Russia) chromatographs. Helium was used as the carrier gas. The OCM reaction was carried out at 700 - 900°C and atmospheric pressure. The catalyst weighed amount was 0.2 g of the 0.25 - 0.5 mm fraction, the volumetric flow rate of the mixture was up to 140 ml/min.

RESULTS AND DISCUSSION

Below are the results of a study of the elemental, phase composition, magnetic properties, morphology, and structural-porous characteristics of the synthesized Na-W-Mn-containing catalysts based on SiO_2 obtained by various preparation methods.

Elemental and phase composition, surface structure and distribution of active elements in catalysts.

Eelectron micrographs show that the duration of the calcination of the samples significantly affects the morphology and structure of the surface. Regarding the effect of the duration of calcination of the samples on the distribution of active components in the catalyst structure, an EDX analyzer of an electron microscope is used and the surfaces of these samples were scanned at 5 randomly selected points of the surface. Comparison of these EDX spectra indicates a noticeable effect of the duration of calcination of the samples at 850°C on the distribution of catalytically active components in the catalyst structure.

X-ray diffraction patterns of samples show the presence of two different phases of the SiO_2 matrix - cristabolite and tridymite and changes in the phase composition of the matrix with an increase in the calcination temperature of the samples from 850 to 1000 °C with the introduction of these active components into SiO2. X-ray diffraction patterns of samples calcined for 4 hours: a)SiO_2 at 850°C; b) SiO_2 at 1000°C; c) $MnNaW/SiO_2$ at 1000°C are given in fig.1.

EMR data

For all samples two types of EPR spectra are observed. The first one with g = 2.000 and an hyperfine constant of ~ 90 G is characteristic for isolated Mn^{2+} ions, and the second with g = 2.01-2.1 and ΔH = 600-1100 G belongs to MnOx, most likely to Mn_2O_3 nanoparticles [3]. Mn^{3+} is not a Kramers ion (3 d^4, S = 2), and it does not show EPR signals at the X-band frequency [4]. Figure 2 shows the EPR spectra of sample 1 at 300 K.

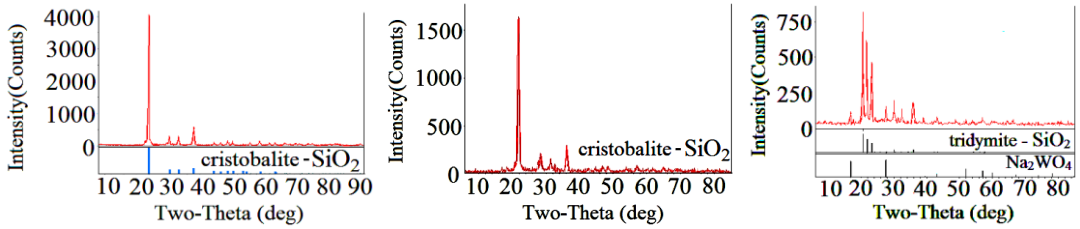

a) *b)* *c)*

Fig.1. X-ray diffraction patterns of samples calcined for 4 hours: a) SiO_2 at 850 °C; b) SiO_2 at 1000°C; c) 2Mn-0.8Na-3.2W/SiO_2 at 1000 °C

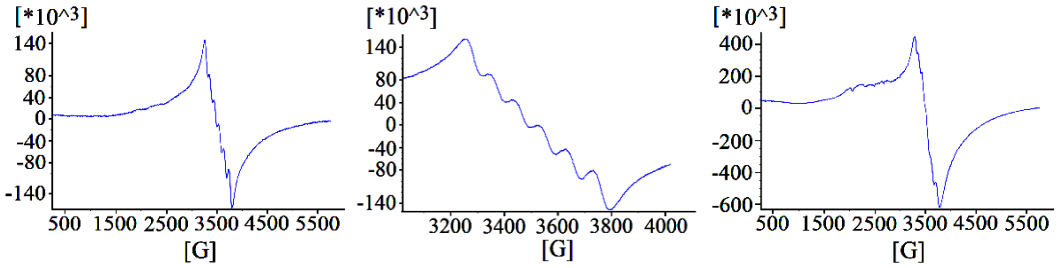

a) b) c)

Fig.2. EPR spectra at 300K of 2Mn -0.8Na-3.2W/SiO_2 sample 1 calcined at 850 ^oC for 4 hours: a,b) before and c) after 10 hours OCM reaction at 798 ^oC; (CH_4/O_2)=4.

It was shown that the observed MnOx nanoparticles are superparamagnetic and weakly ferromagnetic above and below the blocking temperature, accordingly. The dependent of the composition and size of MnOx nanoparticles on the reaction conditions is observed. The evaluated size of the observed MnOx nano- particles is less than 10 nm [5].

Texture properties

In table 1 the values of specific surface area and the volume of pore of these samples before and after 15 hours working in OCM reaction are given. As can be seen from these data effect of the reaction condition on the texture parameters of the samples is significant.

Table 1

The values of specific surface area and the volume of pore of these samples before and after 15 hours working in OCM reaction

Samples*	BET (m^2/g)		Total pore volume, p/p_0 = 0.99 ($cm^3\ g^{-1}$)	
	a*	b*	A	B
1	116.8	46.1	0.590	0.232
2	36.0	4,4	0.206	0.025
3	38.2	8,3	0.373	0.081

***** a, b - accordingly before and after 15 hours testing of the samples in reaction OCM.

ISNN: print 2663-7006; online 2709-2666

Catalysts Testing

The synthesized catalysts exhibit different catalytic activity, depending on their preparation method. Methane conversion of up to 47.7 % and a selectivity of C2 and C3 hydrocarbons in the amount of up to 86.7 % and a yield of up to 27.4 % were observed. The selectivity ratio (C2+C3)/(CO+CO_2) is approximately 1 with a fairly high yield (25.2 %) (C2+C3) for sample 1 and slightly more than 1 for sample 2 (for yield) 24.3 %). The ratio of C_2H_4 / (CO+CO_2) is approximately 1 for both samples with the same yield of C2+C3 hydrocarbons. An increase in temperature from 778 to 874 ^oC leads to an increase in ethylene selectivity and the yield of C2+C3 hydrocarbons. Stability of catalyst as a function of OCM reaction duration is shown in fig.3.

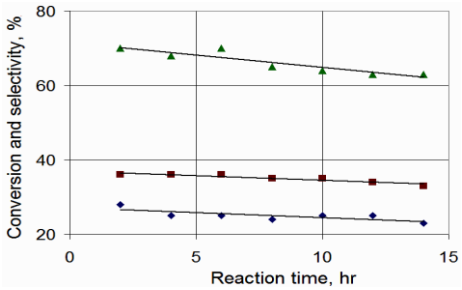

Fig.3. Dependence of methane conversion (■), selectivity of C2+ hydrocarbons (▲) and the yield of C2+ hydrocarbons (♦) on the duration time of the OCM reaction at the ratio CH_4/O_2 = 4, (reaction temperature 812 ^oC, catalyst weight 0.2 g, gas mixture flow rate 120 ml / min.)

Conversion of methane and oxygen without (♦, □,respectively) and in the presence (▲, ▲) of the catalyst in the OCM reaction as a function of the reaction temperature at the ratio CH_4/O_2= 4, (catalyst weight 0.2 g, gas mixture flow rate 120 ml/min.) is demonstrated in fig.4.

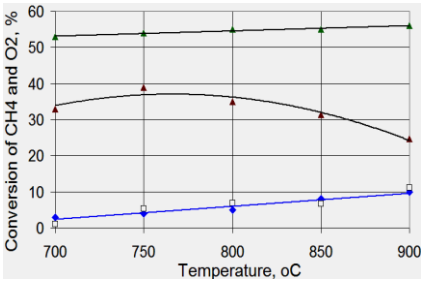

Fig.4. Conversion of methane and oxygen without (♦, □,respectively) and in the presence (▲, ▲) of the catalyst in the OCM reaction as a function of the reaction temperature at the ratio CH_4/O_2= 4, (catalyst weight 0.2 g, gas mixture flow rate 120 ml/min.)

Conversion and selectivity as a function of CH_4/O_2 ratio are The full stoichiometric equation of the OCM reaction according to the output data can be written in the form:

$$aCH_4 + bO_2 \rightarrow cC_2H_6 + dC_2H_4 + eCO_2 + fC_3H_6 + fC_3H_8 + gH_2O + hCO$$

for the case (CH_4/O_2)=2 we have

$$12CH_4 + 6O_2 \rightarrow C_2H_6 + C_2H_4 + CO_2 + C_3H_6 + C_3H_8 + 9H_2O + CO + 3H_2$$

and for the case (CH_4/O_2)=4 we have

$$12CH_4 + 3O_2 \rightarrow C_2H_6 + C_2H_4 + CO_2 + C_3H_6 + C_3H_8 + 3H_2O + CO + 9H_2$$

According to experimental data the ratio $(CH_4/O_2) \geq 4$ more acceptable for OCM reaction.

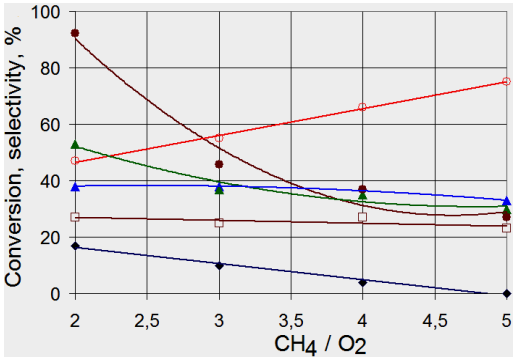

Fig.5. Dependence of the conversion of methane (▲) selectivities of C2+ hydrocarbons (o), CO (▲) and CO_2 (♦), the yield of C2+ hydrocarbons (□), C_2H_4/C_2H_6 ratio (●) in the presence of a catalyst in the OCM reaction on the CH_4/O_2 ratio, (catalyst weight 0.2 g, gas mixture flow rate 120 ml / min.)

Conversion and selectivity as a function of flow rate of gas mixture are given in fig.6.

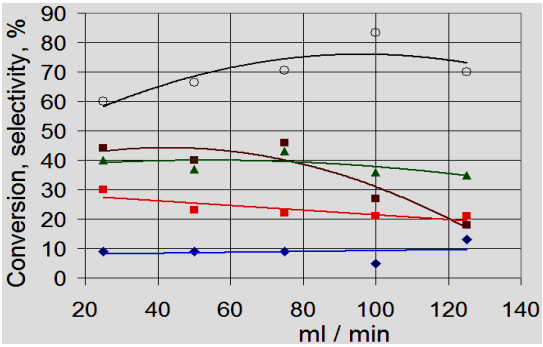

Fig.6. Dependence of the conversion of methane (▲) selectivities of C2+ hydrocarbons (○), CO (♦) and CO2 (■), the yield of C2+ hydrocarbons (■) on the flow rate of gas mixture in OCM reaction at a ratio $(CH_4/O_2) = 4$, (catalyst weight 0.2 g, reaction temperature 798°C)

If we assume that nanosized Mn_2O_3 particles are active centers of the OCM reaction:

$$Mn_2O_3 + 2CH_4 = 2MnO + C_2H_6 + H_2O$$
$$2MnO + \tfrac{1}{2}O_2 = Mn_2O_3$$
$$C_2H_6 = C_2H_4 + H_2$$

then it can also be assumed that methane is activated by oxygen of Mn_2O_3 with the separation of the hydrogen atom and the formation of the methyl radical $CH_3^{\bullet}$ [6,7]. Further, under the reaction conditions, these radicals combine and turn into ethane, and when interacting with oxygen, into $CH_3O_2^{\bullet}$ radicals, which are further oxidized to CO and CO_2. In the case of an excess of oxygen under the reaction conditions, ethylene is also easily oxidized to carbon oxides.

$$2C_2H_4 + 5O_2 = 2CO + 2CO_2 + 4H_2O$$

ISNN: print 2663-7006; online 2709-2666

Radical freezing system in combination with JES-PE-3X, Jeol EPR spectrometer and home made quartz flow reactor connected with radicals freezing Dewar for registration of hydrocarbon and peroxide radicals and investigation of their concentration as a function of reaction condition and type of catalyst is given in fig. 7.

Only $RO_2^{\bullet}$ radicals were detected and their concentration is increased as the ratio CH_4/O_2 is increase. $CH_3^{\bullet}$ radical is not detected because the liquid nitrogen temperature is high enough to detect the $CH_3^{\bullet}$ radical and therefore only $RO_2^{\bullet}$ radicals are detected. The reactions were carried out at temperatures of 550 - 850 °C.

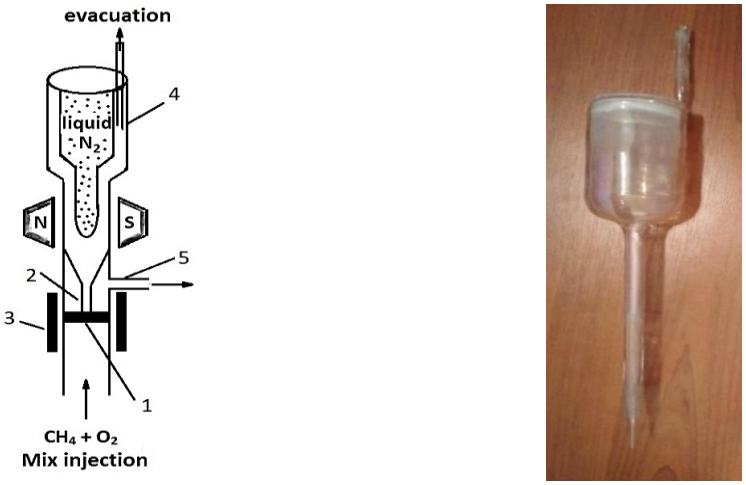

a) b)

Fig.7. Radical freezing system in combination with JES-PE-3XQ, Jeol EPR spectrometer and home made quartz flow reactor connected with Dewar for registration of hydrocarbon and peroxide radicals. Here: a) 1- Catalyst; 2- Capillary with the end beginning from the surface (no more than 0,5 mm); 3- Heater; 4.-Dewar vessel; 5 –Reaction products outlet; b) Dewar vessel with capillary

X-ray diffractometry data show the effect of active elements introduced into the SiO_2 matrix on the phase composition of the matrix. With increasing the calcination temperature from 850 to 1000°C, no noticeable changes are observed in the diffractograms of the matrix. However, the diffraction patterns of the 2Mn-0.8Na-3.2W/SiO_2 samples, along with the formation of the MnOx and Na_2WO_4 phases of active elements, show the presence of two phases of the SiO_2 matrix differing in structure - crisstabolite and tridymite; with an increase in the calcination temperature of samples containing Mn, Na, W, from 850 to 1000°C, the phase composition of the matrix changes. The used MnNaW/SiO_2 catalyst is multicom- ponent and, as shown by the X-ray diffractometry data, consists of the phases MnOx, Na_2WO_4, and SiO_2. At the reaction temperature OCM, i.e. 750-850^{o}C , one of these phases - Na_2WO_4 is in a melted state (the values of the melting and decomposition temperature of Na_2WO_4 are equal to 696 and 1200^{o}C, respectively). The phases MnOx (MnO, Mn_2O_3, MnO_2) and SiO_2 have a melting point above 850°C, i.e. under the reaction conditions Na_2WO_4, covering the surface of crystalline SiO_2 (with cristobalite and/or tridomite structure) in the form of a film, and nanosized MnOx particles contained in it, as shown by EMR data. This example underline the peculiarities of high-temperature reactions catalyzed

by multicom- ponent systems, the components of which are in dif- ferent states of aggregation under the reaction conditions.

CONCLUSİON

The synthesis of a stable OCM catalyst with a conversion of more than 35% and a selectivity for C2 hydrocarbons up to 80% is considered practically acceptable. But:

1. If we use the $MnNaW/SiO_2$ and its modification forms as catalysts for OCM reaction we have to work at the temperature 750-850^oC with the ratio CH_4/O_2 >4 with flow rates of the gas mixture (CH_4+O_2) more than 100 ml/min. In this case we have the quietly high yield of target products, but not enough for practical purposes. The experimental results show that after 15 hours of working in OCM reaction the activity, selectivity and yield of catalysts decrease approximately for 10-15%. We have to take into account the instability of phase composition of these catalysts under reaction conditions also.
2. To use catalysts of new compositions that allow the OCM reaction to be carried out at temperatures below the ignition of ethane and ethylene (~ 600^oC). In this case, we will need to carry out studies using in-situ EPR and Raman spectroscopy in combination with mass spectroscopy of surface and gas-phase products of the OCM reaction. These studies make it possible to find ways to stabilize methyl radicals with their subsequent recombination on the surface with the formation of ethane, to separate and control the stages of recombination of methyl radicals on the surface and in the gas phase, and thereby allow controlling the OCM process. For catalysts with the composition $MnNaW/SiO_2$, prepared using TEOS and CTAB as precursores, methane conversion up to 47.7 % was observed, selectivity for hydrocarbons C_2, C_3 in total up to 86.7 % and yield up to 27 mas.%; the selectivity ratio (C_2 +C_3)/CO was ~1 at a rather high yield (25.2 %) of C_2, C_3 hydrocarbons. An increase in temperature from 778 to 874°C led to an increase in selectivity for C_2,C_3 hydrocarbons. For these catalysts, the specific surface area was 100-120 m^2/g and after 10 hours of operation at a temperature of 800-850° C decreased significantly, but they average pore dia- meter is in the range of 2-50 nm still, so the behavior of these catalysts will be typical for mesoporous materials. Comparison of EDX spectra indicates a noticeable effect of the temperature and duration of calcination of the samples on the distribution of catalytically active components in the catalyst struc- ture. We consider it expedient to carry out, first of all, in situ X-ray diffraction, Raman, and EMR studies in combination with mass spectroscopic analysis of gas-phase products of the reaction to detalize, refine the "structure-activity" models of the OCM reaction with participation of $MnNaW/SiO_2$ catalysts [8].

Acknowledgements: This work is funded by the European Union's Horizon 2020 research and innovation program under grant agreement No.814557. The authors are grateful to Richard Heyn (SINTEF, Oslo, Norway) for help in measuring the texture characteristics of the samples.

REFERENCES

1. Kondratenko E.V., Peppel T., Seeburg D., Kondratenko V.A., Kalevaru N., Martin A., Wohlrab S. “Methane conversion into different hydrocarbons or oxygenates:

ISNN: print 2663-7006; online 2709-2666

current status and future perspectives in catalyst development and reactor operation", Catal. Sci. Technol.2017, 7(2), pp.366–381
2. C. Karakaya, R.J. Kee. "Progress in the direct catalytic conversion of methane to fuels and chemicals", Progr. Energy Combust. Sci.2016, 55, pp. 60–97
3. S.Mukherjee, A.K. Pal, S. Bhattaacharya, J. Raittila. "Magnetism of Mn_2O_3 nanocrystals dispersed in a silica matrix.: Size effects and phase transformations", Phys.RevB.74, 104413 p
4. D.P. Goldberg, J. Telser, J. Krzystek et al., "EPR spectra from "EPR-Silent" species: high-field EPR spectroscopy of manganese(III) porphyrins," J. of the Amer.Chem. Society.1997,119 (37), pp.8722–8723
5. Walter S. D. Folly and Ronaldo S. de Biasi ''Determination of Particle Size Distribution by FMR Measurements'', Braz. J. Phys.2001, 31 (3), pp.398–401
6. A.I. Suleimanov, E.G. Ismailov, S.M. Aliev, V.D. Sokolovskii, "Contribution of one -electron acceptor centers to oxidative dimerization of methane",React. Kinet. Catal. Lett.1987, pp.34, 51–55
7. Wang J., Rosyynek M.P., Lunsford J.H. "Oxidative Coupling of Methane over Oxide-Supported Sodium-Manganese Catalysts", J. Catal.1995,115 (2), pp. 390–402
8. Daniel Kiani, Sagar Sourav, Jonas Baltrusaitis, Israel E.Wachs, "Oxidative Coupling of Methane (OCM) by SiO_2 – supported Tungsten Oxide Catalysts Promoted with Mn and Na", ACS Catal.2019 9, (7), pp.5912–5928

ОКИСЛИТЕЛЬНАЯ КОНВЕРСИЯ МЕТАНА. ЭФФЕКТ КАТАЛИЗАТОРА И ПЕРСПЕКТИВНЫЕ НАПРАВЛЕНИЯ РЕАКЦИИ

[1]Э.Г.Исмаилов, [1]Д.Б. Тагиев, [1] С.М. Зульфугарова, [1]Г.Р.Азимова, [1]С.Н.Османова, [2]Й.У. Тибот

[1]Институт Катализа и Неорганической Химии им.акад.М.Ф. Нагиева НАНА,
[2]Университет Гент, B-9052 Гент, Бельгия
etibar.ismailov@gmail.com

Хорошо известные катализаторы MnNaW на основе SiO2 для окислительной конденсации метана (ОКМ) были синтезированы различными методами, охарактеризованы методами рентгеновской дифрактометрии (XRD), сканирующей электронной микроскопии с энергодисперсионным элементным анализом (SEM/EDX), электронного магнитного резонанса. (ЭМР), текстурные характеристики по адсорбции-десорбции N2 и испытаны в качестве катализаторов реакции ОКМ в углеводороды C_2 и C_{2+}, в смесь этилен + оксиды углерода при атмосферном давлении с целью гидроформилирования последнего в пропилен. Обсуждены структурные и каталитические особенности синтезированных систем. Указаны каталитически активные центры, механизм реакции ОКМ с их участием с образованием связи C-C и углеводородов на этой основе.

Ключевые слова: *окислительная конверсия метана, катализатор MnNaW/SiO2, фазовый состав, магнитные, текстурные свойства, углеводороды C_2, C_{2+}, смесь этилен+оксиды углерода.*

METANIN OKSİDLƏŞDİRİCİ KONDENSASİYASI. KATALİZATORUN TƏSİRİ VƏ REAKSİYANIN PERSPEKTİV İSTİQAMƏTLƏRİ

[1] *E.H. İsmayılov,* [1] *D.B.Tağıyev,*[1] *S.M.Zülfügarova,* [1] *G.R.Əzimova,*
[1] *S.N. Osmanova,* [2] *Joris Thybaut*
[1]*Akad. M.Nağıyev adına Kataliz və Qeyri-üzvi Kimya Institutu, AMEA,*
[2] *Ghent Universiteti, B-9052 Ghent, Belçika*
etibar.ismailov@gmail.com

Metanın oksidləşdirici kondensasiyası (MOK) üçün SiO2 əsaslı məlum MnNaW katalizatorları müxtəlif üsullarla sintez edilmiş, onların rentgen difraktometriyası (XRD), elektron skan mikroskopu enerji dispersion element analizi ilə birgə (SEM/EDX), elektron maqnit rezonansı (EMR) spektroskopiyası, N2 adsorbsiya-desorbsiyası əsasında textur xarakteristikaları müəyyən edilmiş, atmosfer təzyiqində metanın C_2, C_{2+} karbohidrogenlərə, etilen+karbon oksidləri qarışığına və sonuncunun propilenə hidroformilləşdirilməsi reaksiyalarında katalizator kimi sınağı keçirilmişdir. Sintez edilmiş sistemlərin struktur və katalitik xüsusiyyətləri müzakirə olunmuş, katalitik aktiv mərkəzlər göstərilmiş, onların iştirakı ilə C-C rabitəsinin və karbohidrogenlərin əmələ gəlməsinə gətirib çıxaran mexanizm verilmişdir.
Açar sözlər: *metanın oksidləşdirici kondensasiyası, katalizator MnNaW/SiO_2, faza tərkibi, maqnit, tekstur xassələri, C_2, C_{2+} karbohidrogenləri, etilen+karbon oksidləri qarışığı.*

ISNN: print 2663-7006; online 2709-2666

ATTENTION FOR AUTHORS!

Journal "Azerbaijan Journal of Chemical News" approved by the Higher Attestation Commission under the President of Azerbaijan Republic and it is included to the list of journals and periodicals that should be published by major scientific results of dissertations in Azerbaijan Republic.